DERIVATION AND ANALYSIS OF BEHAVIORAL MODELS TO PREDICT POWER SYSTEM DYNAMICS

A Thesis

Submitted to the Faculty

of

Purdue University

by

Chengyi Xu

In Partial Fulfillment of the

Requirements for the Degree

of

Master of Science

August 2020

Purdue University

West Lafayette, Indiana

THE PURDUE UNIVERSITY GRADUATE SCHOOL
STATEMENT OF THESIS APPROVAL

Dr. Steven D. Pekarek, Chair

School of Electrical and Computer Engineering

Dr. Dionysios C. Aliprantis

School of Electrical and Computer Engineering

Dr. Shreyas Sundaram

School of Electrical and Computer Engineering

Approved by:

Dimitrios Peroulis

Head of the School Graduate Program

ACKNOWLEDGMENTS

I would like to acknowledge The Schweitzer Engineering Laboratories(SEL) for the funding and the research opportunity. I could not complete this thesis without the help from SEL and the research group at Purdue University.

I would also like to gratefully acknowledge the support and encouragement of my major professor, Dr. Steven Pekarek. His patience and guidance helped me in all the time of research and writing of this thesis. I could not have imagined having a better advisor and mentor for my graduate study.

My gratitude extends to Dr. Dionysios Aliprantis. Even though he is not my major professor, as a member of my thesis committee and an advisor in the research team, he still constantly gave me encouragement, insightful comments, and hard questions so that I can become a better researcher and successfully finish the thesis.

In addition, I would like to express my sincere gratitude to Dr. Shreyas Sundaram, for spending time in reading my thesis and providing insightful comments.

I also thank my fellow research teammates in the SEL project at Purdue University. Many thanks to Dakota Hamilton, Lucas Peralta and Kiana Pitman for all the research meetings, discussions and all the fun along the journey.

Furthermore, I would like to thank my family: my parents Yinghua Xu and Naihui Jin, for giving birth to me at the first place and supporting me spiritually and financially throughout my life.

TABLE OF CONTENTS

Page

Page

LIST OF TABLES

LIST OF FIGURES

Figure Page

ABSTRACT

Xu, Chengyi Master, Purdue University, August 2020. Derivation and Analysis of Behavioral Models to Predict Power System Dynamics. Major Professor: Steven D. Pekarek.

In this research, a focus is on the development of simplified models to represent the behavior of electric machinery within the time-domain models of power systems. Toward this goal, a generator model is considered in which the states include the machines active and reactive power. In the case of the induction machine, rotor slip is utilized as a state and the steady-state equivalent circuit of the machine is used to calculate active and reactive power. The power network model is then configured to accept the generator and induction machine active and reactive power as inputs and provide machine terminal voltage amplitude and angle as outputs. The potential offered by these models is that the number of dynamic states is greatly reduced compared to traditional machine models. This can lead to increased simulation speed, which has potential benefits in model-based control. A potential disadvantage is that the relationship between the reactive power and terminal voltage requires the solution of nonlinear equations, which can lead to challenges when attempting to predict system dynamics in real-time optimal control. In addition, the accuracy of the generator model is greatly reduced with variations in rotor speed. Evaluation of the models is performed by comparing their predictions to those of traditional machine models in which stator dynamics are included and neglected.

1. INTRODUCTION

1.1 Motivation

The power system is coupled to nearly every aspect of modern life. Thus, ensuring power is provided where desired despite faults, rapid changes in demand, and the potential variability of the energy available from renewable resources is of significant importance. One can argue that in much of the developed world, the engineering community has designed their respective power systems effectively. Indeed, outages are relatively rare events and the cost of electricity remains relatively low. However, the increased reliance on renewables, the integration of wide-bandwidth power electronics in both loads and sources, and the coupling of electrical and transportation infrastructures is increasing the complexity of the system. As a result, many researchers have been considering the role that model-based control methods such as model-predictive control can play in optimizing the performance of the evolving power system [1]. Examples of MPC-based methods applied to power systems include [2], [3], [4], and [5].

One of the critical aspects of model-based control methods is establishing models of components and systems upon which the control can be established. In general, there is a tradeoff between model complexity and its computational requirements. In this research, an initial focus has been placed on developing full-detailed models of a power system proposed in [6] that can serve as a reasonable test case to assess alternative control methods. The system consists of an infinite bus, a turbine generator with associated governor and exciter, a tap-changing transformer, and several transmission lines between the 5 system busses. Loads include those with constant impedance in parallel with induction machines. Herein, the word 'detailed' is used to indicate that the fast (stator) dynamics that are typically neglected in the models of larger power

systems, are represented. Within the models of the machines, the state variables are the stator flux linkages. The inputs to these models are the stator voltages. The network dynamics are represented using a π-based model for each transmission line.

Subsequent to the detailed model derivation, a reduced-order model of the system is created in which the stator dynamics of the machines and transmission lines are neglected [7]. In this form, an algebraic relationship is established between stator terminal voltage and stator current of each machine. Coupling the machine models is performed by representing the stator voltage as a model output and the stator current as a model input. Steady-state forms of the transmission line models are used to establish a network admittance matrix that relate network voltage and current. The traditional advantage of the reduced-order model structure is that it has enabled power system analysts to use a larger time-step when simulating power systems [7]. A similar advantage is likely in MPC-based control.

Finally, to potentially further reduce computational complexity, simplified behavioral models of the turbine generator and induction machine are considered. In the case of the turbine generator, the active and reactive power are utilized as state variables. In the case of the induction machine, rotor slip is utilized as a state variable and the steady-state equivalent circuit of the machine is used to calculate active and reactive power. The network model is then configured to accept the generator and induction machine active and reactive power as input and provide machine terminal voltage amplitude and angle as outputs. The potential offered by these models is that the number of dynamic states is greatly reduced. This can lead to increased simulation speed. In addition, in the case of the turbine generator, the number of model parameters is significantly reduced. Indeed, the only parameters in the behavioral model are several time constants in the machine, governor and exciter. A potential disadvantage is that the relationship between the reactive power and terminal voltage requires the solution of a nonlinear equation, which can lead to challenges in MPC-based control.

In this research, the details of each of the models is provided along with their implementation structure within MATLAB.

1.2 Description of 5-Bus System

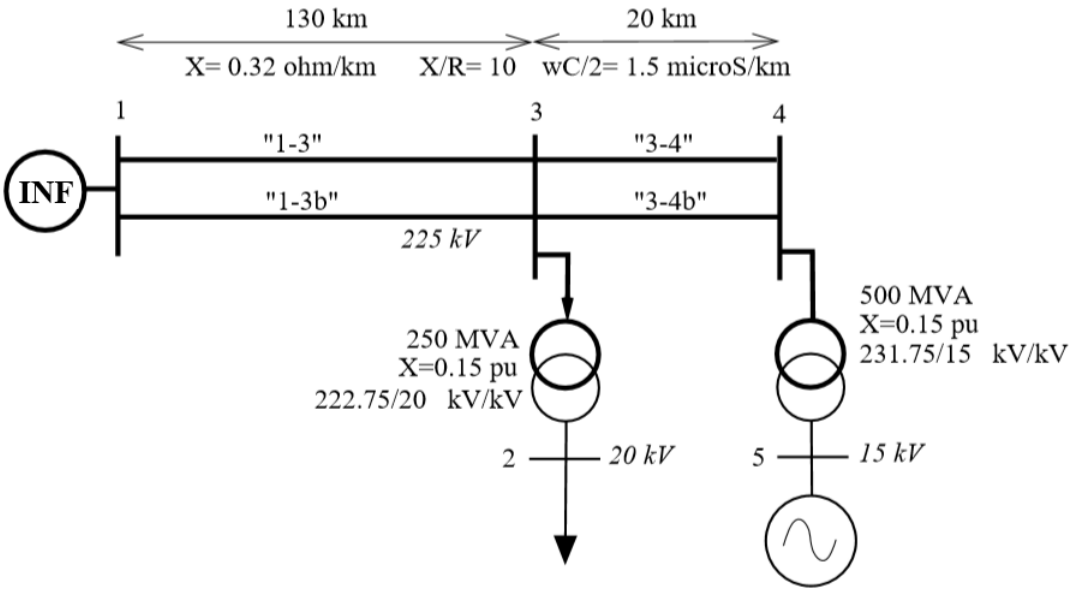

Fig. 1.1.: 5-bus System

The 5-bus system that is considered in this research has a one-line diagram shown in the Figure 1.1 and is described in [6]. The reason the system was selected is that it has several key traditional power system components and the parameters of all components and controls are provided. As shown, the 5-bus system consists of an infinite bus 1, a load bus 2, a generator bus 5 and transmission lines coupling bus 3 and bus 4. In addition, there is a load tap changing transformer between bus 3 and bus 2, and a fixed turns transformer between bus 4 and bus 5. The machine sources and loads are highlighted in subsequent chapters. Some details of the network components are highlighted in the following subsections.

1.2.1 Infinite Bus

The infinite bus represents an ideal AC source voltage with a voltage magnitude and frequency independent of the bus current. In 3-phase electrical circuit analysis,

it is convenient to use reference frame theory to transform systems into a frame in which steady-state currents and voltages are constant [8]. This allows one to solve algebraic expressions for steady-state operating points. In addition, It also provides convenience for controls, since the input variables are constant in the steady-state, rather than time-varying. As a result, the infinite bus would provide the synchronous reference angle for the utilization of the reference-frame theory.

1.2.2 Generator Bus

At bus 2, there are three components: a wound-rotor synchronous machine with excitation and governor. The excitation system controls the field voltage to the generator. There are various types of excitation systems [9], in the [6] a DC excitation system is utilized. For the governor system, there are multiple types of governors, including steam- gas-, and hydro-turbine-based. In the thesis, a steam governor system is considered . For the wound-rotor synchronous generator, the machines is a three-phase, wye-connected, salient-pole model with two damper windings on the q-axis, one damper winding on the d- axis and one field winding on the d-axis.

1.2.3 Load Bus

Load bus 2 includes two induction machines and a constant-impedance load. Based on [10], this combination is common practice in American power system research. For the constant-impedance load, a symmetrical three-phase wye-connected series-connected RC load is assumed. The use of the induction as part of the load model is based on three factors [11]: first, it is a fast-restoring load in the time frame of a second; second, it is a low power factor load with a high reactive power demand; third, it is prone to stalling when the voltage is low, or the mechanical load is increased, which can lead to issues of power system stability. For the induction machines, both are three-phase, wye-connected, symmetrical induction machines. The main difference between the two machines is their inertia. One has an inertia

consistent with a large-power machine. The second has a lower inertia that is representative of many smaller-power machines connected to a bus, which often occurs in manufacturing plants.

1.2.4 Transmission Line

For the network, a π model of the transmission lines is used, as described in [12]. Physically, between bus 1/2 and bus 3/4, there is a conductor that is modeled using a π circuit. Hence for the system, there are twelve π circuits representing the transmission lines. The π model of the transmission is shown in Figure (1.2). The per-unit impedance (value of R_l, X_l) and admittance (b_l) for the transmission lines are the same; the differences are their length. The lines between bus 1 and bus 3 are longer than the lines between bus 3 and bus 4.

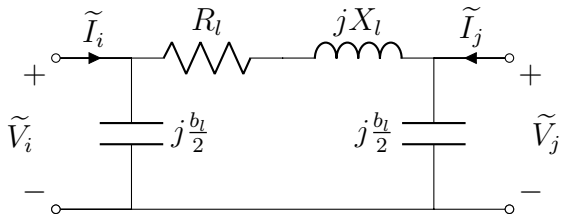

Fig. 1.2.: Transmission Line π-Equivalent Circuit

1.2.5 Transformer

A load-tap-changer transformer (LTC) is used to step the voltage from transmission levels to distribution levels and regulate bus 2 voltage. A fixed-turn transformer is used to step the voltage from transmission to distribution levels at bus 5. The only difference between the two transformers is that the LTC can vary its turns ratio, whereas the fixed-turn transformer has a fixed value. In this research, both transformers are modeled using the circuit shown in Figure 1.3. Therein, one can observe that the input-to-output relationship consists of an ideal turns ratio in series with a

reactance that is representative of the transformer's leakage reactances. As shown, all both primary and secondary resistances are assumed negligible. Similarly, the transformer magnetizing reactance is assumed to be sufficiently large that it can be neglected. Again, for the load tap changer between bus 3 and bus 4, $\frac{V_{in}}{V_t}$ varies in order to control V_{out} to a desired value.

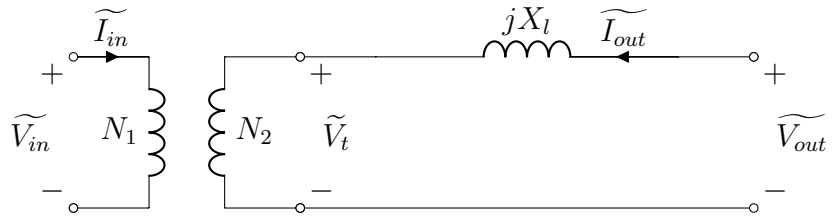

Fig. 1.3.: Transformer Equivalent Circuit

2. DETAILED MODEL

2.1 Introduction

In this chapter, the detailed model for each of the components is described. For all electrical components, the state equations are represented in a suitable reference-frame. Brief details of reference frame transformation are provided in the Appendix. For the transmission lines, transformers and constant admittance loads, the corresponding differential equations are based upon equivalent circuits described in [12]. In the generator and induction machines, model details are provided in [8] and [11]. Herein magnetic saturation in all machines is neglected. All models are built based on the per-unit quantities for all the variables. Parameters described in the appendix.

2.2 Infinite Bus

Description

The infinite bus 1 provides phase voltages expressed (2.1) in per-unit form:

$$v_{ainf} = V_s \cos(\omega_e t) \tag{2.1a}$$

$$v_{binf} = V_s \cos(\omega_e t - \frac{2\pi}{3}) \tag{2.1b}$$

$$v_{cinf} = V_s \cos(\omega_e t + \frac{2\pi}{3}) \tag{2.1c}$$

Transforming the infinite bus voltage to the synchronous reference frame using equation (B.1) with $\theta_e = \omega_e t$, the infinite bus is modeled in the synchronous reference frame can be expressed as:

$$v_{qinf} = V_s \tag{2.2a}$$

$$v_{dinf} = 0 \tag{2.2b}$$

$$v_{0inf} = 0 \tag{2.2c}$$

Simulink Implementation

The infinite bus voltage magnitude and electrical frequency are constant. As a result, the bus voltage in the $qd0$ variables and the synchronous reference frame angle θ_e can be calculated. Hence the Simulink block diagram is shown in Figure 2.1

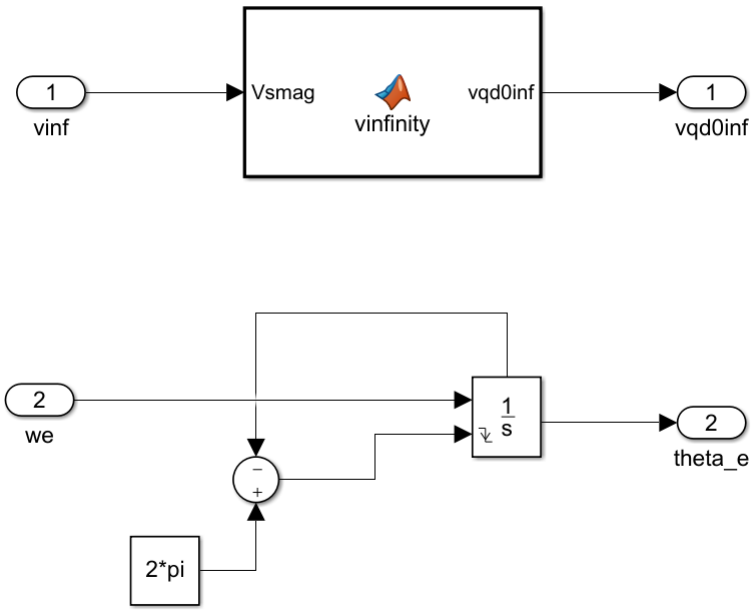

Fig. 2.1.: Infinite Bus Simulink Implementation

2.3 Detailed Generator Model

2.3.1 Wound-Rotor Synchronous Machine

The detailed model for the generator utilized is fully described in [7] page 42. The derivation of the model starts from the cross section of a two-pole, three-phase, wye-connected salient-pole synchronous machine depicted in Figure 2.2. Analysis of the relationship between winding current and magnetic flux and voltage and current is used to generate the ordinary differential equations (ODEs) used to predict machine performance. Reference frame theory is then applied to establish the common Park's equivalent circuit described in [8] that can be modeled using ODEs of the form:

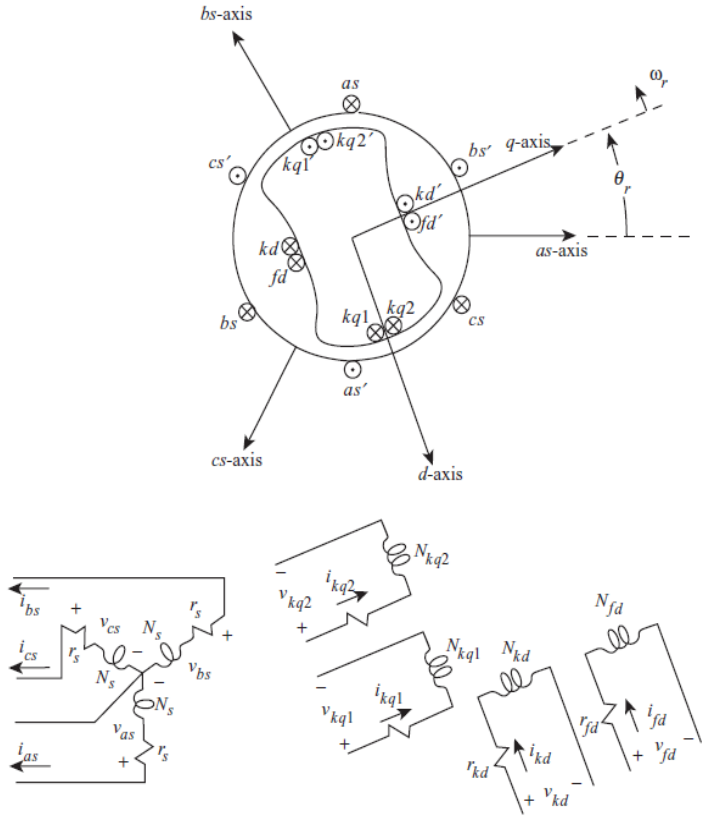

Fig. 2.2.: Two-pole, three-phase, wye-connected salient-pole synchronous machine

$$v_{qs}^{r} = -r_s i_{qs}^{r} + \omega_r \lambda_{ds}^{r} + \frac{d\lambda_{qs}^{r}}{dt} \tag{2.3a}$$

$$v_{ds}^{r} = -r_s i_{ds}^{r} - \omega_r \lambda_{qs}^{r} + \frac{d\lambda_{ds}^{r}}{dt} \tag{2.3b}$$

$$v_{0s} = -r_s i_{0s} + \frac{d\lambda_{0s}}{dt} \tag{2.3c}$$

$$v_{fd}^{'r} = r_{fd}^{'} i_{fd}^{'r} + \frac{d\lambda_{fd}^{'r}}{dt} \tag{2.3d}$$

$$v_{kd}^{'r} = r_{kd}^{'} i_{kd}^{'r} + \frac{d\lambda_{kd}^{'r}}{dt} \tag{2.3e}$$

$$v_{kq1}^{'r} = r_{kq1}^{'} i_{kq1}^{'r} + \frac{d\lambda_{kq1}^{'r}}{dt} \tag{2.3f}$$

$$v_{kq2}^{'r} = r_{kq2}^{'} i_{kq2}^{'r} + \frac{d\lambda_{kq2}^{'r}}{dt} \tag{2.3g}$$

where v is used to represent respective winding voltage, r winding resistance, and ω_r is the rotor electrical angular velocity. The variable λ is used for winding flux linkage. The winding flux linkages can be expressed in terms of winding currents using (2.4):

$$\lambda_{qs}^{r} = -L_{ls} i_{qs}^{r} + L_{mq}(-i_{qs}^{r} + i_{kq1}^{'r} + i_{kq2}^{'r}) \tag{2.4a}$$

$$\lambda_{ds}^{r} = -L_{ls} i_{ds}^{r} + L_{md}(-i_{ds}^{r} + i_{fd}^{'r} + i_{kd}^{'r}) \tag{2.4b}$$

$$\lambda_{0s} = -L_{ls} i_{0s} \tag{2.4c}$$

$$\lambda_{fd}^{'r} = L_{lfd}^{'} i_{fd}^{'r} + L_{md}(-i_{ds}^{r} + i_{fd}^{'r} + i_{kd}^{'r}) \tag{2.4d}$$

$$\lambda_{kd}^{'r} = L_{lkd}^{'} i_{kd}^{'r} + L_{md}(-i_{ds}^{r} + i_{fd}^{'r} + i_{kd}^{'r}) \tag{2.4e}$$

$$\lambda_{kq1}^{'r} = L_{lkq1}^{'} i_{kq1}^{'r} + L_{mq}(-i_{qs}^{r} + i_{kq1}^{'r} + i_{kq2}^{'r}) \tag{2.4f}$$

$$\lambda_{kq2}^{'r} = L_{lkq2}^{'} i_{kq2}^{'r} + L_{mq}(-i_{qs}^{r} + i_{kq1}^{'r} + i_{kq2}^{'r}) \tag{2.4g}$$

In (2.3) and (2.4), the subscripts s and r refer to stator and rotor quantities respectively. The superscript r is used to indicate the variables are in the rotor frame of reference, and the prime $'$ is used to indicate that the respective winding is referred to the stator winding through an appropriate turns ratio. The inductances in (2.4)

with a subscript l are leakage values of the respective winding while those with a subscript md and mq are the d- and q-axis magnetizing values, respectively. Since the parameters of the synchronous machine are often provided in terms of reactances rather than inductances, it is convenient to multiply (2.3) and (2.4) on both sides by a base angular velocity ω_e and express the result in a state model form:

$$\frac{1}{\omega_e}\frac{d\psi^r_{qs}}{dt} = r_s i^r_{qs} - \frac{\omega_r}{\omega_e}\psi^r_{ds} + v^r_{qs} \tag{2.5a}$$

$$\frac{1}{\omega_e}\frac{d\psi^r_{ds}}{dt} = r_s i^r_{ds} + \frac{\omega_r}{\omega_e}\psi^r_{qs} + v^r_{ds} \tag{2.5b}$$

$$\frac{1}{\omega_e}\frac{d\psi_{0s}}{dt} = r_s i_{0s} + v_{0s} \tag{2.5c}$$

$$\frac{1}{\omega_e}\frac{d\psi^{'r}_{fd}}{dt} = -r'_{fd} i^{'r}_{fd} + v^{'r}_{fd} \tag{2.5d}$$

$$\frac{1}{\omega_e}\frac{d\psi^{'r}_{kd}}{dt} = -r'_{kd} i^{'r}_{kd} + v^{'r}_{kd} \tag{2.5e}$$

$$\frac{1}{\omega_e}\frac{d\psi^{'r}_{kq1}}{dt} = -r'_{kq1} i^{'r}_{kq1} + v^{'r}_{kq1} \tag{2.5f}$$

$$\frac{1}{\omega_e}\frac{d\psi^{'r}_{kq2}}{dt} = -r'_{kq2} i^{'r}_{kq2} + v^{'r}_{kq2} \tag{2.5g}$$

where

$$\psi^r_{qs} = -X_{ls} i^r_{qs} + X_{mq}(-i^r_{qs} + i^{'r}_{kq1} + i^{'r}_{kq2}) \tag{2.6a}$$

$$\psi^r_{ds} = -X_{ls} i^r_{ds} + X_{md}(-i^r_{ds} + i^{'r}_{fd} + i^{'r}_{kd}) \tag{2.6b}$$

$$\psi_{0s} = -X_{ls} i_{0s} \tag{2.6c}$$

$$\psi^{'r}_{fd} = X'_{lfd} i^{'r}_{fd} + X_{md}(-i^r_{ds} + i^{'r}_{fd} + i^{'r}_{kd}) \tag{2.6d}$$

$$\psi^{'r}_{kd} = X'_{lkd} i^{'r}_{kd} + X_{md}(-i^r_{ds} + i^{'r}_{fd} + i^{'r}_{kd}) \tag{2.6e}$$

$$\psi^{'r}_{kq1} = X'_{lkq1} i^{'r}_{kq1} + X_{mq}(-i^r_{qs} + i^{'r}_{kq1} + i^{'r}_{kq2}) \tag{2.6f}$$

$$\psi^{'r}_{kq2} = X'_{lkq2} i^{'r}_{kq2} + X_{mq}(-i^r_{qs} + i^{'r}_{kq1} + i^{'r}_{kq2}) \tag{2.6g}$$

To continue the description, it is convenient to define several reactances of the machine. The d- and q-axis reactances are expressed:

$$X_d \triangleq X_{ls} + X_{md} \tag{2.7a}$$

$$X_q \triangleq X_{ls} + X_{mq} \tag{2.7b}$$

The d- and q-axis transient reactances are expressed:

$$X'_d \triangleq X_{ls} + \frac{1}{\frac{1}{X_{md}} + \frac{1}{X'_{lfd}}} \tag{2.8a}$$

$$X'_q \triangleq X_{ls} + \frac{1}{\frac{1}{X_{mq}} + \frac{1}{X'_{lkq}}} \tag{2.8b}$$

Finally, the d- and q-axis subtransient reactances are expressed:

$$X''_d \triangleq X_{ls} + \frac{1}{\frac{1}{X_{md}} + \frac{1}{X'_{lfd}} + \frac{1}{X'_{lkd}}} \tag{2.9a}$$

$$X''_q \triangleq X_{ls} + \frac{1}{\frac{1}{X_{mq}} + \frac{1}{X'_{lkq1}} + \frac{1}{X'_{lkq2}}} \tag{2.9b}$$

The transient and subtransient time constants are defined as:

$$T'_{do} \triangleq \frac{X'_{lfd}}{\omega_e r'_{fd}} \tag{2.10a}$$

$$T'_{qo} \triangleq \frac{X'_{lkq1}}{\omega_e r'_{kq1}} \tag{2.10b}$$

$$T''_{do} \triangleq \frac{1}{\omega_e r'_{kd}} \left(X'_{lkd} + \frac{1}{\frac{1}{X_{md}} + \frac{1}{X'_{lfd}}} \right) \tag{2.10c}$$

$$T''_{qo} \triangleq \frac{1}{\omega_e r'_{kq2}} \left(X'_{lkq2} + \frac{1}{\frac{1}{X_{mq}} + \frac{1}{X'_{lkq1}}} \right) \tag{2.10d}$$

Finally, three additional variables associated with the rotor windings are defined:

$$E'_q \triangleq \frac{X_{md}}{X'_{lfd}}\psi'^r_{fd} \tag{2.11a}$$

$$E'_{fd} \triangleq \frac{X_{md}}{r'_{fd}}V'^r_{fd} \tag{2.11b}$$

$$E'_d \triangleq -\frac{X_{mq}}{X'_{lkq1}}\psi'^r_{kq1} \tag{2.11c}$$

These are substituted into (2.5) and (2.6), and the result rearranged to establish a final detailed model:

$$\frac{1}{\omega_e}p\psi^r_{qs} = r_s i^r_{qs} - \frac{\omega_r}{\omega_e}\psi^r_{ds} + v^r_{qs} \tag{2.12a}$$

$$\frac{1}{\omega_e}p\psi^r_{ds} = r_s i^r_{ds} + \frac{\omega_r}{\omega_e}\psi^r_{qs} + v^r_{ds} \tag{2.12b}$$

$$\frac{1}{\omega_e}p\psi_{0s} = r_s i_{0s} + v_{0s} \tag{2.12c}$$

$$T'_{qo}pE'_d = -E'_d + (X_q - X'_q)[i^r_{qs} - \frac{X'_q - X''_q}{(X'_q - X_{ls})^2}(\psi'^r_{kq2} + (X'_q - X_{ls})i^r_{qs} + E'_d)] \tag{2.12d}$$

$$T''_{qo}p\psi'^r_{kq2} = -\psi'^r_{kq2} - E'_d - (X'_q - X_{ls})i^r_{qs} \tag{2.12e}$$

$$T'_{do}pE'_q = -E'_q - (X_d - X'_d)[i^r_{ds} - \frac{X'_d - X''_d}{(X'_d - X_{ls})^2}(\psi'^r_{kd} + (X'_d - X_{ls})i^r_{ds} - E'_q)] + E'_{fd} \tag{2.12f}$$

$$T''_{do}p\psi'^r_{kd} = -\psi'^r_{kd} + E'_q - (X'_d - X_{ls})i^r_{ds} \tag{2.12g}$$

$$p\delta = \omega_r - \omega_e \tag{2.12h}$$

$$J\frac{2}{P}p\omega_r = T_M - T_e \tag{2.12i}$$

$$T_e = \frac{3}{2}\frac{P}{2}\frac{1}{\omega_e}(\psi^r_{ds}i^r_{qs} - \psi^r_{qs}i^r_{ds}) \tag{2.12j}$$

where δ is the rotor angle with respect to the synchronous reference frame, J is the rotor inertia, T_e is the electromagnetic torque, P is the number of poles of the machine, T_M is the mechanical torque, and p is the $\frac{d}{dt}$ operator.

This model can be expressed in a per-unit form:

$$\frac{1}{\omega_e}p\psi^r_{qs} = r_s i^r_{qs} - \frac{\omega_r}{\omega_e}\psi^r_{ds} + v^r_{qs} \tag{2.13a}$$

$$\frac{1}{\omega_e}p\psi^r_{ds} = r_s i^r_{ds} + \frac{\omega_r}{\omega_e}\psi^r_{qs} + v^r_{ds} \tag{2.13b}$$

$$\frac{1}{\omega_e}p\psi_{0s} = r_s i_{0s} + v_{0s} \tag{2.13c}$$

$$T'_{qo}pE'_d = -E'_d + (X_q - X'_q)[i^r_{qs} - \frac{X'_q - X''_q}{(X'_q - X_{ls})^2}(\psi^{'r}_{kq2} + (X'_q - X_{ls})i^r_{qs} + E'_d)] \tag{2.13d}$$

$$T''_{qo}p\psi^{'r}_{kq2} = -\psi^{'r}_{kq2} - E'_d - (X'_q - X_{ls})i^r_{qs} \tag{2.13e}$$

$$T'_{do}pE'_q = -E'_q - (X_d - X'_d)[i^r_{ds} - \frac{X'_d - X''_d}{(X'_d - X_{ls})^2}(\psi^{'r}_{kd} + (X'_d - X_{ls})i^r_{ds} - E'_q)] + E'_{fd} \tag{2.13f}$$

$$T''_{do}p\psi^{'r}_{kd} = -\psi^{'r}_{kd} + E'_q - (X'_d - X_{ls})i^r_{ds} \tag{2.13g}$$

$$p\delta = \omega_r - \omega_e \tag{2.13h}$$

$$\frac{2H}{\omega_e}p\omega_r = T_M - T_e \tag{2.13i}$$

$$T_e = \psi^r_{ds}i^r_{qs} - \psi^r_{qs}i^r_{ds} \tag{2.13j}$$

The per-unitization assumes that base voltage is the peak value of the rated phase voltage, base power is the machine volt-ampere rating, and base rotor angular velocity is ω_e=377 rad/s. The corresponding current base, torque base and impedance base is calculated from the base voltage, power, and angular velocity. These are then used to rewrite (2.12a)- (2.12g), to form (2.13a)-(2.12g). For the rotor mechanical dynamics, (2.12i)-(2.12j), the base torque is first expressed:

$$T_B = \frac{P_B}{(2/P)\omega_e} \tag{2.14}$$

Subsequently, (2.12i) is expressed in terms of per-unit values of speed and torque, which yields the inertia constant defined as:

$$H = \left(\frac{1}{2}\right)\left(\frac{2}{P}\right)\frac{J\omega_e}{T_B} = \left(\frac{1}{2}\right)\left(\frac{2}{P}\right)^2\frac{J\omega_e^2}{P_B} \tag{2.15}$$

Equations (2.13a)-(2.13j) represents the state model of the synchronous machine. Within the machine detailed model, the following expressions are used to relate winding currents to the states:

$$i_{qs}^r = \frac{1}{X_q''}(-\psi_{qs}^r - \frac{X_q'' - X_{ls}}{X_q' - X_{ls}}E_d' + \frac{X_q' - X_q''}{X_q' - X_{ls}}\psi_{kq2}^{'r}) \tag{2.16a}$$

$$i_{ds}^r = \frac{1}{X_d''}(-\psi_{ds}^r + \frac{X_d'' - X_{ls}}{X_d' - X_{ls}}E_q' + \frac{X_d' - X_d''}{X_d' - X_{ls}}\psi_{kd}^{'r}) \tag{2.16b}$$

$$i_{0s} = -\frac{1}{X_{ls}}\psi_{0s} \tag{2.16c}$$

$$i_{kq2}^{'r} = \frac{X_q' - X_q''}{(X_q' - X_{ls})^2}[\psi_{kq2}^{'r} + (X_q' - X_{ls})i_{qs}^r + E_d'] \tag{2.16d}$$

$$i_{kq1}^{'r} = \frac{1}{X_{mq}}[-E_d' + (X_q - X_q')(i_{qs}^r - i_{kq2}^{'r})] \tag{2.16e}$$

$$i_{kd}^{'r} = \frac{X_d' - X_d''}{(X_d' - X_{ls})^2}[\psi_{kd}^{'r} + (X_d' - X_{ls})i_{ds}^r + E_q'] \tag{2.16f}$$

$$i_{fd}^{'r} = \frac{1}{X_{md}}[E_q' + (X_d - X_d')(i_{ds}^r - i_{kd}^{'r})] \tag{2.16g}$$

The active and reactive power are also calculated in per-unit using:

$$P = v_{qs}^r i_{qs}^r + v_{ds}^r i_{ds}^r + 2v_{0s}^r i_{0s}^r \tag{2.17a}$$

$$Q = v_{qs}^r i_{ds}^r - v_{ds}^r i_{qs}^r \tag{2.17b}$$

2.3.2 Generator Exciter system

The exciter model used comes from [6]. A block diagram of the exciter model is shown in Figure 2.3. The output of the exciter system is the field winding voltage E_{fd}', which labeled as v_f in Figure 2.3. The field winding voltage value is expected to be 1 per-unit when the generator operates unloaded at rated speed with a 1 per-unit terminal voltage.

The control input to the exciter model is the V_0 in Figure 2.3, which is used to control the stator terminal voltage magnitude of the synchronous machine. By

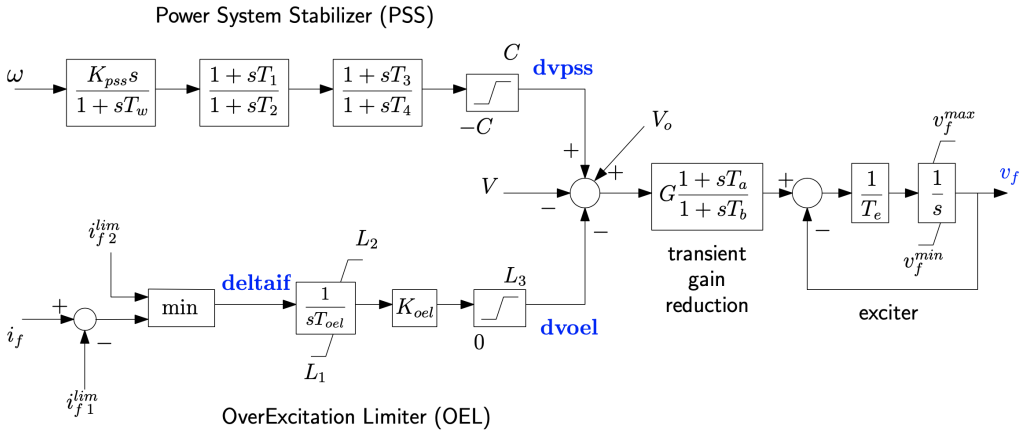

Fig. 2.3.: Exciter System

using the measured machine stator terminal phase voltage magnitude, labeled as V, a relation among E'_{fd}, V_0 and V can be expressed under steady state:

$$E'_{fd} = G(V - V_0)\frac{T_a}{T_b} \tag{2.18}$$

The control described in (2.18) is commonly referred as an Automatic Voltage Regulator(AVR), which is used to control the field winding voltage value based on the measured machine stator terminal voltage. In Figure 2.3, also shown are the control sections in the top part of the figure labeled *Power System Stabilizer (PSS)*, *transient gain reduction*, and another control section in the bottom part of the figure labeled *OverExcitation Limiter (OEL)*,which is related to the field winding current limit.

To briefly explain the OEL, i_{fd}^{lim1} is the field current limit that is established by the generator manufacturer. Under normal operation, if the field current, labeled i_f in Figure 2.3, is lower than the field current limit, a negative value is input into the *min* block. Since i_{fd}^{lim2} is a positive number, a negative signal of $i_f - i_{fd}^{lim1}$ results as an inmput to the integrator. Since the output of the OEL is bounded between 0 to L_3, the output of the OEL is then 0 under normal operation. However, when the field current exceeds i_{fd}^{lim1}, the signal that goes to the OEL integrator is based on the *min*

gate. In the end, the more the field current exceeds the limit, the higher the output of the OEL will be.

The transient gain reduction is used to limit the overshoot in the terminal voltage following a step disturbance. The Bode response of this block is shown in Figure 2.4. If the frequency of the input signal to the block is greater than 1Hz, the output is reduced by 8 dB. Otherwise the gain is fixed at G. Thus, any low frequency disturbances receive greater response compared to high frequency disturbances.

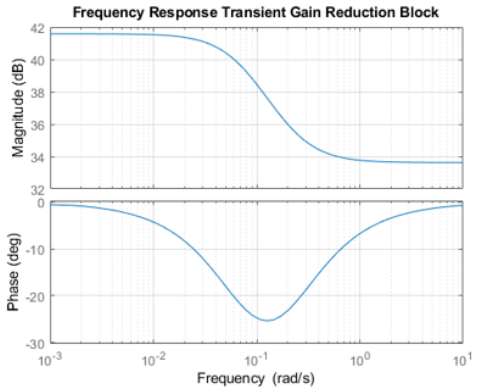

Fig. 2.4.: Frequency Response for Transient Gain Reduction Block

The PSS uses rotor electrical speed ω_r as an input. It includes a high pass filter and two identical lead filters in cascade. The overall PSS transfer function is shown in Figure 2.5. As shown, it filters signals at very low frequencies (below 0.01 rad/s) while providing significant gain to signals above 100 rad/s.

2.3.3 Governor System

The governor model system is a steam turbine based model, shown in Figure 2.6. It also comes from [11]. In the bottom half of the figure, one can observe that the steam turbine is divided into three different pressure stages (labeled LP, MP, HP) which add to yield commanded mechanical torque.

From the top of Figure 2.6 one can observe that the model accepts the rotor mechanical speed (shown as ω) and desired generator electrical power (shown as P_o)

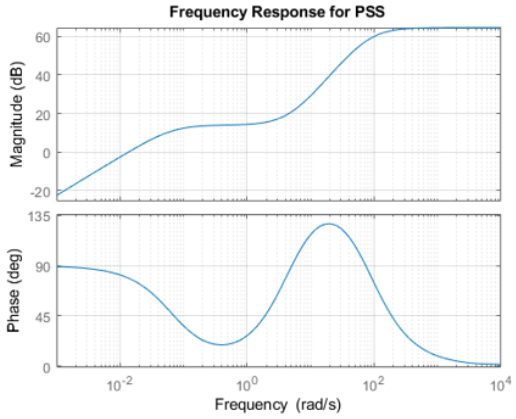

Fig. 2.5.: Frequency Response for Power System Stabilizer

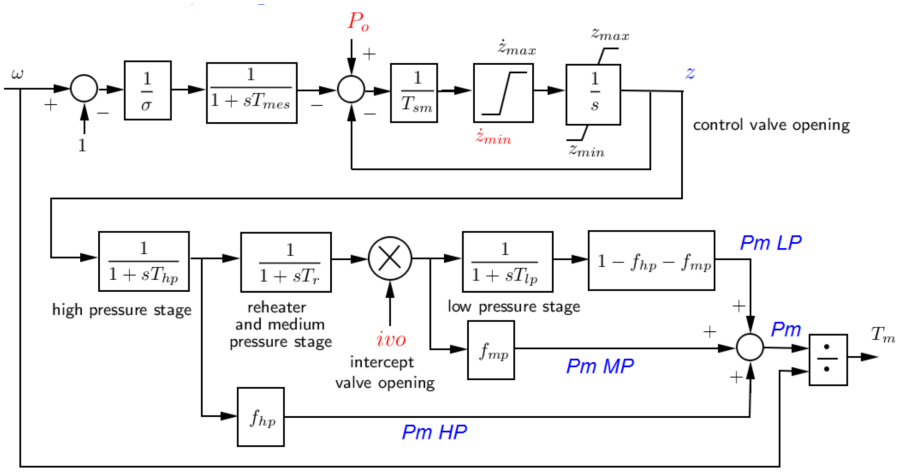

Fig. 2.6.: Governor System

as inputs. The valve open z is added to the speed error. This results in a droop-type of action between power and speed. Specifically, assuming steady-state, one can assume the input to the valve opening integrator is 0. Under this condition, one can express

$$z = P_o + \frac{1-\omega}{\sigma} \tag{2.19}$$

Assuming no loss in the mechanical system, it can be shown that $T_m = z = P_o$. As speed varies away from 1, the load torque varies from the commanded power.

2.3.4 Detailed Generator/Infinite Bus Implementation

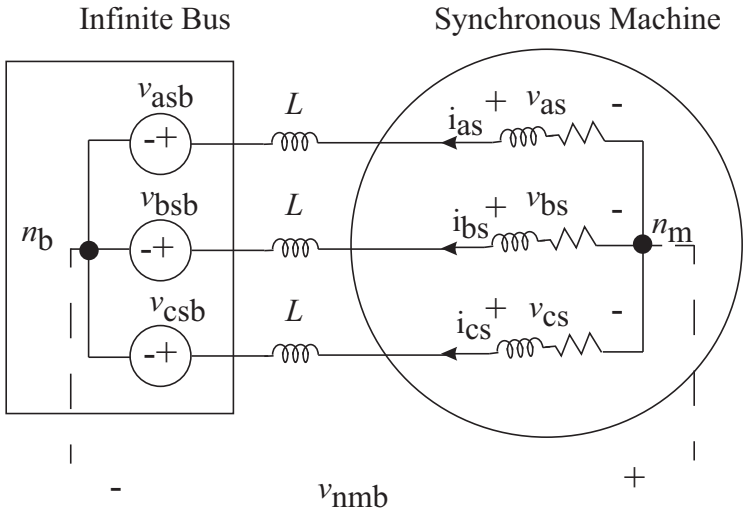

Fig. 2.7.: Detailed Generator/Infinite Bus Implementation

With the infinite bus and the generation system described, a simple system including an infinite bus and a generator can be readily developed, shown in Figure 2.7. Such a system is often used for the purpose of generator stability studies and excitation/governor control design. In subsequent behavioral model development, this system is used for model derivation and characterization. Hence, a Simulink model of an infinite/bus generator has been constructed. The Simulink model of the generator accepts as inputs the qd stator terminal voltage expressed in the rotor reference frame, the load torque (from the governor model) and the field voltage excitation E'_{fd} (from the excitation system model). In addition to the states, the simulation is used to solve for field winding current, d- and q-axis stator currents, electromagnetic torque, rotor angular velocity, rotor angle, active and reactive power and the terminal voltage magnitude. The machine is connected to the infinite bus through a 0.15 per-unit series reactance X. This enables implementation of the Exciter system to control the machine terminal voltage (machine terminal voltage magnitude would be the infinite bus voltage without this reactance).

Within the Simulink model, the series reactance is incorporated within the synchronous machine model by adding its value to the leakage reactance of each phase. From the definition of the parameters in (2.9) and (2.8), it can be shown that equation (2.13) does not need to change with the addition of the series reactance, since the terms involving the parameters of the wound-rotor machine do not rely on its leakage inductance. However, it is important to note that the stator voltage and stator flux linkage per second in (2.8) is influence by the series reactance since the lumped leakage reactance is the infinite-bus voltage and the total flux linkage per second after including the series reactance. Hence, in addition to use the equation (2.13) to calculate the states variables, further calculation is needed for the calculation of the machine terminal voltage and stator flux linkage per second.

The infinite bus voltage is expressed:

$$\theta_e = \omega_e t \tag{2.20}$$

$$v_{abcsb} = \begin{pmatrix} V_i \cos(\theta_e) \\ V_i \cos(\theta_e - \frac{2\pi}{3}) \\ V_i \cos(\theta_e + \frac{2\pi}{3}) \end{pmatrix} \tag{2.21}$$

where V_i is the peak voltage of the infinite bus and

$$\theta_e = \omega_e t \tag{2.22}$$

Using Kirchhoff's law around the loop from nb to nm the relationship between the infinite bus voltage and the machine terminal voltage can be expressed:

$$v_{abcsb} = -\frac{X}{\omega_e}\frac{di_{abcs}}{dt} + v_{abcs} + \begin{pmatrix} 1 \\ 1 \\ 1 \end{pmatrix} v_{nmb} \tag{2.23}$$

Transforming (2.23) and (2.21) to the rotor reference frame yields:

$$v^r_{qsb} = -\frac{X}{\omega_e}\frac{di^r_{qs}}{dt} - \omega_r\frac{X}{\omega_e}i^r_{ds} + v^r_{qs} \tag{2.24a}$$

$$v^r_{dsb} = -\frac{X}{\omega_e}\frac{di^r_{ds}}{dt} + \omega_r\frac{X}{\omega_e}i^r_{qs} + v^r_{ds} \tag{2.24b}$$

$$v_{0sb} = -\frac{X}{\omega_e}\frac{di_{0s}}{dt} + v_{0s} + v_{nmb} \tag{2.24c}$$

As shown in the equation (2.64), the derivatives of the generator stator currents are needed for the calculation of the generator stator voltage. The derivatives can be calculated based on equation (2.16) by using the derivative operator $\frac{d}{dt}$ on both sides.

$$pi^r_{qs} = \frac{1}{X''_q}(-p\psi^r_{qs} - \frac{X''_q - X_{ls}}{X'_q - X_{ls}}pE'_d + \frac{X'_q - X''_q}{X'_q - X_{ls}}p\psi'^r_{kq2}) \tag{2.25a}$$

$$pi^r_{ds} = \frac{1}{X''_d}(-p\psi^r_{ds} + \frac{X''_d - X_{ls}}{X'_d - X_{ls}}pE'_q + \frac{X'_d - X''_d}{X'_d - X_{ls}}p\psi'^r_{kd}) \tag{2.25b}$$

$$pi_{0s} = -\frac{1}{X_{ls}}p\psi_{0s} \tag{2.25c}$$

Where $p = \frac{d}{dt}$ and all the terms on the right hand sides with p are the states and their derivatives are calculated based on the equation (2.13).

In addition, it is assumed the machine windings are balanced and wye-connected, in which case one can show that $v_{nmb} = 0$. These steps enable one to express the transformed stator phase voltages in terms of the infinite bus voltage as:

$$v^r_{qsb} = V_i\cos(\delta) \tag{2.26a}$$

$$v^r_{dsb} = V_i\sin(\delta) \tag{2.26b}$$

$$v_{0sb} = 0 \tag{2.26c}$$

Simulink Implementation

The overall implementation of the generator/infinite bus in Simulink is shown in Figure 2.8. At the **source** function block, the infinite bus voltage v^r_{qd0sb} in the rotor frame of reference is calculated using (2.26) and where the angle difference is the state variable δ.

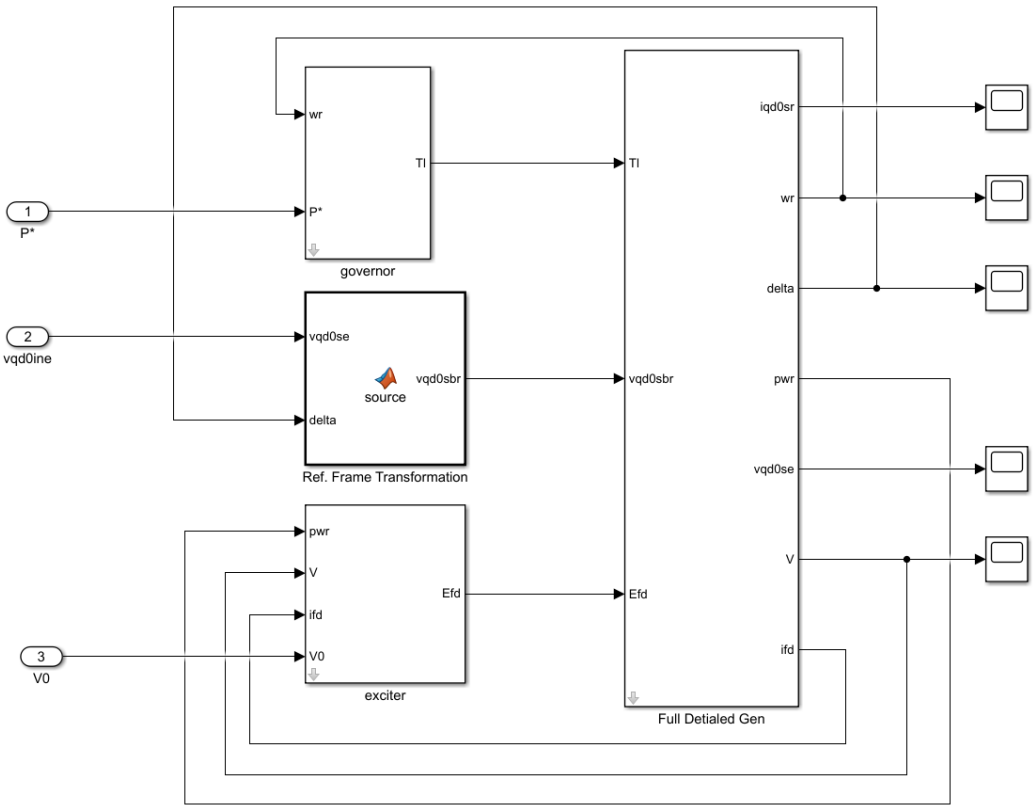

Fig. 2.8.: Detailed Generator/Infinite Bus System Simulink Implementation

Inside the **governor** block and **exciter** block, the dynamics of the governor and exciters are implemented. The implementation of the governor dynamics are shown in Figure 2.9, Figure 2.10 and Figure 2.11; the implementation of the exciter dynamics are shown in Figure 2.12, Figure 2.13 and Figure 2.14.

Inside the **Full Detailed Gen** block, the dynamics of the generator are implemented, which is shown in Figure 2.15.

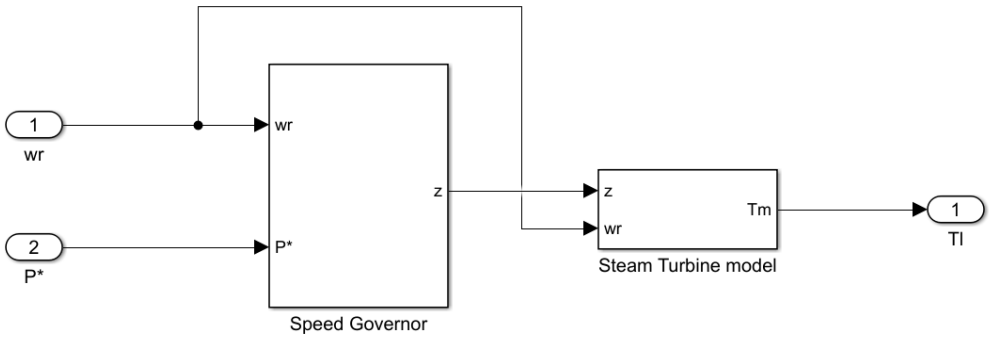

Fig. 2.9.: Governor Simulink Implementation

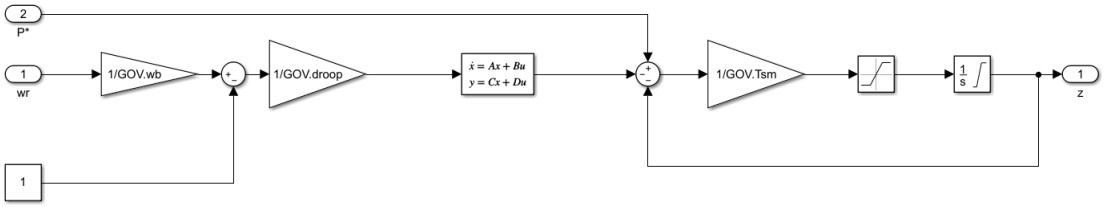

Fig. 2.10.: Speed Governor Simulink Implementation

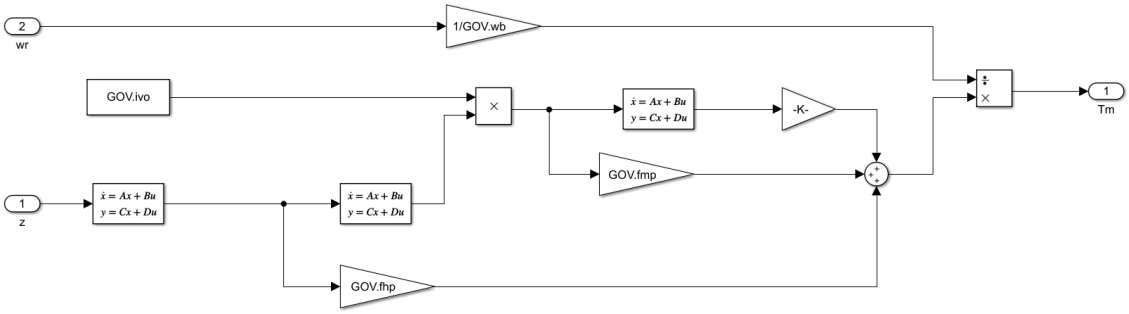

Fig. 2.11.: Steam Turbines Simulink Implementation

In the **ElectricalDynamics** and **MechanicalDynamics** function block,(2.13) are implemented. In the **Current** function block, (2.16) are used to calculate the stator and damper windings currents. In the **Additional Info** block, shown in Figure 2.16. In the **Voltage** function block, the machine voltage is calculated using (2.24).

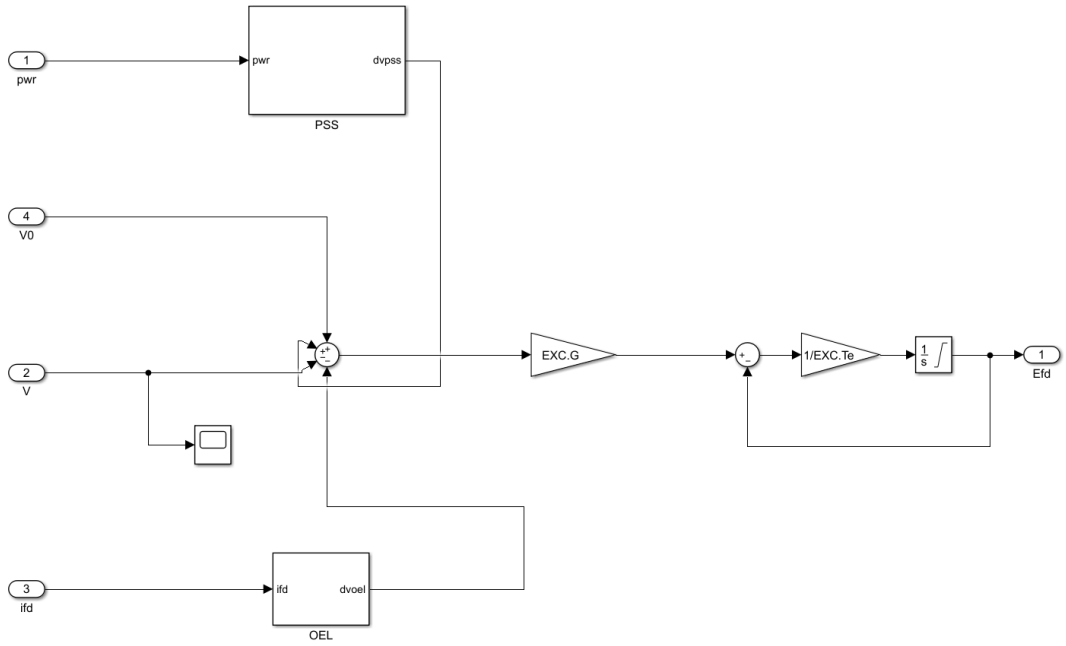

Fig. 2.12.: Exciter Simulink Implementation

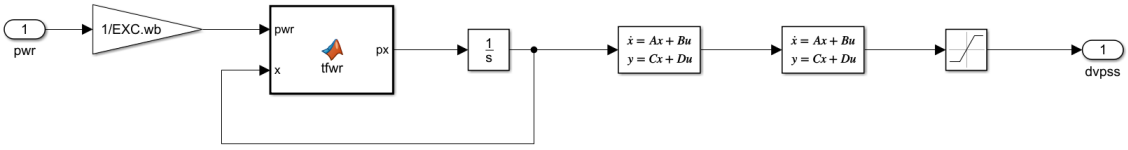

Fig. 2.13.: PSS Simulink Implementation

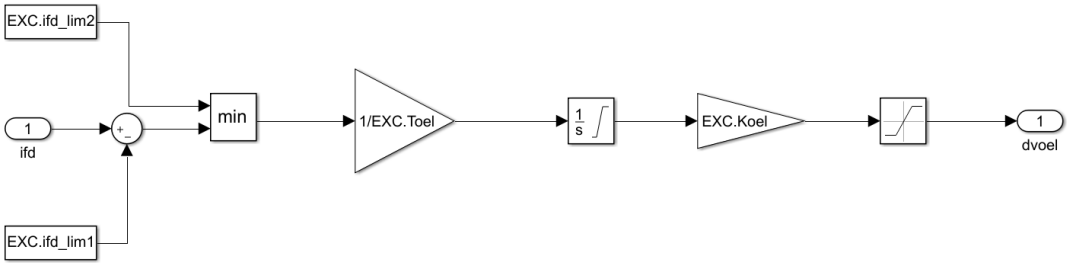

Fig. 2.14.: OEL Simulink Implementation

In the **synchV** function block, the stator terminal voltage is transformed back to the synchronous reference frame for the bus information calculation.

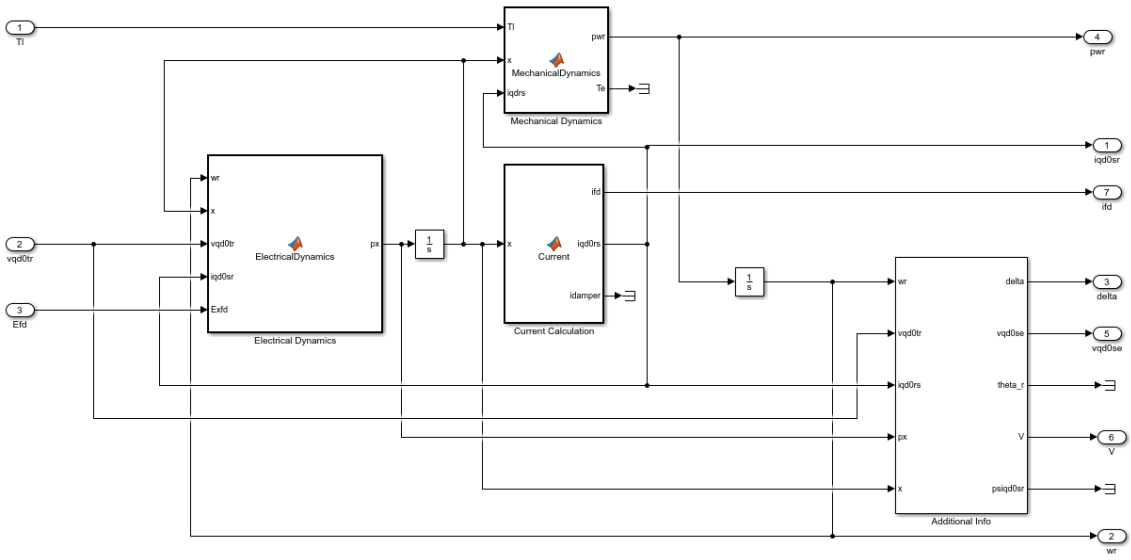

Fig. 2.15.: Generator Simulink Implementation

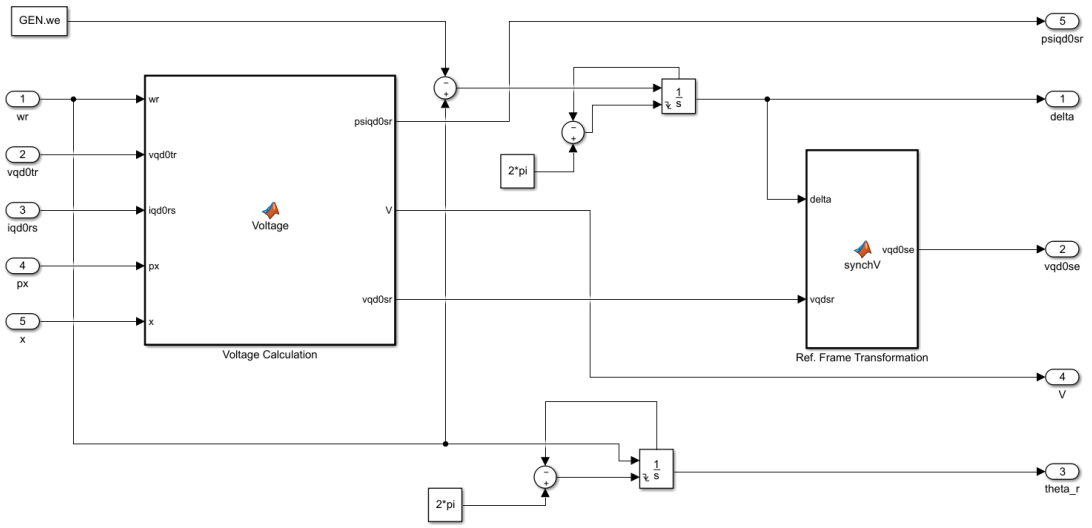

Fig. 2.16.: Generator Subblock Simulink Implementation

2.4 Load Model

2.4.1 Constant RC Load

The constant impedance load modeled in this section is a three phase symmetrical wye-connected series RC load. In the physical *abc* variable representation, the equations:

$$\mathbf{v}_{abcLoad} = \mathbf{R}\mathbf{i}_{abcR} + \mathbf{v}_{abcC} \tag{2.27a}$$

$$\mathbf{i}_{abcC} = \mathbf{C}p\mathbf{v}_{abcC} \tag{2.27b}$$

are used to relate load voltage and current. In (2.27), the $\mathbf{v}$ and $\mathbf{i}$ are vectors of voltage and current, respectively. The variable p is the d/dt operator, and $\mathbf{R}$ and $\mathbf{C}$ are three-by-three square diagonal matrices with diagonal entries R and C. The load model can be transformed to the synchronous reference frame using the transformation (B.3), resulting in:

$$v^e_{qload} = i^e_{qR}R + v^e_{qC} \tag{2.28a}$$

$$v^e_{dload} = i^e_{dR}R + v^e_{dC} \tag{2.28b}$$

$$v^e_{0load} = i^e_{0R}R + v^e_{0C} \tag{2.28c}$$

where

$$pv^e_{qC} = \frac{i^e_{qC}}{C} - \omega_e v^e_{dC} \tag{2.29a}$$

$$pv^e_{dC} = \frac{i^e_{dC}}{C} + \omega_e v^e_{qC} \tag{2.29b}$$

$$pv^e_{0C} = \frac{i^e_{0C}}{C} \tag{2.29c}$$

In (2.29), the currents with subscript C are the capacitor currents. Since the load is series connected, then $\mathbf{i}_{qd0R} = \mathbf{i}_{qd0C} = \mathbf{i}_{qd0RC}$.

Simulink Implementation

For the constant admittance, with the load currents given, the load voltages can be calculated using (2.28). The Simulink diagram is shown in Figure 2.17.

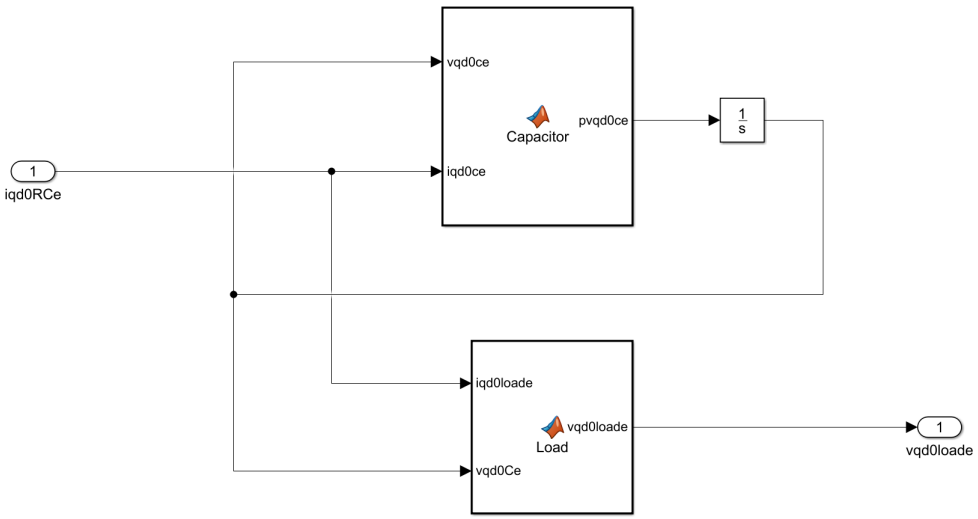

Fig. 2.17.: Constant Admittance Simulink Implementation

2.4.2 Detailed Induction Machine Model

The induction machine model used is derived in [8] based upon the cross section of the two-pole, three-phase, wye-connected symmetrical induction machine shown in Figure 2.18. Similar to the synchronous generator described in Section 2.3, the relationship between winding current, magnetic flux, and voltage is used to express the ODEs used to predict machine performance. The ODEs expressed in the *abc* variables are described in detail in [8] starting from page 216. Since the model used in this work is all based on reference-frame theory, the ODEs in machine *abc* variables are not discussed here. Rather, the common $qd0$ representation of the induction machine in the synchronous reference frame is expressed in (2.30).

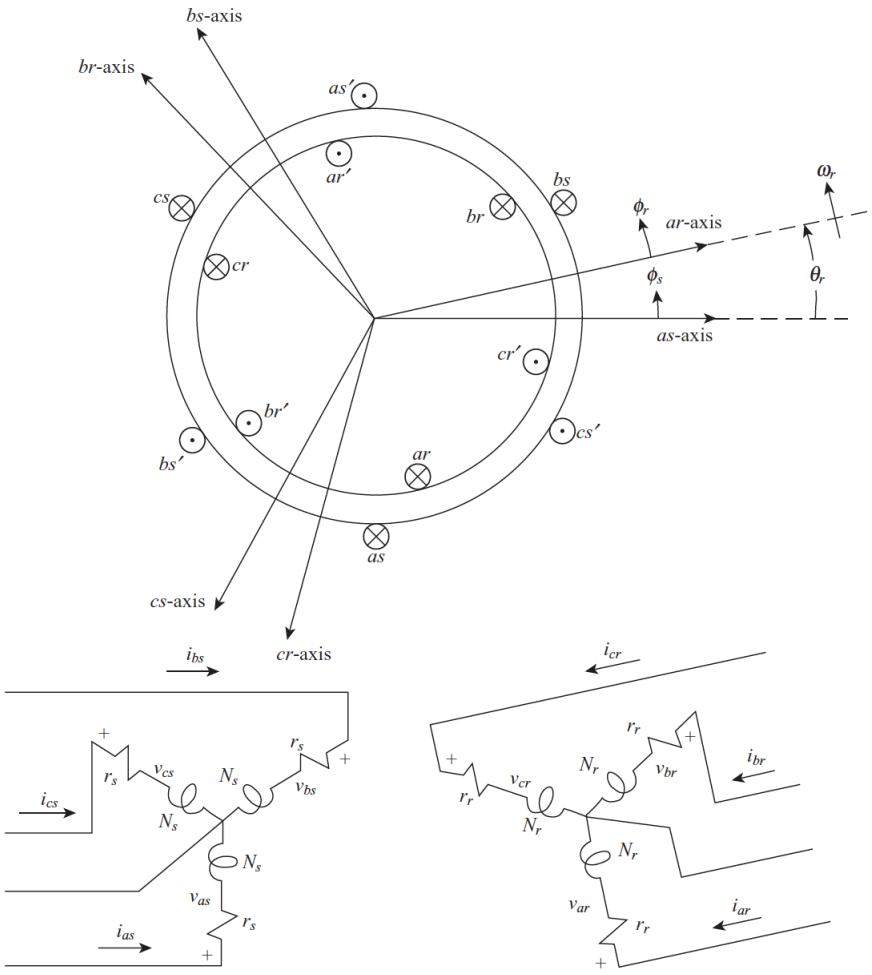

Fig. 2.18.: Two-pole, Three-phase, Wye-connected Symmetrical Induction Machine

$$v_{qs}^{e} = r_s i_{qs}^{e} + \omega_e \lambda_{ds}^{e} + \frac{d\lambda_{qs}^{e}}{dt} \tag{2.30a}$$

$$v_{ds}^{e} = r_s i_{ds}^{e} - \omega_e \lambda_{qs}^{e} + \frac{d\lambda_{ds}^{e}}{dt} \tag{2.30b}$$

$$v_{0s} = r_s i_{0s} + \frac{d\lambda_{0s}}{dt} \tag{2.30c}$$

$$v_{qr}^{'e} = r_r' i_{qr}^{'e} + (\omega_e - \omega_r)\lambda_{dr}^{'e} + \frac{d\lambda_{qr}^{'e}}{dt} \tag{2.30d}$$

$$v_{dr}^{'r} = r_r' i_{dr}^{'e} - (\omega_e - \omega_r)\lambda_{qr}^{'e} + \frac{d\lambda_{dr}^{'e}}{dt} \tag{2.30e}$$

$$v_{0r}^{'} = r_r' i_{0r}^{'} + \frac{d\lambda_{0r}^{'}}{dt} \tag{2.30f}$$

where v is used to represent respective winding voltage, r winding resistance, ω_e is the synchronous electrical angular velocity from the infinite bus, and ω_r is the rotor electrical angular velocity. The variable λ is used for winding flux linkage. The winding flux linkages can be expressed in terms of winding currents using (2.31):

$$\lambda^e_{qs} = L_{ls} i^e_{qs} + L_M (i^e_{qs} + i^{'e}_{qr}) \tag{2.31a}$$

$$\lambda^e_{ds} = L_{ls} i^e_{ds} + L_M (i^e_{ds} + i^{'e}_{dr}) \tag{2.31b}$$

$$\lambda_{0s} = L_{ls} i_{0s} \tag{2.31c}$$

$$\lambda^{'e}_{qr} = L'_{lr} i^{'e}_{qr} + L_M (i^e_{qs} + i^{'e}_{qr}) \tag{2.31d}$$

$$\lambda^{'e}_{dr} = L'_{lr} i^{'e}_{dr} + L_M (i^e_{ds} + i^{'e}_{dr}) \tag{2.31e}$$

$$\lambda^{'}_{0r} = L'_{lr} i^{'}_{0r} \tag{2.31f}$$

Subscripts s and r refer to stator and rotor quantities respectively. The superscript e is used to indicate the variables are in the synchronous frame of reference, and the prime $'$ is used to indicate that the respective winding is referred to the stator winding through an appropriate turns ratio. The inductances in (2.31) with a subscript l are leakage values of the respective winding while those with a subscript M magnetizing values. Since the parameters of the induction machine are often provided in terms of reactances rather than inductances, it is convenient to multiply (2.30) and (2.31) on both sides by a base angular velocity ω_e and express the result in equations (2.32):

$$\omega_e v^e_{qs} = \omega_e r_s i^e_{qs} + \omega_e \psi^e_{ds} + p\psi^e_{qs} \tag{2.32a}$$

$$\omega_e v^e_{ds} = \omega_e r_s i^e_{ds} - \omega_e \psi^e_{qs} + p\psi^e_{ds} \tag{2.32b}$$

$$\omega_e v_{0s} = \omega_e r_s i_{0s} + p\psi_{0s} \tag{2.32c}$$

$$\omega_e v^{'e}_{qr} = \omega_e r'_r i^{'e}_{qr} + (\omega_e - \omega_r)\psi^{'e}_{dr} + p\psi^{'e}_{qr} \tag{2.32d}$$

$$\omega_e v^{'r}_{dr} = \omega_e r'_r i^{'e}_{dr} - (\omega_e - \omega_r)\psi^{'e}_{qr} + p\psi^{'e}_{dr} \tag{2.32e}$$

$$\omega_e v^{'}_{0r} = \omega_e r'_r i^{'}_{0r} + p\psi^{'}_{0r} \tag{2.32f}$$

Where p is the $\frac{d}{dt}$ operator and:

$$\psi^e_{qs} = X_{ls} i^e_{qs} + X_M (i^e_{qs} + i^{'e}_{qr}) \tag{2.33a}$$

$$\psi^e_{ds} = X_{ls} i^e_{ds} + X_M (i^e_{ds} + i^{'e}_{dr}) \tag{2.33b}$$

$$\psi_{0s} = X_{ls} i_{0s} \tag{2.33c}$$

$$\psi^{'e}_{qr} = X'_{lr} i^{'e}_{qr} + X_M (i^e_{qs} + i^{'e}_{qr}) \tag{2.33d}$$

$$\psi^{'e}_{dr} = X'_{lr} i^{'e}_{dr} + X_M (i^e_{ds} + i^{'e}_{dr}) \tag{2.33e}$$

$$\psi^{'}_{0r} = X'_{lr} i^{'}_{0r} \tag{2.33f}$$

In (2.33), the currents can be readily calculated using (2.34).

$$i^e_{qs} = \frac{1}{X_{ls}} (\psi^e_{qs} - \psi^e_{mq}) \tag{2.34a}$$

$$i^e_{ds} = \frac{1}{X_{ls}} (\psi^e_{ds} - \psi^e_{md}) \tag{2.34b}$$

$$i_{0s} = \frac{1}{X_{ls}} \psi_{0s} \tag{2.34c}$$

$$i^{'e}_{qr} = \frac{1}{X'_{lr}} (\psi^{'e}_{qr} - \psi^e_{mq}) \tag{2.34d}$$

$$i^{'e}_{dr} = \frac{1}{X'_{lr}} (\psi^{'e}_{dr} - \psi^e_{md}) \tag{2.34e}$$

$$i_{0r} = \frac{1}{X'_{lr}} \psi^{'}_{0r} \tag{2.34f}$$

where ψ^e_{mq} and ψ^e_{md} are defined as:

$$\psi^e_{mq} \triangleq X_M (i^e_{qs} + i^{'e}_{qr}) \tag{2.35a}$$

$$\psi^e_{md} \triangleq X_M (i^e_{ds} + i^{'e}_{dr}) \tag{2.35b}$$

It is useful to express ψ^e_{mq} and ψ^e_{md} in terms of the states in the equations (2.32) and the reactances for Simulink implementation:

$$\psi^e_{mq} = X_{aq}(\frac{\psi^e_{qs}}{X_{ls}} + \frac{\psi'^e_{qr}}{X'_{lr}}) \tag{2.36a}$$

$$\psi^e_{md} = X_{ad}(\frac{\psi^e_{ds}}{X_{ls}} + \frac{\psi'^e_{dr}}{X'_{lr}}) \tag{2.36b}$$

where

$$X_{aq} = X_{ad} \triangleq (\frac{1}{X_M} + \frac{1}{X_{ls}} + \frac{1}{X'_{lr}})^{-1} \tag{2.37}$$

With ψ^e_{mq} and ψ^e_{md}, (2.32) can be readily written in a form:

$$p\psi^e_{qs} = \omega_e[v^e_{qs} - \psi^e_{ds} + \frac{r_s}{X_{ls}}(\psi^e_{mq} - \psi^e_{qs})] \tag{2.38a}$$

$$p\psi^e_{ds} = \omega_e[v^e_{ds} + \psi^e_{qs} + \frac{r_s}{X_{ls}}(\psi^e_{md} - \psi^e_{ds})] \tag{2.38b}$$

$$p\psi_{0s} = \omega_e[v_{0s} - \frac{r_s}{X_{ls}}\psi_{0s}] \tag{2.38c}$$

$$p\psi'^e_{qr} = \omega_e[v'^e_{qr} - \frac{\omega_e - \omega_r}{\omega_e}\psi'^e_{dr} + \frac{r'_r}{X'_{lr}}(\psi^e_{mq} - \psi'^e_{qr})] \tag{2.38d}$$

$$p\psi'^e_{dr} = \omega_e[v'^e_{dr} + \frac{\omega_e - \omega_r}{\omega_e}\psi'^e_{qr} + \frac{r'_r}{X'_{lr}}(\psi^e_{md} - \psi'^e_{dr})] \tag{2.38e}$$

$$p\psi_{0r} = \omega_e[v'_{0r} - \frac{r'_r}{X'_{lr}}\psi'_{0r}] \tag{2.38f}$$

The rotor dynamics of the machine can be expressed using:

$$J\frac{2}{P}\frac{d\omega_r}{dt} = T_M - T_e \tag{2.39a}$$

where J is the rotor inertia, P the number of poles, T_M the mechanical torque, and T_e the electromagnetic torque that can be expressed in terms of stator flux linkages and currents as:

$$T_e = \frac{3}{2}\frac{P}{2}\frac{1}{\omega_e}(\psi^e_{ds}i^e_{qs} - \psi^e_{qs}i^e_{ds}) \tag{2.40}$$

The induction machine implemented within the power system is in per-unit. The per-unitization applied assumes that base voltage is the peak value of the rated phase voltage, base power is the machine volt-ampere rating, and base rotor angular velocity is ω_e=377 rad/s. The corresponding current base, torque base and impedance base is calculated from the base voltage, power, and angular velocity. To apply to the rotor mechanical dynamics in (2.39), the base torque is first expressed:

$$T_B = \frac{P_B}{(2/P)\omega_e} \tag{2.41}$$

Subsequently, (2.39) is expressed in terms of per-unit values of speed and torque, which yields

$$\frac{2H}{\omega_e} p\omega_r = T_M - T_e \tag{2.42a}$$

$$T_e = \psi^e_{ds} i^e_{qs} - \psi^e_{qs} i^e_{ds} \tag{2.42b}$$

where

$$H = \left(\frac{1}{2}\right)\left(\frac{2}{P}\right)\frac{J\omega_e}{T_B} = \left(\frac{1}{2}\right)\left(\frac{2}{P}\right)^2 \frac{J\omega_e^2}{P_B} \tag{2.43}$$

The active and reactive power are also calculated in per-unit using:

$$P_e = v^e_{qs} i^e_{qs} + v^e_{ds} i^e_{ds} + 2v^e_{0s} i^e_{0s} \tag{2.44a}$$

$$Q_e = v^e_{qs} i^e_{ds} - v^e_{ds} i^e_{qs} \tag{2.44b}$$

Simulink Implementation

The Simulink implementation of the induction machine is shown in Figure 2.19. In the **dynamics** block, the states equations (2.38) are calculated. In the **current** block, the stator and rotor currents are calculated based on equation (2.34). In the

torque block, the torque and rotor speed are calculated. In the **loadtorque** block, the load torque is calculated, which is in the general form of:

$$T_l = T_{m0}(0.5\omega^2 + 0.5) \tag{2.45}$$

Where ω are the per-unit rotor speed, $\frac{\omega_r}{\omega_e}$.

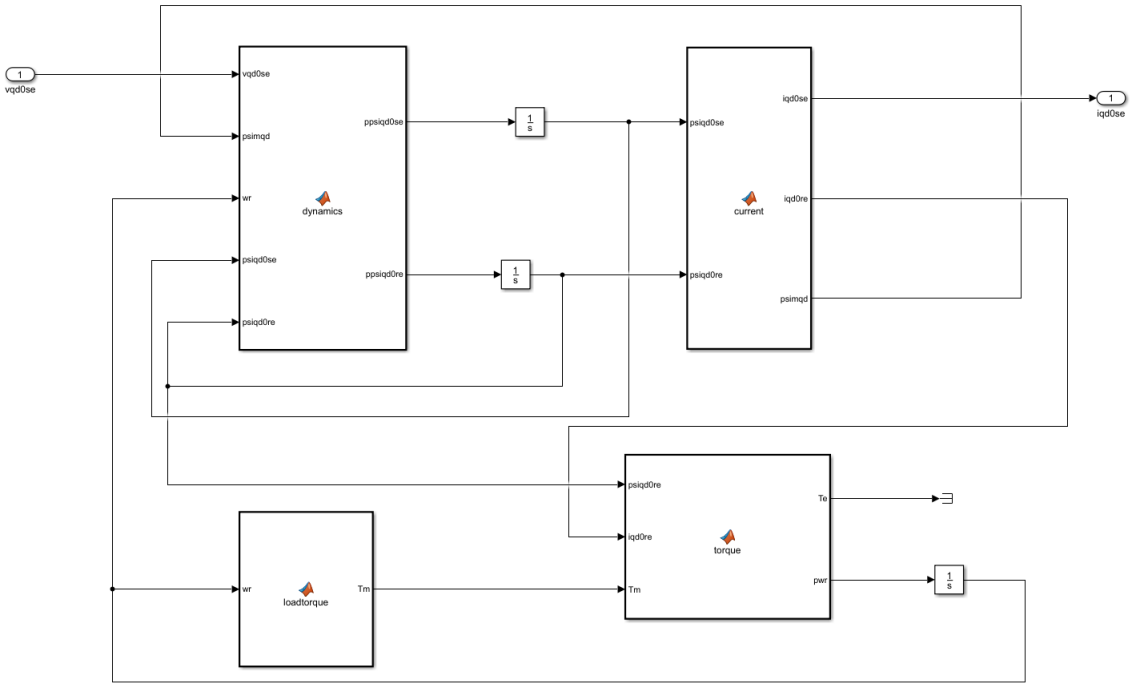

Fig. 2.19.: Induction Machine Detailed Model Simulink Implementation

2.5 Transmission Line

As mentioned in Chapter 1, the π circuit is used to model the transmission line. In Figure 1.1, there are twelve transmission lines, where six of them are connecting bus 1 and bus 3 with two transmission lines for each phase; the other six are connecting bus 3 and bus 4. For simplicity, only the phase a connection is shown in Figure 2.20. To model parallel lines, the values of resistance and inductance of the individual

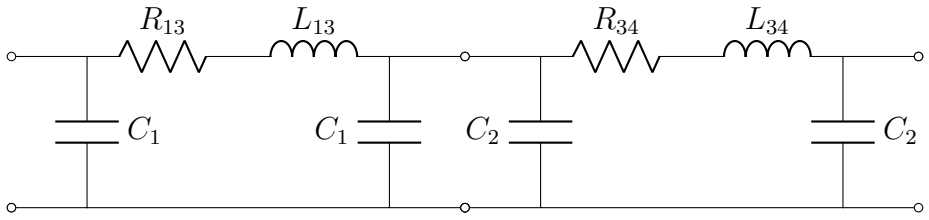

Fig. 2.20.: 5-Bus System Transmission Line Equivalent Circuit

conductors are divided by two and the values of the capacitance are multiplied by two.

In the implementation, the capacitors across bus 3 share the same voltages as the primary side of the LTC transformer. Therefore, the capacitors with admittance b_{13} and b_{34} are combined to form a single capacitance. In addition, within the Simulink implementation to avoid algebraic loops, and based upon the fact the the capacitor should not directly connect to a voltage source (the infinite bus) because of the continuity of capacitive voltage, a small resistor is added between the infinite bus and the transmission line. Hence, the final topology shown in Figure 2.21 is used.

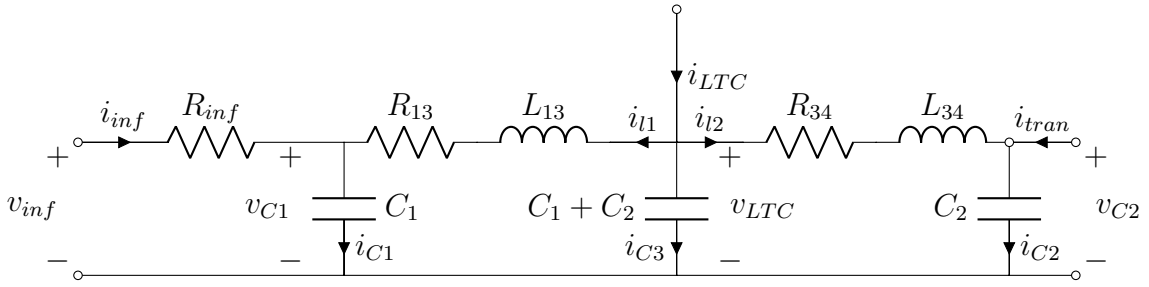

Fig. 2.21.: 5-Bus Transmission Line Implementation Model

Currents in inductor L_{13}

In the Figure 2.21, the currents and voltages can all be calculated. For the inductor L_{13}, the equations for the currents states in *abc* variables are: (2.46):

$$\mathbf{v}_{abcl1} = \mathbf{v}_{abcLTC} - \mathbf{v}_{abcC1} \tag{2.46a}$$

$$\mathbf{v}_{abcl1} = \mathbf{L}_{13} p\mathbf{i}_{\mathbf{abcl1}} + \mathbf{R}_{13}\mathbf{i}_{abcl1} \tag{2.46b}$$

Where $\mathbf{L}_{13}$ and $\mathbf{R}_{13}$ are three-by-three square diagonal matrices with diagonal entries L_{13} and R_{13} respectively. To transform the *abc* variables to $qd0$ variables, a reference frame transformation to the synchronous reference frame is applied, yielding a state model of the form:

$$pi^e_{ql1} = \frac{v^e_{qLTC} - v^e_{qC1} - R_{13} i^e_{ql1}}{L_{13}} - \omega_e i^e_{dl1} \tag{2.47a}$$

$$pi^e_{dl1} = \frac{v^e_{dLTC} - v^e_{dC1} - R_{13} i^e_{dl1}}{L_{13}} + \omega_e i^e_{ql1} \tag{2.47b}$$

$$pi^e_{0l1} = \frac{v^e_{0LTC} - v^e_{0C1} - R_{13} i^e_{0l1}}{L_{13}} \tag{2.47c}$$

In (2.47), voltages with subscript LTC are calculated based on the capacitor in Figure 2.21 labeled with $C_1 + C_2$; voltages with subscript C_1 are calculated based on the capacitor in Figure 2.21 labeled with C_1, and the currents are states for the inductor L_1.

Currents in inductor L_{34}

In the same fashion, the currents in the transmission lines connecting bus 3 and bus 4 can be calculated. First of all, the voltage in the lines can be calculated:

$$\mathbf{v}_{abcl2} = \mathbf{v}_{abcLTC} - \mathbf{v}_{abcC2} \tag{2.48a}$$

$$\mathbf{v}_{abcl2} = \mathbf{L}_{34} p\mathbf{i}_{abcl2} + \mathbf{R}_{34}\mathbf{i}_{abcl2} \tag{2.48b}$$

Following the same procedure described for the calculation of current in L_{13}, the derivatives of the currents through the L_{34} can be calculated in the equation (2.49) in the synchronous reference frame.

$$pi^e_{ql2} = \frac{v^e_{qLTC} - v^e_{qC2} - R_{34} i^e_{ql2}}{L_{34}} - \omega_e i^e_{dl2} \tag{2.49a}$$

$$pi^e_{dl2} = \frac{v^e_{qLTC} - v^e_{qC2} - R_{34} i^e_{ql2}}{L_{34}} + \omega_e i^e_{ql2} \tag{2.49b}$$

$$pi^e_{0l2} = \frac{v^e_{qLTC} - v^e_{qC2} - R_{34} i^e_{ql2}}{L_{34}} \tag{2.49c}$$

In the equation (2.49), voltages with subscript LTC will be calculated based on the capacitor in Figure 2.21 labeled with $C_1 + C_2$; voltages with subscript C_2 will be calculated based on the capacitor in Figure 2.21 labeled with C_2, and the currents are states for the inductor L_2.

Voltages in shunt capacitor $C_1 + C_2$

With the currents through the inductor calculated, the voltage across the capacitors can also be calculated. For the capacitor $C_1 + C_2$,

$$\mathbf{i}_{abcC3} = \mathbf{i}_{abcLTC} - \mathbf{i}_{abcl1} - \mathbf{i}_{abcl2} \tag{2.50a}$$

$$\mathbf{i}_{abcC3} = (\mathbf{C}_1 + \mathbf{C}_2) p\mathbf{v}_{abcLTC} \tag{2.50b}$$

These can be transformed to the the synchronous reference frame, yielding (2.51)

$$pv^e_{qLTC} = \frac{i^e_{qLTC} - i^e_{ql1} - i^e_{ql2}}{C_1 + C_2} - \omega_e v^e_{dLTC} \tag{2.51a}$$

$$pv^e_{dLTC} = \frac{i^e_{dLTC} - i^e_{dl1} - i^e_{dl2}}{C_1 + C_2} + \omega_e v^e_{qLTC} \tag{2.51b}$$

$$pv^e_{0LTC} = \frac{i^e_{0LTC} - i^e_{0l1} - i^e_{0l2}}{C_1 + C_2} \tag{2.51c}$$

In (2.51), currents with subscript LTC are calculated based on the LTC model, which will be described in later sections.Currents with subscript l_1 and l_2 are calculated using (2.47) and (2.49) respectively, and the voltages are states for the capacitor $C_1 + C_2$.

Voltages in shunt capacitor C_1

For the capacitor C_1, the model in *abc* variables can be expressed in the form: (2.52)

$$\mathbf{i}_{abcC1} = \mathbf{i}_{abcinf} + \mathbf{i}_{abcl1} \tag{2.52a}$$

$$\mathbf{i}_{abcC1} = \mathbf{C}_1 p\mathbf{v}_{abcC1} \tag{2.52b}$$

Transforming (2.52) to the synchronous reference frame and expanding the equation, the derivatives can be calculated as:

$$pv^e_{qC1} = \frac{i^e_{qinf} + i^e_{ql1}}{C_1} - \omega_e v^e_{dC1} \tag{2.53a}$$

$$pv^e_{dC1} = \frac{i^e_{dinf} + i^e_{dl1}}{C_1} + \omega_e v^e_{qC1} \tag{2.53b}$$

$$pv^e_{0C1} = \frac{i^e_{0inf} + i^e_{0l1}}{C_1} \tag{2.53c}$$

In (2.53), currents with subscript inf are those through through the resistor R_{inf}, placed between the infinite bus and the capacitor of the transmission line. These currents are determined using:

$$i^e_{qinf} = \frac{v^e_{qinf} - v^e_{qC1}}{R_{inf}} \tag{2.54a}$$

$$i^e_{dinf} = \frac{v^e_{dinf} - v^e_{dC1}}{R_{inf}} \tag{2.54b}$$

$$i^e_{0inf} = \frac{v^e_{0inf} - v^e_{0C1}}{R_{inf}} \tag{2.54c}$$

The currents with subscript L_1 are calculated based on equation (2.47).

Voltages in shunt capacitor C_2

Similarly, for the capacitor C_2, the equations in abc variables can be expressed in the form: (2.55)

$$\mathbf{i}_{abcC2} = \mathbf{i}_{abctran} + \mathbf{i}_{abcl2} \tag{2.55a}$$

$$\mathbf{i}_{abcC2} = \mathbf{C}_2 p \mathbf{v}_{abcC2} \tag{2.55b}$$

Transforming these equations (2.52) to the synchronous reference frame and expanding yields:

$$pv^e_{qC2} = \frac{i^e_{qtran} + i^e_{ql2}}{C_2} - \omega_e v^e_{dC2} \tag{2.56a}$$

$$pv^e_{dC2} = \frac{i^e_{dtran} + i^e_{dl2}}{C_2} + \omega_e v^e_{qC2} \tag{2.56b}$$

$$pv^e_{0C2} = \frac{i^e_{0tran} + i^e_{0l2}}{C_2} \tag{2.56c}$$

In (2.56), currents with subscript $tran$ are calculated based on the transformer model, which will be described in a later section. Currents with subscript L_2 are calculated using (2.49).

Simulink Implementation

As all the equations describing the currents and voltages are shown, one can notice that there are only three quantities shown in the Figure 2.21 that are not states: $\mathbf{i}_{qd0LTC}$, $\mathbf{i}_{qd0tran}$ and $\mathbf{v}_{qd0inf}$. These quantities are used as input to the transmission line subsystem. Specifically, $\mathbf{i}_{qd0LTC}$ are calculated from the Load-tap-changer section, $\mathbf{i}_{qd0tran}$ are calculated from the transformer section and $\mathbf{v}_{qd0inf}$ are calculated in the infinite bus section. The outputs are the $\mathbf{v}_{qd0LTC}$, which are used in the LTC system (between bus 2 and bus 3), and $\mathbf{v}_{qd0C2}$, which are used in the transformer system (between bus 4 and bus 5). The implementation of the transmission line is shown in Figure 2.22.

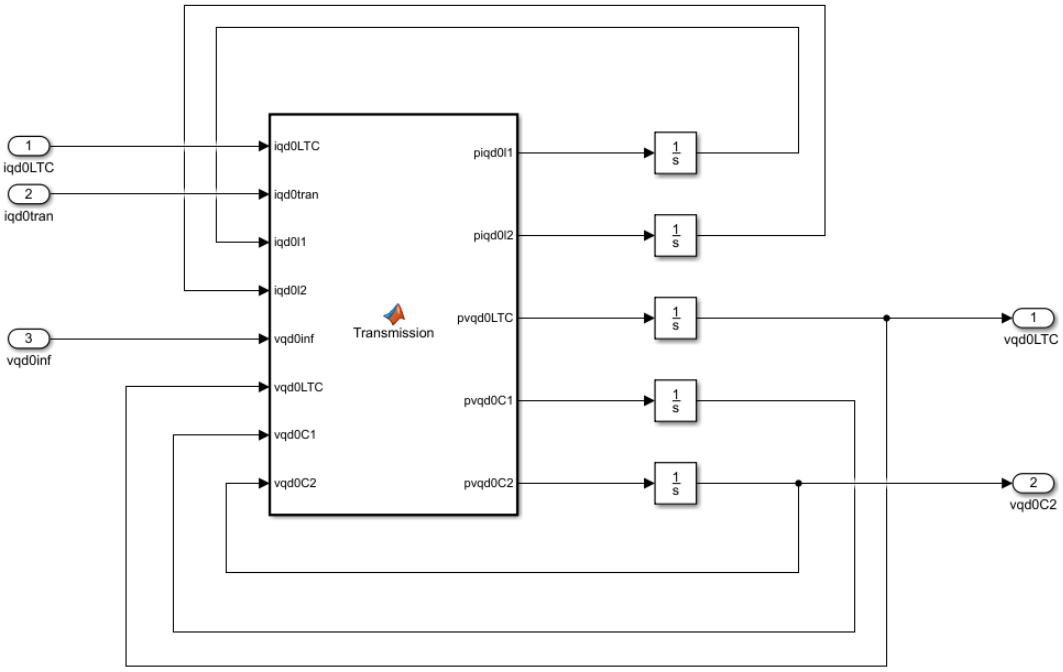

Fig. 2.22.: Transmission Line Simulink Implementation

2.6 Transformer Model

Transformer

The transformer model is shown in Figure 1.3. To aid description, the same figure with additional current labels are shown in Figure 2.25. The model is derived from an analysis of two magnetically coupled coils shown in Figure 2.23 from [8]. With saturation neglected. An T-equivalent circuit for the transformer can be derived shown in Figure 2.24 with a detailed described in [8] page 2-7.In power system analysis, the resistance in the windings, namely r_1 and $r_2^{'}$ in Figure 2.24, are assumed negligible. In addition, it is assumed the permeability of the core is relatively large compared to the air so that the magnetizing inductance l_{m1} is relatively large compared to the leakage inductances L_{l1} and L_{l2}. Thus, the shunt impedance of the L_{m1} is ignored. In the end, the transformer is modeled using a single inductor with the two leakage inductances lumped together. To accommodate the LTC, where the turns ratio can be varied, the left part in the Figure 2.25 is added. By changing the turns ratio of $\frac{N_1}{N_2}$, the voltage ratio $\frac{V_{in}}{V_t}$ is changed accordingly. Hence the left of the Figure 2.25 acts as a voltage regulator.

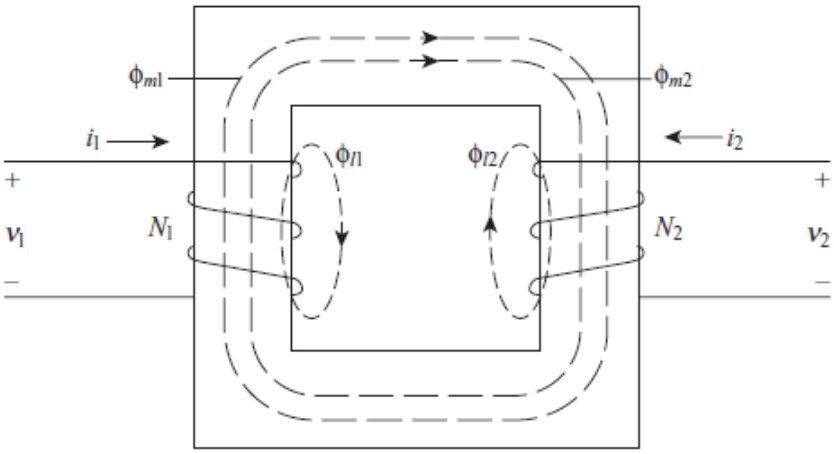

Fig. 2.23.: Two Wingdings Magnetically Coupled Circuits

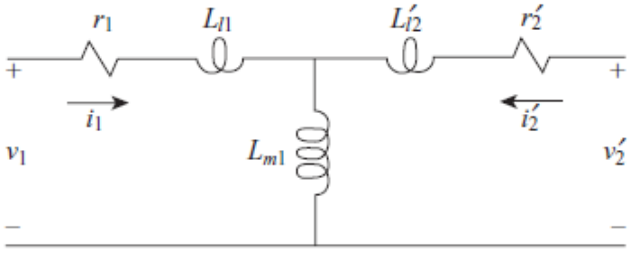

Fig. 2.24.: Transformer T-Equivalent Circuit

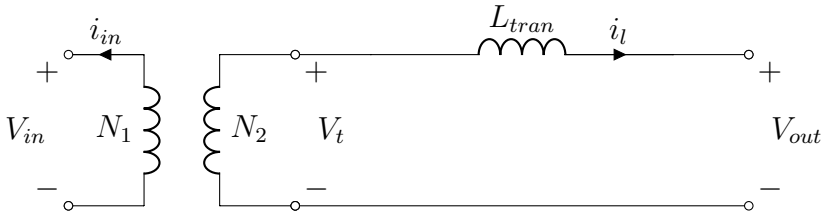

Fig. 2.25.: Transformer Implementation

Finally, in assuming there is no coupled between the phase leakages of a 3-phase transformer, the voltages equations in *abc* variables can be expressed as: (2.57).

$$\mathbf{v}_{abcin} = \frac{N_1}{N_2}\mathbf{v}_{abct} \tag{2.57a}$$

$$\mathbf{v}_{abct} - \mathbf{v}_{abcout} = (\mathbf{L}_{tran})p\mathbf{i}_{abcl} \tag{2.57b}$$

Where the $\mathbf{L}_{tran}$ is a diagonal matrix with entries of the lumped leakage inductance of the transformer. Using a transformation to the synchronous frame of reference, the model can be expressed:

$$p\psi^e_{ql} = (\frac{v^e_{qin}}{r}v^e_{qin} - v^e_{qout} - \psi^e_{dl})\omega_e \tag{2.58a}$$

$$p\psi^e_{dl} = (\frac{v^e_{qin}}{r}v^e_{din} - v^e_{dout} - \psi^e_{dl})\omega_e \tag{2.58b}$$

$$p\psi_{0l} = \frac{v^e_{qin}}{r}v^e_{0in} - v^e_{0out} \tag{2.58c}$$

where $r = \frac{N_1}{N_2}$, and

$$\psi^e_{ql} = X_{tran} i^e_{ql} \tag{2.59a}$$

$$\psi^e_{dl} = X_{tran} i^e_{dl} \tag{2.59b}$$

$$\psi_{0l} = X_{tran} i_{0l} \tag{2.59c}$$

With the inductors obtained by solving the state model, the input currents and can also be calculated. On the input side, there is a voltage regulator, with the relationship shown in equation (2.57a). Based on the conservation of energy, i.e., the input power should equal to the output power, the currents can be expressed:

$$\mathbf{i}_{abcin} = \frac{N_2}{N_1} \mathbf{i}_{abcl} \tag{2.60}$$

Furthermore, from the direction of the i_{in}, the input currents are expressed in the synchronous reference frame as:

$$i^e_{qin} = -\frac{i^e_{ql}}{r} \tag{2.61a}$$

$$i^e_{din} = -\frac{i^e_{dl}}{r} \tag{2.61b}$$

$$i^e_{0in} = -\frac{i^e_{0l}}{r} \tag{2.61c}$$

Simulink Implementation

The Simulink implementation of the transformer is shown in Figure 2.26. In the **PsiCalculation** block, (2.58) is utilized. In the **CurrentCal** block, (2.59) and (2.61) are used.

LTC Tap-Changing Mechanism

The LTC tap-changing mechanism is developed from [13]. The LTC is able change its turn ratios in distinct steps to regulate the output voltage magnitude within a

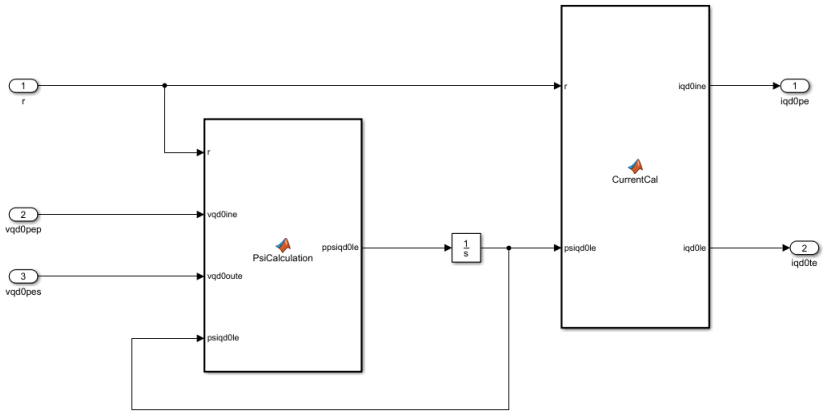

Fig. 2.26.: Transformer Simulink Implementation

desired range. The typical parameters of the LTC include the maximum and minimum turns ratio, r_{min} and r_{max} respectively, the tap position N_{tap}, a voltage dead-band V_d, a delay time before the first tap change t_{d1}, a delay time between subsequent tap change t_{d2}, and a voltage sampling time t_s.

The $\frac{N_1}{N_2}$ can vary and the number of the tap position specifies how much the turns ratio can vary between each tap position. The incremental turns ratio change δr, due to change of one tap position, is calculated based upon:

$$\delta r = \frac{r_{max} - r_{min}}{N_{tap} - 1} \tag{2.62}$$

The voltage dead-band is the control objective of the LTC. Typically, the voltage dead band represents the objective voltage $V_o \pm V_d$ in per-unit, which means the LTC measures the voltage V_{out} shown in Figure 2.25 and the tap changes if V_{out} does not fall into the voltage dead-band. The last two parameters are used as time delay for the tap-position change to prevent the LTC making unnecessary tap-changing due to transient voltage responses. To be more clear, the LTC checks V_{out} at every sampling time t_s. At these sampling times, if the V_{out} is within the voltage dead-band, the LTC does not make any changes. However, if V_{out} is not within the voltage dead band, the

LTC changes its turns ratio by $\pm\delta r$ after a time delay of t_{d1}. If V_{out} is in the voltage dead-band as desired after the first tap-change, the the LTC stops making changes and checks the voltage again after t_s. However, if V_{out} is still not in the voltage dead-band after the first tap-change, it makes subsequent changes after a time delay of t_{d2}.

In Simulink, since there is no direct time domain delay block to be conveniently used in the LTC operation, a combination of a triangle signal T and hit crossing check block is used to mimic the LTC signal sampling and time delay. The magnitude of the triangle signal is set to a value T_{max} and the frequency of the triangle signal is varied based on V_{out}. The LTC makes necessary changes to its turns ratio and the slope k_T of the signal when the triangle signal T hits its maximum value T_{max}. Even though the voltage magnitude V_{out} can be calculated at every time step in the simulation, it is not used in the LTC operation decision until the triangle signal T hits its maximum value T_{max}. The slope of the triangle signal k_T is based on the V_{out} and the delay or the sampling time. The operation flow chart is shown in Figure 2.28. The inputs to the LTC operation are LTC turns ratio r, output voltage V_{out}, triangle signal T, and the slope of the triangle signal k_T and the outputs are the LTC turns ratio r and triangle signal slope k_T.

Simulink Implementation

The Simulink implementation of the tap-changing mechanism is shown in Figure 2.27. The **TapChaning** block contains the logic described in Figure 2.28, with an additional signal e, which represents the condition "$V_o - V_d \leq V_{out} \leq V_o + V_d$?". On the right hand side, there is an integrator used to create the triangle signal, which resets to 0 when it reaches 1. The hit crossing block is used for the condition "$T = T_{max}$?".

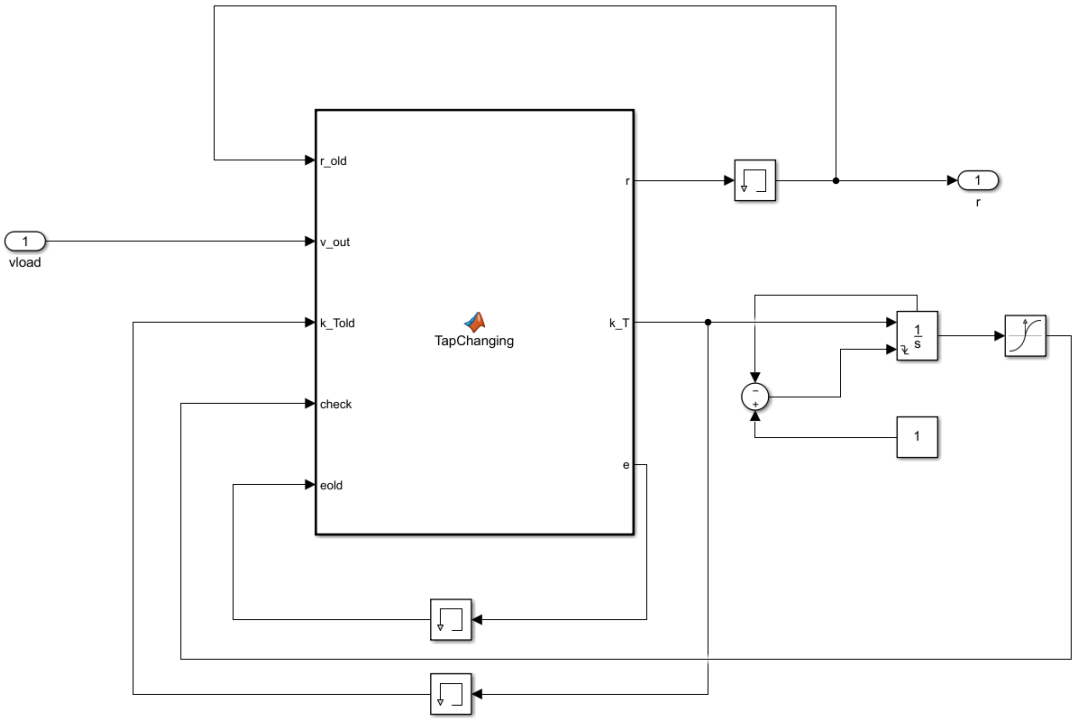

Fig. 2.27.: LTC Tap-changing Mechanism Simulink Implementation

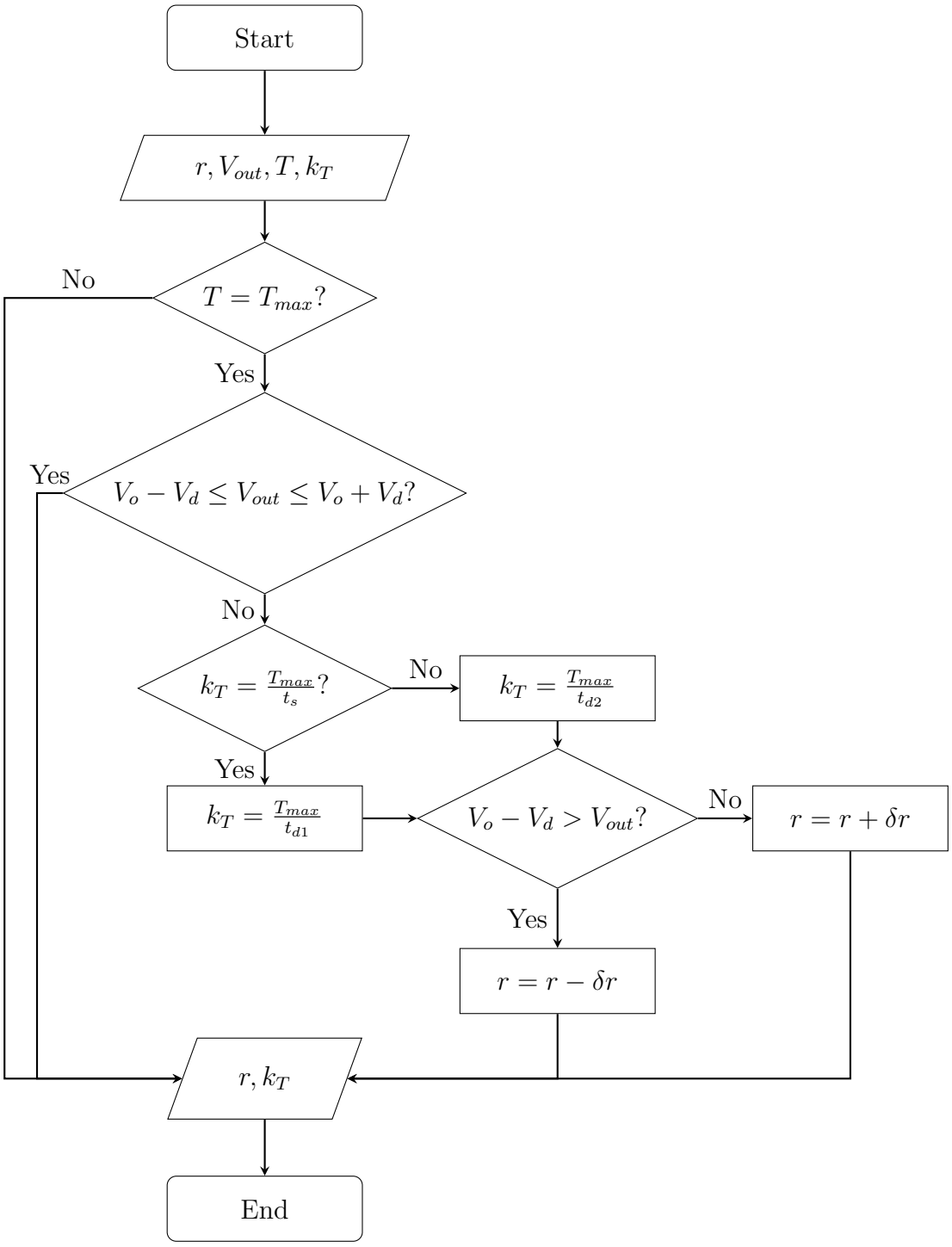

Fig. 2.28.: LTC Flow Chart

2.7 System Level Simulink Implementation

2.7.1 Simulink Block Diagram

The overall 5-bus system Simulink block diagram is shown in Figure 2.29, which is a combination of all the aforementioned components. The inputs to the system is the infinite bus voltage, P_o for the generator governor and V_0 generator exciter. Furthermore, the input and output voltages and currents of each bus are all in the synchronous reference frame.

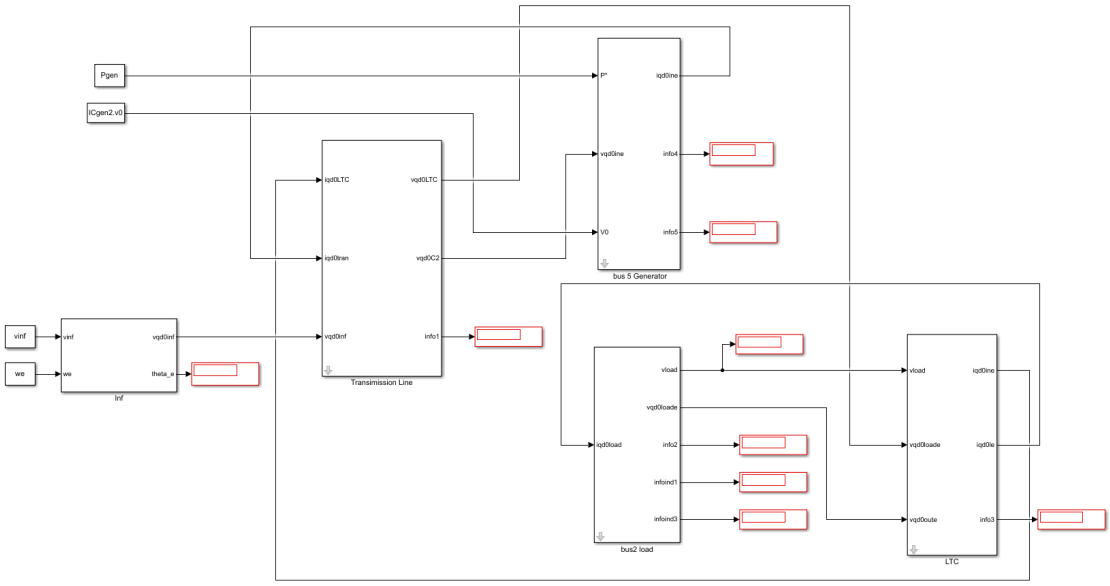

Fig. 2.29.: 5-bus System Detailed Model Simulink Implementation

For each bus, an **info** block is added in addition to blocks described in previous sections. This block uses a **busdata** function block, shown in Figure 2.30, to calculate the bus information in steady state. The bus voltage and current magnitude, voltage and current angle are obtained based on the (B.9) in the Appendix.Then the active and reactive power are calculated based on (C.2). Hence, the inputs to this block are the bus voltages and currents in the synchronous reference frame, and the outputs are the steady-state voltage magnitude, voltage angle, active power and reactive power.

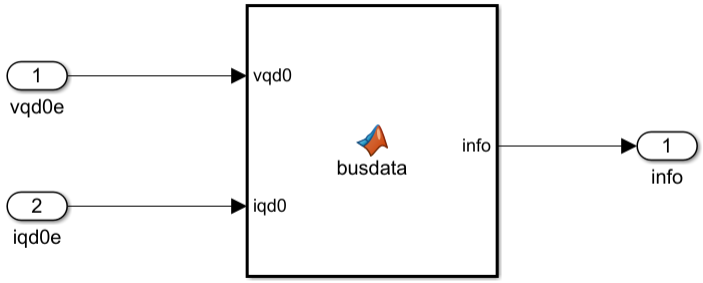

Fig. 2.30.: Bus Information Simulink Implementation

Infinite Bus

The **Inf** block is shown in Figure 2.1. The inputs to this block are the fixed infinite bus voltage magnitude and the electrical frequency. The outputs are the infinite bus voltage in the synchronous frame reference.

Transmission Line

The **Transmission Line** block is shown in Figure 2.22 with an additional info calculation. Hence, the inputs to the block are the currents of the LTC between bus 2 and bus 3, currents of the transformer between bus 4 and bus 5 and the infinite bus voltages. The outputs of the block are the LTC input voltages and the transformer input voltages.

Generator System

The generator and the transformer are lumped into a single in the Simulink implementation, similar to the generator/infinite bus implementation. Since the reactances of the transformer are series connected to the generator, they are treated as part of the leakage reactances of the generator. Hence, the transformer reactance is incor-

porated within the synchronous machine model by adding its value to the leakage reactance of each phase.

Similar to the generator/infinite bus implementation described in section 2.3.4, the correct machine stator terminal voltage needs to be calculated. The series connected transformer and the generator can be described by using Kirchhoff's law from the transformer input terminal to the generator terminal. The relationship between the transformer input voltage and the machine terminal voltage can be expressed:

$$\mathbf{v}_{abcin} = r\mathbf{v}_{abct} \tag{2.63a}$$

$$\mathbf{v}_{abct} = -\frac{X}{\omega_e}\frac{di_{abcs}}{dt} + v_{abcs} \tag{2.63b}$$

Where the voltage with subscript in are the transformer input terminal voltage shown in Figure 2.25, the voltages with subscript t are the transformer internal voltage after the voltage regulator and the quantities with subscript s are the generator stator quantities.

Transforming (2.63) to the rotor reference frame:

$$v^r_{qsin} = rv^r_{qst} \tag{2.64a}$$

$$v^r_{dsin} = rv^r_{dst} \tag{2.64b}$$

$$v^r_{0sin} = rv^r_{0st} \tag{2.64c}$$

$$v^r_{qst} = -\frac{X}{\omega_e}\frac{di^r_{qs}}{dt} - \omega_r\frac{X}{\omega_e}i^r_{ds} + v^r_{qs} \tag{2.64d}$$

$$v^r_{dst} = -\frac{X}{\omega_e}\frac{di^r_{ds}}{dt} + \omega_r\frac{X}{\omega_e}i^r_{qs} + v^r_{ds} \tag{2.64e}$$

$$v_{0st} = -\frac{X}{\omega_e}\frac{di_{0s}}{dt} + v_{0s} \tag{2.64f}$$

The overall implementation in Simulink is shown in Figure 2.31. At the upper right corner, a constant block represents the constant tap setting r is used for the transformer, as shown in equations (2.64a) to equation (2.64c).

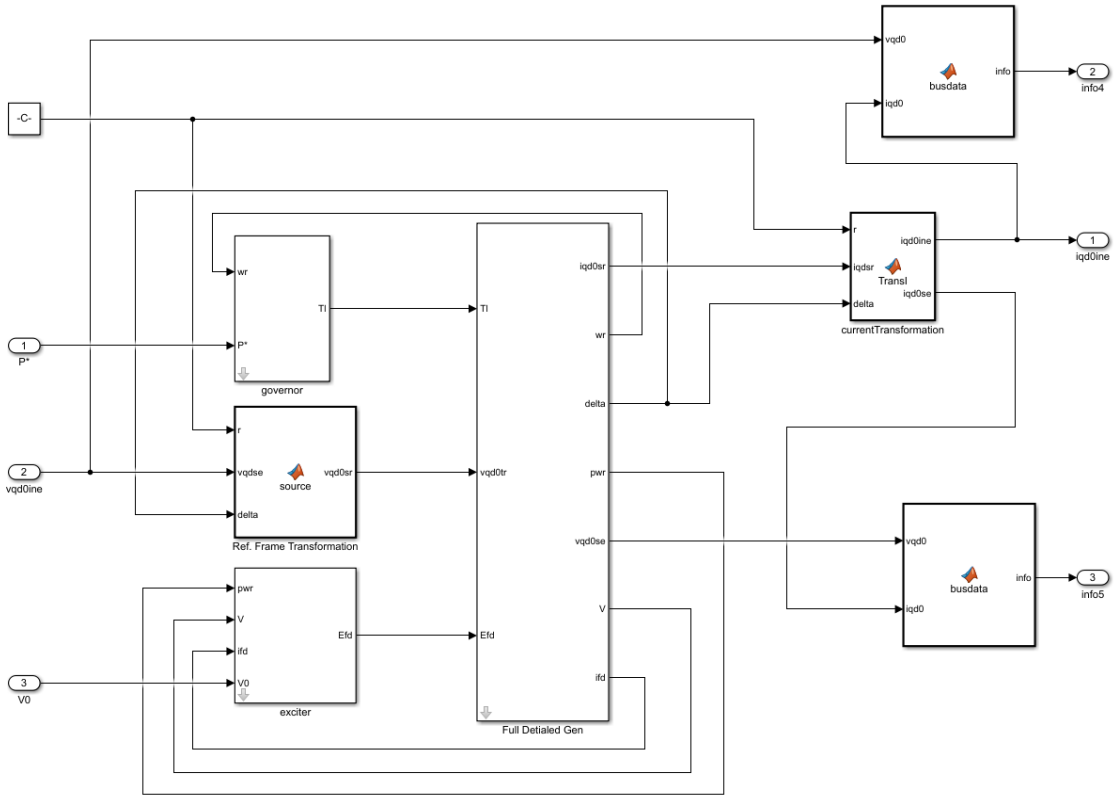

Fig. 2.31.: Generator/Transformer Simulink Implementation

All the sub-blocks are the described in section 2.3.4. hence they are not discussed further. The inputs to the generation system block are the commanded power P_o for the governor, V_0 for the exciter and the input is the transformer input voltages The output of the system is the bus information for bus 4 and bus 5, and the transformer input currents in the synchronous reference frame.

Load Bus

The load bus includes three components as described, which is implemented as shown in Figure 2.32.

The three blocks on the left are the constant admittance load,induction machine 1 and induction machine 2. The constant admittance load is shown in Figure 2.17. The inputs are the load currents and the outputs are the load voltages. The details of

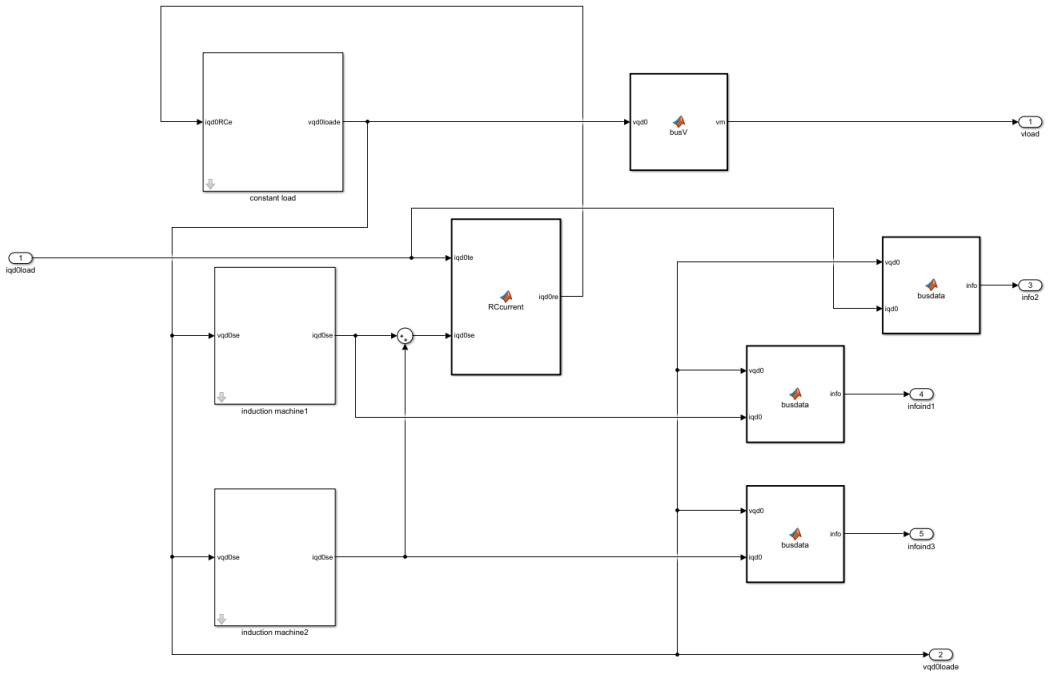

Fig. 2.32.: Load Bus Simulink Implementation

induction machine blocks are shown in Figure 2.19. Both blocks use the same model with different machine parameters. Inputs to the induction machine blocks are the machine stator voltages and the outputs are the machine stator currents.

The **RCcurrent** function block is used to calculate the input currents to the constant admittance block, which is based on KCL and can be expressed as:

$$\mathbf{i}^e_{qd0RC} = \mathbf{i}^e_{qd0load} - (\mathbf{i}^e_{qd0ind1} + \mathbf{i}^e_{qd0ind2}) \tag{2.65}$$

Where the currents with subscript *ind* are the induction machines currents, the currents with the subscript *load* are the total currents at the load bus.

The **busV** function block is used to calculate the voltage magnitude, which is calculated based on:

$$V_m = \sqrt{v_q^{e2} + v_d^{e2}} \tag{2.66}$$

And three more **businfo** blocks are used to calculate the induction machine terminal information and the bus information.

Therefore, the inputs to the load bus are the LTC output currents and the outputs are the bus load voltage magnitude, the load voltage in the synchronous reference frame, and three info for the load bus and induction machine.

LTC

The **LTC** block is shown in Figure 2.33. Underneath sub-block, shown in Figure 2.34), is the transformer dynamics, shown in Figure 2.26, and the tap position control mechanism, shown in Figure 2.27.

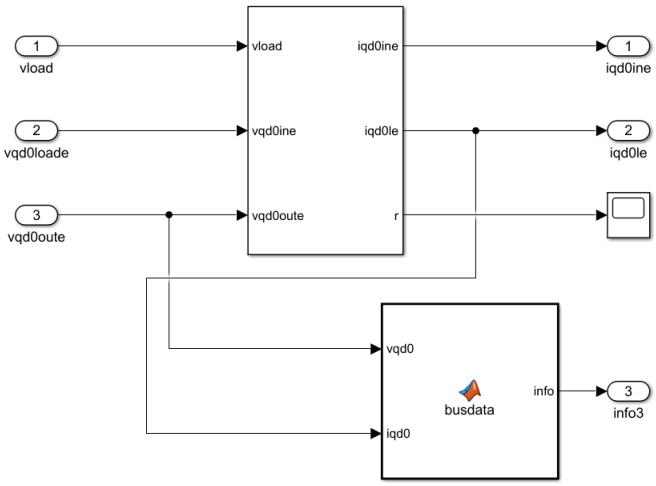

Fig. 2.33.: LTC Simulink Implementation

The inputs to the LTC block are the load voltage magnitude at bus 3, the input and output voltages of the LTC in the synchronous reference frame. The outputs for the LTC blocks are the input and output currents of the LTC in the synchronous reference frame.

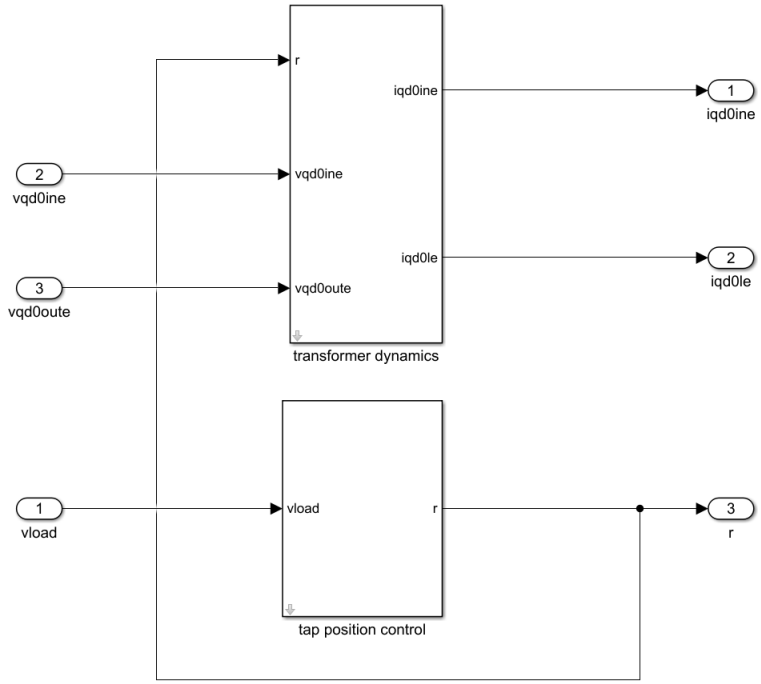

Fig. 2.34.: LTC Subblock Simulink

2.7.2 State Initial Condition

The initial conditions of all states are calculated based on the power flow solution described in the Appendix. Using the bus voltages and complex power, the initial condition of the states in each components is calculated. The main idea is to use the power flow solution as known quantities, and solve the differential equations mentioned in this chapter with the derivative terms set to 0. All zero sequence quantities are set to zero because it is assumed that all the currents, voltages and flux linkage are balanced.

Infinite Bus

The infinite bus block only has a state, θ_e, which is angle of the synchronous reference frame. The initial condition of this state is set to 0.

Synchronous Generator

There are 9 states for the wound-rotor synchronous machine, 5 states for the governor system, and 5 states for the exciter. From the Matpower solution, the generator terminal voltage phasor and the complex electrical power produced by the generator are obtained. In the power system generator steady-state analysis, the angle δ is used for the power and rotor stability studies. From [8], chapter 5 starting from page 160, the steady-state equations relating the angle δ and the voltages and currents in steady state are shown to be:

$$\widetilde{E_a} = [(X_d - X_q)I_{ds}^r + X_{md}I_{fd}^{'r}]e^{j\delta} \tag{2.67a}$$

$$\widetilde{V_{as}} = -(r_s + jX_q)\widetilde{I_{as}} + \widetilde{E_a} \tag{2.67b}$$

Using (C.2) from the Appendix, the $\widetilde{I_{as}}$ is calculated based on the Matpower solution, and the δ is calculated based on the angle of $\widetilde{E_a}$.

From the equation (B.11), the q- and d- axis quantities can be calculated. After expansion:

$$v_{qs0}^r = |\widetilde{V_{as}}| \cos(\theta_v - \delta) \tag{2.68a}$$

$$v_{ds0}^r = -|\widetilde{V_{as}}| \sin(\theta_v - \delta) \tag{2.68b}$$

$$i_{qs0}^r = |\widetilde{I_{as}}| \cos(\theta_i - \delta) \tag{2.68c}$$

$$i_{ds0}^r = -|\widetilde{I_{as}}| \sin(\theta_i - \delta) \tag{2.68d}$$

$$\tag{2.68e}$$

Where θ_v and θ_i are the voltage and current phasor angle respectively. The subscript 0 represents initial condition at $t = 0s$.

As mentioned in the Simulink Implementation section, the transformer connecting the generator and the rest of the power system network is lumped into the generation block. The reactance of the transformer, shown in Figure 2.25, is added to the leakage

reactance of the synchronous machine. Hence, the stator flux linkage per second in the implementation is the total flux linkage per second including the generator and the transformer. Letting the subscript t represent the transformer input terminal voltage. From equation (2.5):

$$v^r_{qst0} = \psi^r_{ds0} \tag{2.69a}$$

$$v^r_{dst0} = -\psi^r_{qs0} \tag{2.69b}$$

$$v_{0st0} = 0 \tag{2.69c}$$

$$v^{'r}_{fd0} = r'_{fd} i^{'r}_{fd0} \tag{2.69d}$$

$$v^{'r}_{kd0} = r'_{kd} i^{'r}_{kd0} \tag{2.69e}$$

$$v^{'r}_{kq10} = r'_{kq1} i^{'r}_{kq10} \tag{2.69f}$$

$$v^{'r}_{kq20} = r'_{kq2} i^{'r}_{kq20} \tag{2.69g}$$

Since the rotor windings $kq1$, $kq2$ and kd are short circuits, the currents in these windings are 0 in the steady state.

From (2.13), (2.16) and using the fact that the the winding currents are zero:

$$E'_{d0} = (X_q - X'_q) i^r_{qs0} \tag{2.70a}$$

$$\psi^{'r}_{kq20} = -E'_{d0} - (X'_q - X_{ls}) i^r_{qs0} \tag{2.70b}$$

$$E'_{q0} = -(X_d - X'_d) i^r_{ds0} + E'_{fd0} \tag{2.70c}$$

$$\psi^{'r}_{kd0} = E'_{q0} - (X'_d - X_{ls}) i^r_{ds0} \tag{2.70d}$$

$$\omega_r 0 = \omega_e \tag{2.70e}$$

$$T_M = T_e \tag{2.70f}$$

Based on (2.70), the initial conditions of the E'_d, $\psi^{'r}_{kq2}$, E'_q, $\psi^{'r}_{kd}$ and ω_r can be calculated if the initial condition of the E'_{fd0} is known.

From the equation (2.6), and the definition of the X_q, X_d and E'_{fd}, the q- and d-axis voltage is calculated based on:

$$v^r_{qs0} = -X_d i^r_{ds0} + E'_{fd0} \tag{2.71a}$$

$$v^r_{ds0} = X_q i^r_{qs0} \tag{2.71b}$$

From (2.17) and (2.71), the excitation voltage is calculated using:

$$E'_{fd0} = \frac{P_{e0} - (X_q - X_d) i^r_{qs0} i^r_{ds0}}{i^r_{qs0}} \tag{2.72}$$

Where P_e is the same as the commanded P_o in the exciter if the stator resistance r_s is neglected. If the stator resistance is not 0, there are power losses in the stator, which can be calculated:

$$i_{s0} = \sqrt{{i^r_{qs0}}^2 + {i^r_{ds0}}^2} \tag{2.73a}$$

$$P_{loss0} = i^2_{s0} r_s \tag{2.73b}$$

Then the electrical power produced by the generator (2.72) is:

$$P_{e0} = P_o - P_{loss0} \tag{2.74}$$

To this end, the initial conditions for the synchronous generators are all calculated except ψ^r_{qs}, ψ^r_{ds} and ψ^r_{0s}. The initial condition of the stator flux linkage per second is calculated from: (2.64):

$$v^r_{qst0} = -X i^r_{ds0} + v^r_{qs0} \tag{2.75a}$$

$$v^r_{dst0} = X i^r_{qs0} + v^r_{ds0} \tag{2.75b}$$

$$v_{0st0} = v_{0s0} \tag{2.75c}$$

Hence, by plugging (2.75) into (2.69):

$$\psi^r_{qs0} = -Xi^r_{qs0} - v^r_{ds0} \tag{2.76a}$$

$$\psi^r_{ds0} = -Xi^r_{ds0} + v^r_{qs0} \tag{2.76b}$$

$$\psi_{0s0} = 0 \tag{2.76c}$$

Governor System

In the governor, there are several first order transfer functions. To specify the initial condition for these transfer functions, the state model form of these transfer functions are used. For the first block, which is used to control the valve opening, the initial condition for the first transfer function is assumed 0 and the initial condition for the integral of the valve opening z is set to the commanded power P_o. For the second block of the governor system, all the initial condition for the transfer functions are set to be the commanded power P_o multiplied with their respective time constant.

Excitation System

In the excitation system, there are three components. To specify the initial condition for these transfer functions, their state space versions are used. The initial conditions for all the transfer functions in the power system stabilizer is set to zero. For the first high pass filter, the state in this block is the derivative of the rotor speed, which is zero under steady state. For the two lead filters, the state initial condition is 0. In the OEL block, the initial condition for the integrator is 0 as explained in the previous sections. In the last exciter integrator, the initial condition is E'_{fd} calculated in (2.72).

Transmission Lines, Transformer and Constant Admittance

The initial conditions of transmission lines, transformer states and constant admittance at the load are readily calculated using the power flow solution. For the voltage states at the capacitors, the initial condition of the voltage is calculated based on (B.9) with the corresponding steady-state voltage phasor; and setting the initial condition for the zero-sequence quantites to zero. For example, for the initial condition for the voltages described in (2.51), the voltage at bus 3 is found from the solution of Matpower. Then the initial conditions are:

$$v^e_{qLTC} = |\widetilde{V}_3| \cos\theta_{v3} \tag{2.77a}$$

$$v^e_{dLTC} = -|\widetilde{V}_3| \sin\theta_{v3} \tag{2.77b}$$

$$v^e_{0LTC} = 0 \tag{2.77c}$$

Where $\widetilde{V}_3$ is the voltage phasor at bus 3 and θ_{v3} is the voltage phasor angle.

Similarly, for the currents, the first step is to find the current phasor. However, since Matpower only provides solution of the complex power flow and the voltage phasor, the currents are calculated using:

$$\widetilde{I}_i = (\frac{\widetilde{S}_i}{\widetilde{V}_i})^* \tag{2.78}$$

Where the $\widetilde{S}_i$ is the corresponding complex power flow of the current and $*$ is the conjugate operator. With the current phasor, the $qd0$ states initial condition are calculated using (B.9).

Induction Machine

The induction machine initial conditions are calculated using (2.32) and (2.33). From (2.33), the currents can be expressed in terms of the flux linkages per second matrix form:

$$\begin{bmatrix} i^e_{qs} \\ i^e_{ds} \\ i_{0s} \\ i'^e_{qr} \\ i'^e_{qr} \\ i'_{0r} \end{bmatrix} = \frac{1}{D} \begin{bmatrix} X'_{rr} & 0 & 0 & -X_M & 0 & 0 \\ 0 & X'_{rr} & 0 & 0 & -X_M & 0 \\ 0 & 0 & \frac{D}{X_{ls}} & 0 & 0 & 0 \\ -X_M & 0 & 0 & X_{ss} & 0 & 0 \\ 0 & -X_M & 0 & 0 & X_{ss} & 0 \\ 0 & 0 & 0 & 0 & 0 & \frac{D}{X'_{lr}} \end{bmatrix} \begin{bmatrix} \psi^e_{qs} \\ \psi^e_{ds} \\ \psi_{0s} \\ \psi'^e_{qs} \\ \psi'^e_{ds} \\ \psi'_{0s} \end{bmatrix} \tag{2.79}$$

Where

$$X_{ss} = X_{ls} + X_M \tag{2.80a}$$

$$X'_{rr} = X'_{lr} + X_M \tag{2.80b}$$

$$D = X_{ss}X'_{rr} - X^2_M \tag{2.80c}$$

By substituting (2.79) into (2.32), the voltages are expressed in terms of the flux linkages per second in the matrix form:

$$\begin{bmatrix} v^e_{qs} \\ v^e_{ds} \\ v_{0s} \\ v'^e_{qr} \\ v'^e_{qr} \\ v'_{0r} \end{bmatrix} = \frac{1}{D} \begin{bmatrix} \frac{r_s X'_{rr}}{D} & 1 & 0 & -\frac{r_s X_M}{D} & 0 & 0 \\ -1 & \frac{r_s X'_{rr}}{D} & 1 & 0 & -\frac{r_s X_M}{D} & 0 \\ 0 & 0 & \frac{r_s}{X_{ls}} & 0 & 0 & 0 \\ -\frac{r'_r X_M}{D} & 0 & 0 & \frac{r'_r X_{ss}}{D} & s & 0 \\ 0 & -\frac{r'_r X_M}{D} & 0 & -s & \frac{r'_r X_{ss}}{D} & 0 \\ 0 & 0 & 0 & 0 & 0 & \frac{r'_r}{X_{ls}} \end{bmatrix} \begin{bmatrix} \psi^e_{qs} \\ \psi^e_{ds} \\ \psi_{0s} \\ \psi'^e_{qs} \\ \psi'^e_{ds} \\ \psi'_{0s} \end{bmatrix} \tag{2.81}$$

Where s is the slip in the induction machine, defined as:

$$s = \frac{\omega_e - \omega_r}{\omega_e} \tag{2.82}$$

To solve (2.81) the initial conditions of the induction machine electrical states (all the flux linkage per second in the stator and rotor), the steady-state slip is needed. This is calculated based on the torque speed relationship, described in detail in [8]. Under steady state, the electrical torque created by the machine equals the load torque. From [8], the relationship used to calculate the slip in steady state is:

$$T_e = \frac{X_M^2 r'_r s |\widetilde{V_{as}}|^2}{[r_s r'_r + s(X_M^2 - X_{ss}X'_{rr})]^2 + (r'_r X_{ss} + s r_s X'_{rr})^2} \tag{2.83}$$

Where s is the initial slip, $|\widetilde{V_{as}}|$ is the induction machine terminal voltage magnitude. From (2.83), the initial condition is solved using the MATLAB non-linear equation solver command **fsolve** given the load torque T_l and $T_e = T_l$ under steady state.

The initial rotor speed is then calculated:

$$\omega_{r0} = \omega_e(1 - s_0) \tag{2.84}$$

Where ω_e is synchronous speed.

To summarize, the initial conditions of all the states of the induction machine are calculated based on the machine voltages in the synchronous reference frame. To calculate these voltages, the power flow solution from the Matpower is used. Again, the stator voltages are calculated based on the induction machine terminal voltage phasor from the Matpower and (B.9) with zero-sequence quantity set to zero.

2.7.3 Representative System Response

With the mathematical model of the system components and Simulink Implementation described, a study is done to provide some details on quantities that are of

interest and can be predicted using the model. In this study, starting with the system at steady state at the operating point described in the Appendix, with the constant admittance bus drawing 60% of the load power, the two induction machines each drawing 20% of the load power. Subsequently, at 50 s, A change in the power command P_o is made. Specifically, the commanded power of the generator steps from 0.6 per-unit to 0.4 per-unit. Under normal operation, power system operators attempt to keep the voltages and the frequencies of each bus within a fixed range to ensure stability of the system. The results are shown in Figure 2.35 and Figure 2.36.

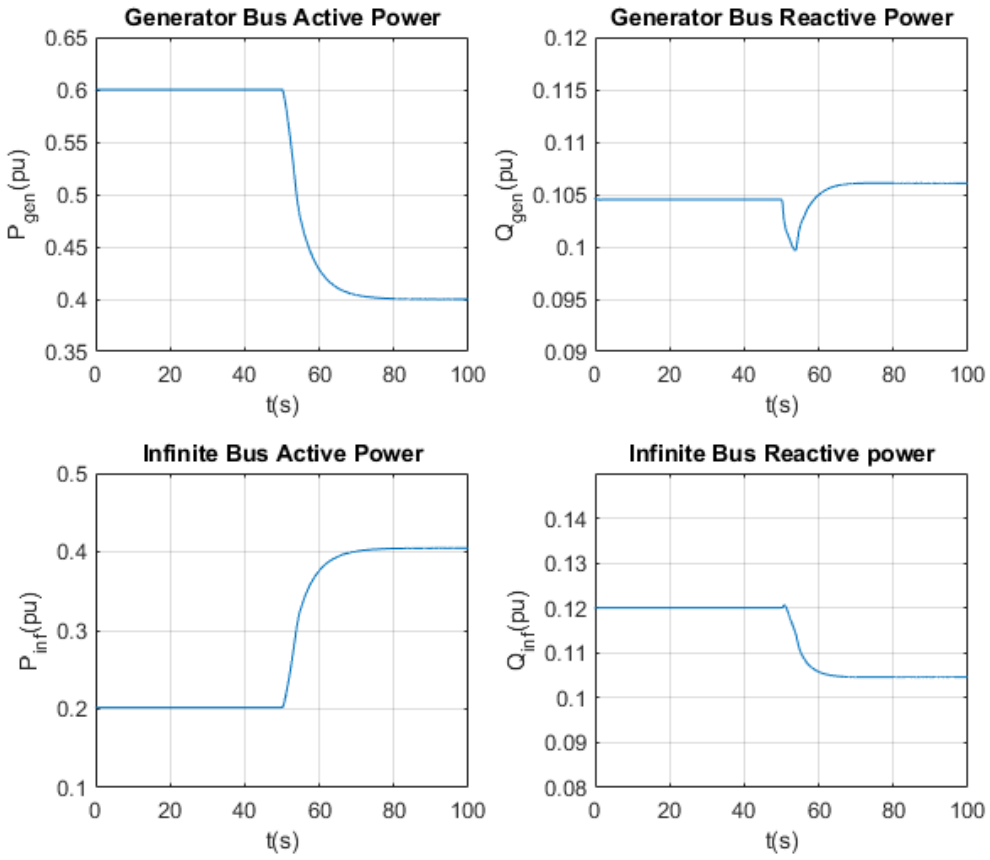

Fig. 2.35.: Detailed Model Simulation Results due to Generator Commanded Power Change(a)

In Figure 2.35, the simulation results for the active power and reactive power of both the generator and the infinite bus are plotted. One can observe that before 50s

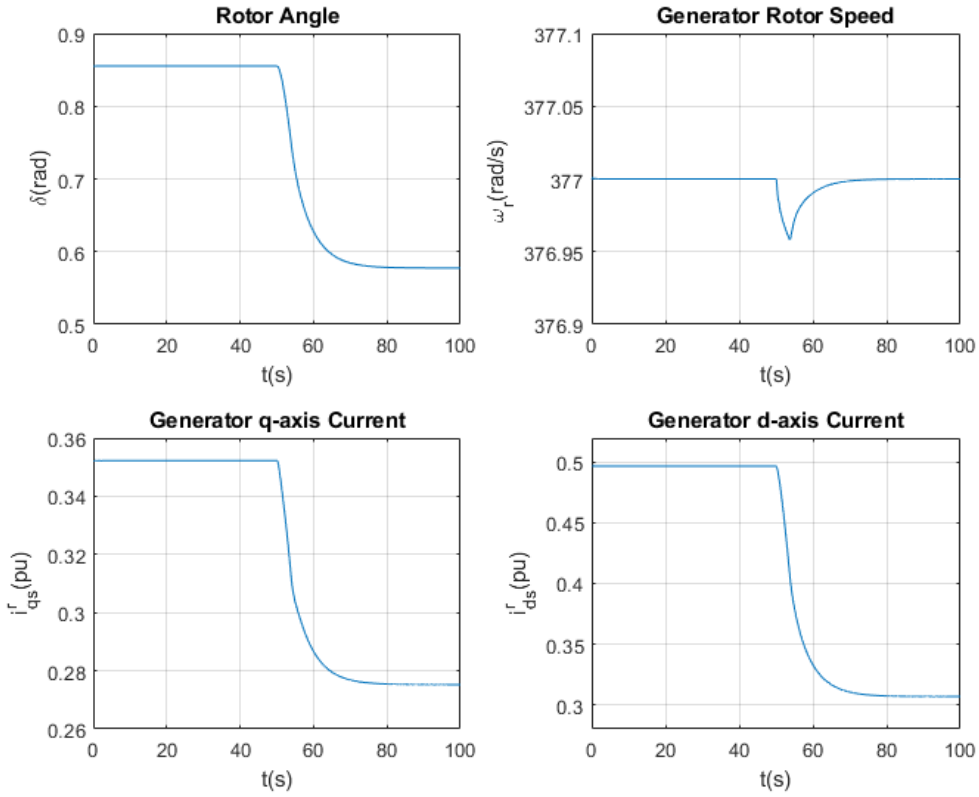

Fig. 2.36.: Detailed Model Simulation Results due to Generator Commanded Power Change(b)

each component in the system is operating at steady state, which validates initial steady-state condition calculations. At 50s, when the commanded power drops for the generator, the active power produced by the generator drops and reaches the commanded power. Due to the 0.2 per-unit active power decrease in the generator output, the infinite bus must increase its output power to keep the power balance in the system. For the reactive power, since the control of the active power does not directly related to the control of the reactive power, the reactive power of both the generator and the infinite bus does not change significantly. The minor change (0.005 per-unit for the generator and 0.015 per-unit for the infinite bus) is caused by the network power flow changes. In the Figure 2.36, some dynamics of the generator are plotted. As a result of the change in the commanded power, the mechanical torque

also changes as expected. Hence, a small transient can be seen in the rotor speed. As the load torque decreases, the rotor reduces its speed until the electrical torque and the load torque are equal. In addition, the change in the rotor angle δ is caused by the rotor speed change based on equation (2.13h). Last but not least, since the voltage regulator keeps the voltage at the generator machine terminal relatively fixed, the q- and d- axis currents are reduced so that the output active power of the generator is reduced to the commanded value. Apart from a step change in power command, many different types of studies can performed using the detailed model. This will be demonstrated in Chapter 5, where several studies are considered to compare the performance of alternative models.

3. REDUCED-ORDER MODEL

In traditional power system analysis, the so-called fast dynamics of the electrical system are often neglected [7]. In machine models, formal methods based upon singular perturbation techniques have been applied to derive the reduced forms [14]. Alternatively, reference frame theory has been used to justify the reference frame where derivatives of state variables are most appropriately neglected [8]. The reduction of the electrical dynamics of the stators of machines is typically applied in tandem with a reduced-order representation of the electrical network. Reduced-order network models typically consist of sinusoidal-steady-state phasor forms of the transmission line circuits. In this chapter, reduced-order forms of the detailed models described in Chapter 2 are provided. The means of coupling the component models to form a system-level model of the microgrid of Figcure 1.1 is then described. A representative study is used to highlight the model dynamics under changes in system input.

3.1 Reduced-Order Generator Model

To establish a reduced-order model of the generator, the stator electrical transients are neglected, which enables one to utilize larger time steps when solving the ODEs. This in turn leads to a faster model that is typically utilized in transient stability studies. A formal process to derive a reduced-order model from a detailed model utilizes a mathematical technique referred to as singular perturbation theory [14] For the generator, the reduced-order model is obtained by setting the terms with the derivative p to 0 and $\omega_r = \omega_e$ in (2.13) [8] for stator equations. This yields the per-unit reduced-order model:

$$0 = r_s i^r_{qs} - \psi^r_{ds} + v^r_{qs} \tag{3.1a}$$

$$0 = r_s i^r_{ds} + \psi^r_{qs} + v^r_{ds} \tag{3.1b}$$

$$0 = r_s i_{0s} + v_{0s} \tag{3.1c}$$

$$T'_{qo} p E'_d = -E'_d + (X_q - X'_q)[i^r_{qs} - \frac{X'_q - X''_q}{(X'_q - X_{ls})^2}(\psi^{'r}_{kq2} + (X'_q - X_{ls})i^r_{qs} + E'_d)] \tag{3.1d}$$

$$T''_{qo} p \psi^{'r}_{kq2} = -\psi^{'r}_{kq2} - E'_d - (X'_q - X_{ls})i^r_{qs} \tag{3.1e}$$

$$T'_{do} p E'_q = -E'_q - (X_d - X'_d)[i^r_{ds} - \frac{X'_d - X''_d}{(X'_d - X_{ls})^2}(\psi^{'r}_{kd} + (X'_d - X_{ls})i^r_{ds} - E'_q)] + E'_{fd} \tag{3.1f}$$

$$T''_{do} p \psi^{'r}_{kd} = -\psi^{'r}_{kd} + E'_q - (X'_d - X_{ls})i^r_{ds} \tag{3.1g}$$

$$p\delta = \omega_r - \omega_e \tag{3.1h}$$

$$\frac{2H}{\omega_e} p\omega_r = T_M - T_e \tag{3.1i}$$

$$T_e = \psi^r_{ds} i^r_{qs} - \psi^r_{qs} i^r_{ds} \tag{3.1j}$$

3.1.1 Reduced-Order Generator/Infinite Bus Implementation

Similar to the detailed model, a reduced-order form of the generator/infinite-bus system, shown in Figure 2.7is convenient to consider machine dynamics/performance. The implementation of the reduced-order model is similar to the detailed model, described in the Chapter 2 in Section 2.3.4; however, there are changes in the calculation of stator currents. Specifically, to obtain an expression for the currents, (2.16a)-(2.16b) is substituted into (3.1a)-(3.1b) and the q- and d-axis currents are solved using:

$$\begin{bmatrix} X_q'' + X & -r_s \\ -r_s & -X_d'' - X \end{bmatrix} \begin{bmatrix} i_{qs}^r \\ i_{ds}^r \end{bmatrix} = \begin{bmatrix} v_{ds}^r + \psi_{qs}^{''r} \\ v_{qs}^r - \psi_{ds}^{''r} \end{bmatrix} \tag{3.2}$$

where X is the series reactance between the machine and infinite bus and where $\psi_{qs}^{''r}$ and $\psi_{ds}^{''r}$ are the last 2 term of (2.16a)-(2.16b):

$$\psi_{qs}^{''r} = -\frac{X_q'' - X_{ls}}{X_q' - X_{ls}} E_d' + \frac{X_q' - X_q''}{X_q' - X_{ls}} \psi_{kq2}^{'r} \tag{3.3a}$$

$$\psi_{ds}^{''r} = +\frac{X_d'' - X_{ls}}{X_d' - X_{ls}} E_q' + \frac{X_d' - X_d''}{X_d' - X_{ls}} \psi_{kd}^{'r} \tag{3.3b}$$

The machine stator terminal voltage is calculated from the stator currents and infinite bus voltage using the relationships in (3.4), which are derived from (2.24) by setting the derivative terms to 0 and $\omega_r = \omega_e$.

$$v_{qsb}^r = -X i_{ds}^r + v_{qs}^r \tag{3.4a}$$

$$v_{dsb}^r = X i_{qs}^r + v_{ds}^r \tag{3.4b}$$

$$v_{0sb} = v_{0s} \tag{3.4c}$$

The Simulink Implementation of the generator/infinite-bus system is shown in Figure 3.1. In the Figure 3.1, the **governor** and the **exciter** blocks are identical to those used in the detailed model and described in Chapter 1. The **source** function

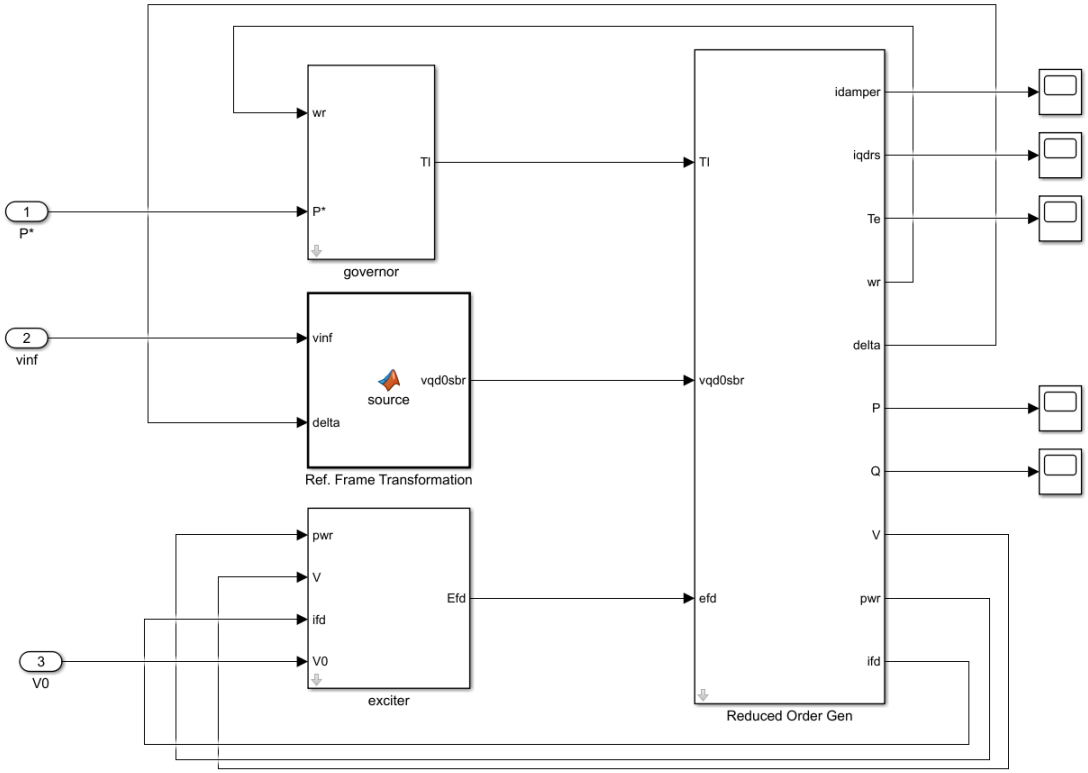

Fig. 3.1.: Reduced-Order Generator/Infinite Bus Implementation

block transforms the infinite bus voltage from the synchronous to the rotor reference frame based on (2.2). Inside the **Reduced Order Gen** subsystem, the generator reduced-order model is implemented, shown in Figure 3.2

The **ElectricDynamic** function block is used to calculate the state variables of the rotor electrical system. In the same block, the stator currents are also calculated based on (3.2). In the **MechanicalDynamic** function block, the electromagnetic torque and rotor speed are calculated. In the **Current** function block, the damper winding currents, the active and reactive power are established. Within the **psis** function block, the stator flux linkages per second and the stator voltages are all calculated. Last, inside **delta Calculation** block, the rotor angle with respect to the synchronous reference frame δ is calculated, shown in Figure 3.3 .

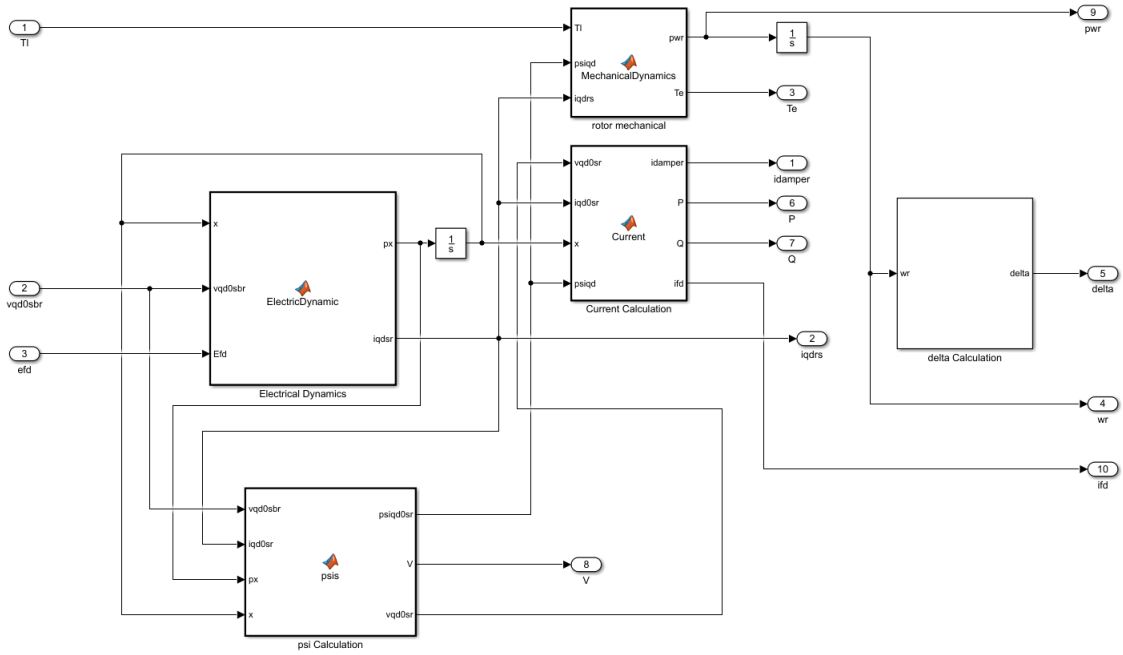

Fig. 3.2.: Generator Reduced-Order Model Implementation

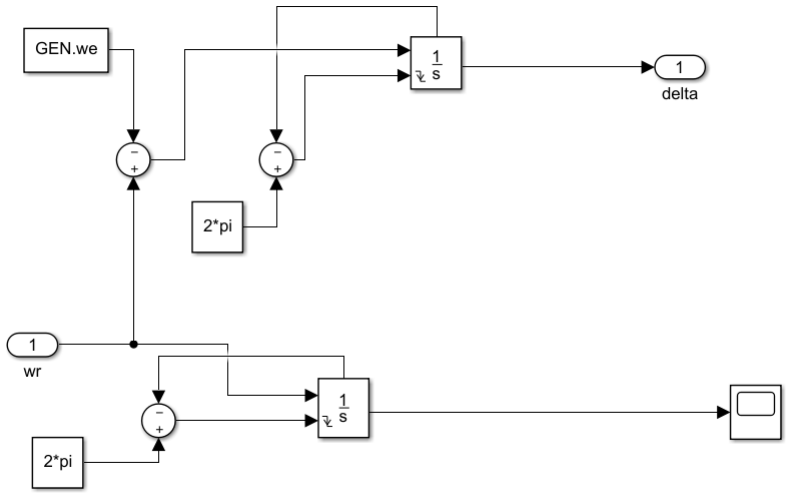

Fig. 3.3.: Generator Reduced-Order Model Rotor Angle calculation

3.1.2 Generator Detailed Model and Reduced-Order Model Comparison

Up to this point, two models have been constructed for the generator/infinite-bus system. Hence, a study has been performed to compare the two models. The

parameters used for the study are provided in the Appendix. The study consists of step changes in infinite bus voltage, the commanded power P_o and V_0. To be more specific, the infinite bus voltage magnitude drops from 1 per-unit to 0.9 per-unit at 50s and returns to 1 per-unit at 70s; the V_0 increases 0.1 per-unit at 100s; and finally, the P_o steps from 1 per-unit to 0.6 per-unit at 200s. The results are shown in Figure 3.4.

From the results, one can observe that as the infinite bus voltage drops, the machine d-axis voltage drops as well. As a result, the q-axis current drops as shown. However, since the commanded power is maintained at 1 per-unit, the d-axis current increases so that the generator will generate sufficient power. Another result of the drop in bus voltage is that the electric torque is less than the load torque, which leads to a decrease in the rotor speed and rotor angle. After the disturbance on the infinite bus voltage at 70s, one observes that all quantities go back to the pre-disturbance value, as expected. At 100s, an increase in the V_0 results in an increase in the machine terminal voltage, which proves the effectiveness of the exciter. Further, at 200s, an decrease in the P_o results in an decrease in the machine electrical power output, which demonstrates the control in the generator governor acts as expected.

From the step responses shown in Figure 3.4, it can be observed that detailed model has more high-frequency oscillation compared with a frequency of 60Hz that the reduced-order model does not capture. This is due to the neglecting of the fast stator transient in the reduced-order models. One notes that the slower dynamics are nearly identical. Comparing the simulation time, the time required for detailed model using a Simulink built-in ODE4(Runge-Kutta) algorithm, with a time-step of 1ms is 9.02s, whereas the reduced-order model with the same algorithm, but a time-step of 10ms is 1.21s. Hence, reduced-order model can be used to represent the slower dynamics of the generator electrical and mechanical systems, with an improvement in the simulation speed.

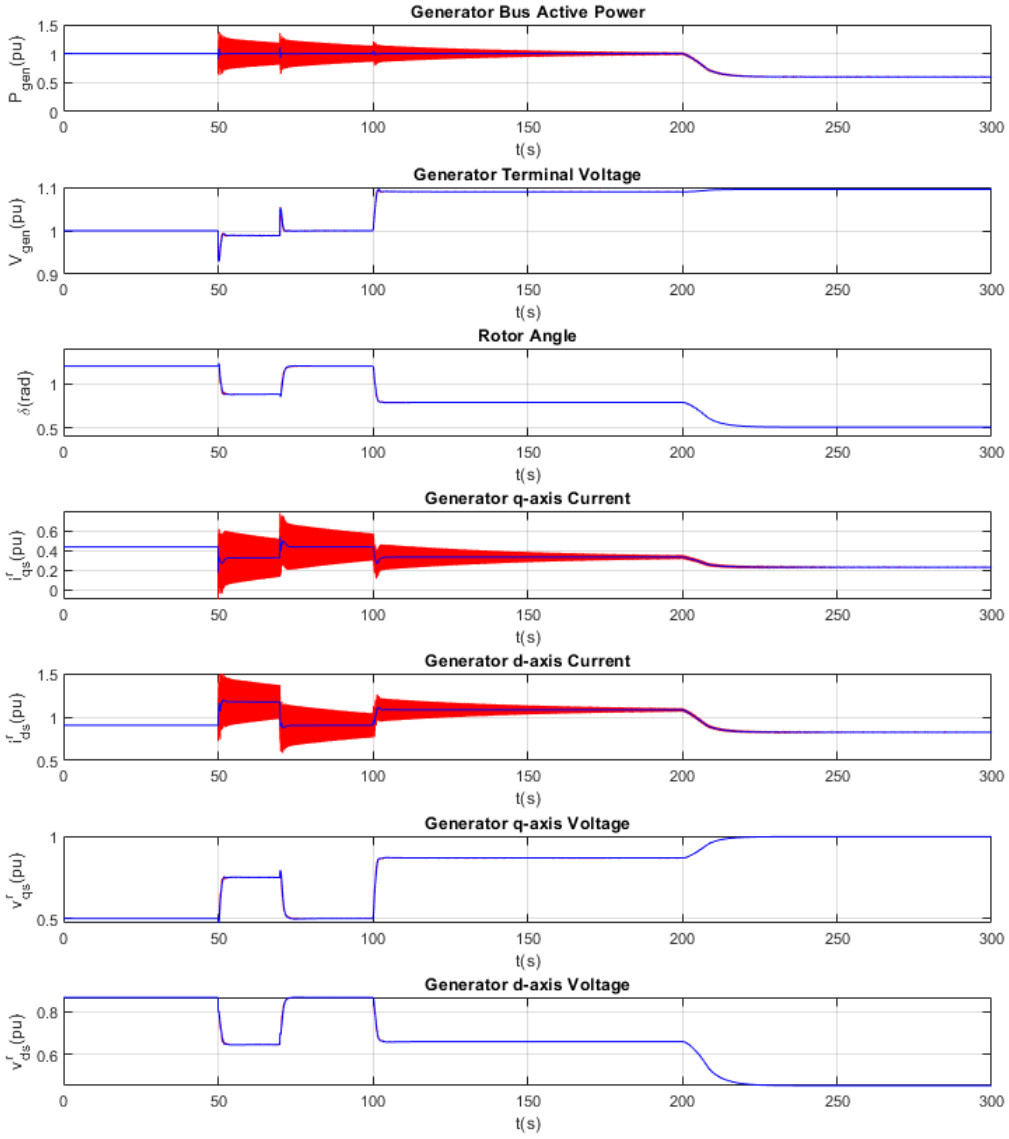

Fig. 3.4.: Generator/Infinite Bus Model Comparison for Detailed and Reduced-Order Model,blue lines are reduced-order model results and red lines are detailed model results

3.1.3 Structuring Models for Coupling to Network

A goal of using reduced-order models is to ignore the fast dynamics of the stator of the generators and induction machines, and the network. To couple the machine models to the network models, it is assumed that the voltages and the currents of the machine stator and the network are in steady state, details can be found in Purdue ECE 6330 lecture notes from Prof. Aliprantis. Thus, to integrate the generator reduced-order model in a system level, a phasor representation of the machine is used in the network calculation. To be more specific, in the per-unit system, by using (B.10):

$$\widetilde{V_{as}} = (v_{qs}^r - jv_{ds}^r)e^{j\delta} \tag{3.5a}$$

$$\widetilde{I_{as}} = (i_{qs}^r - ji_{ds}^r)e^{j\delta} \tag{3.5b}$$

Where δ is the angle between the synchronous reference frame and the local machine rotor reference frame, one can couple the generator and network models.

To represent the machine in phasor form, one can use (3.1), to express

$$\psi_{qs}^r = -X_q'' i_{qs}^r - \frac{X_q'' - X_{ls}}{X_q' - X_{ls}} E_d' + \frac{X_q' - X_q''}{X_q' - X_{ls}} \psi_{kq2}^{'r} \tag{3.6a}$$

$$\psi_{ds}^r = -X_d'' i_{ds}^r + + \frac{X_d'' - X_{ls}}{X_d' - X_{ls}} E_q' + \frac{X_d' - X_d''}{X_d' - X_{ls}} \psi_{kd}^{'r} \tag{3.6b}$$

Using (3.1a) to (3.1b), (3.6) and (3.5), a phasor voltage can be expressed:

$$\begin{aligned}
\widetilde{V_{as}} =&(v_{qs}^r - jv_{ds}^r)e^{j\delta} \\
=&\{(-X_d''i_{ds}^r + \frac{X_d'' - X_{ls}}{X_d' - X_{ls}}E_q' + \frac{X_d' - X_d''}{X_d' - X_{ls}}\psi_{kd}^{'r}) - r_s i_{qs}^r \\
&- j[-(-X_q''i_{qs}^r - \frac{X_q'' - X_{ls}}{X_q' - X_{ls}}E_d' + \frac{X_q' - X_q''}{X_q' - X_{ls}}\psi_{kq2}^{'r}) - r_s i_{ds}^r]\}e^{j\delta} \\
=&-(r_s + jX_d'')(i_{qs}^r - ji_{ds}^r)e^{j\delta} + \{(\frac{X_d'' - X_{ls}}{X_d' - X_{ls}}E_q' + \frac{X_d' - X_d''}{X_d' - X_{ls}}\psi_{kd}^{'r}) \\
&+ j[(X_d'' - X_q'')i_{qs}^r - \frac{X_q'' - X_{ls}}{X_q' - X_{ls}}E_d' + \frac{X_q' - X_q''}{X_q' - X_{ls}}\psi_{kq2}^{'r})]\}e^{j\delta} \\
=&-(r_s + jX_d'')\widetilde{I_{as}} + \{(\frac{X_d'' - X_{ls}}{X_d' - X_{ls}}E_q' + \frac{X_d' - X_d''}{X_d' - X_{ls}}\psi_{kd}^{'r}) \\
&+ j[(X_d'' - X_q'')i_{qs}^r - \frac{X_q'' - X_{ls}}{X_q' - X_{ls}}E_d' + \frac{X_q' - X_q''}{X_q' - X_{ls}}\psi_{kq2}^{'r})]\}e^{j\delta}
\end{aligned} \tag{3.7}$$

Defining a new phasor variable $\widetilde{E_{as}}$, the voltage can be expressed

$$\widetilde{E_{as}} = \{\frac{X_d'' - X_{ls}}{X_d' - X_{ls}}E_q' + \frac{X_d' - X_d''}{X_d' - X_{ls}}\psi_{kd}^{'r} - \frac{X_q'' - X_{ls}}{X_q' - X_{ls}}E_d' + \frac{X_q' - X_q''}{X_q' - X_{ls}}\psi_{kq2}^{'r}\}e^{j\delta} \tag{3.8}$$

which can be expressed

$$\widetilde{V_{as}} = -(r_s + jX_d'')\widetilde{I_{as}} + j(X_d'' - X_q'')i_{qs}^r e^{j\delta} + \widetilde{E_{as}} \tag{3.9}$$

and can be rearranged to express the phasor current as

$$\widetilde{I_{as}} = \frac{1}{(r_s + jX_d'')}[j(X_d'' - X_q'')i_{qs}^r e^{j\delta} + \widetilde{E_{as}} - \widetilde{V_{as}}] \tag{3.10}$$

From these expressions, one can observe that the generator terminal voltage phasor can be calculated as the summation of an internal voltage source and the voltage across a series RL impedance. Defining $Y_s = \frac{1}{(r_s + jX_d'')}$ and $S = j(X_d'' - X_q'')i_{qs}^r e^{j\delta}$, the voltage can be expressed in a form:

$$\widetilde{I_{as}} = Y_s(S + \widetilde{E_{as}} - \widetilde{V_{as}}) \tag{3.11}$$

3.2 Load Model

Identical to the detailed system model, in the reduced-order system model, the constant admittance and two induction machines. To couple to the network model, the three components are treated as distinct load buses.

3.2.1 Constant Admittance Model

The constant admittance (RC) load is added to the system admittance matrix as shown in the Appendix equation (C.12). The constant admittance is the load that is connected to ground, described by Y_i.

3.2.2 Reduced-Order Induction Machine Model

To establish a reduced-order model of an induction machine, which is similar to a reduced-order model of a synchronous machine, the stator transients are neglected. This is done by setting the p to 0 and $\omega_r = \omega_e$ in (2.32). This yields the model in per-unit form:

$$v_{qs}^{e} = r_s i_{qs}^{e} + \psi_{ds}^{e} \tag{3.12a}$$

$$v_{ds}^{e} = r_s i_{ds}^{e} - \psi_{qs}^{e} \tag{3.12b}$$

$$v_{0s} = r_s i_{0s} \tag{3.12c}$$

$$\omega_e v_{qr}^{'e} = \omega_e r_r^{'} i_{qr}^{'e} + (\omega_e - \omega_r)\psi_{dr}^{'e} + p\psi_{qr}^{'e} \tag{3.12d}$$

$$\omega_e v_{dr}^{'r} = \omega_e r_r^{'} i_{dr}^{'e} - (\omega_e - \omega_r)\psi_{qr}^{'e} + p\psi_{dr}^{'e} \tag{3.12e}$$

$$\omega_e v_{0r}^{'} = \omega_e r_r^{'} i_{0r}^{'} + p\psi_{0r}^{'} \tag{3.12f}$$

To couple the machine and network models, the phasor relationship:

$$\widetilde{V_{as}} = (v_{qs}^e - jv_{ds}^e) \tag{3.13a}$$

$$\widetilde{I_{as}} = (i_{qs}^e - ji_{ds}^e) \tag{3.13b}$$

is utilized. Using (3.12a) to (3.12c), (2.33), and (3.13), one can express the phasor voltge as:

$$\begin{aligned}
\widetilde{V_{as}} &= (v_{qs}^e - jv_{ds}^e) \\
&= r_s i_{qs}^e + \psi_{ds}^e - j(r_s i_{ds}^e - \psi_{qs}^e) \\
&= r_s(i_{qs}^e - ji_{ds}^e) + \psi_{ds}^e + j\psi_{qs}^e \\
&= r_s\widetilde{I_{as}} + j(\psi_{qs}^e - j\psi_{ds}^e) \\
&= r_s\widetilde{I_{as}} + j[X_{ss}i_{qs}^e + X_M i_{qr}^{'e} - j(X_{ss}i_{ds}^e + X_M i_{dr}^{'e})] \\
&= r_s\widetilde{I_{as}} + j(X_{ss}\widetilde{I_{as}} + X_M i_{qr}^{'e} - jX_M i_{dr}^{'e}) \\
&= (r_s + jX_{ss})\widetilde{I_{as}} + jX_M(i_{qr}^{'e} - ji_{dr}^{'e})
\end{aligned} \tag{3.14}$$

where $X_{ss} = X_{ls} + X_M$.

From (2.33), the rotor winding currents can be expressed in terms of the rotor flux linkages per second and the stator currents:

$$i_{qr}^{'e} = \frac{\psi_{qr}^{'e} - X_M i_{qs}^e}{X_{rr}} \tag{3.15a}$$

$$i_{dr}^{'e} = \frac{\psi_{dr}^{'e} - X_M i_{ds}^e}{X_{rr}} \tag{3.15b}$$

Where $X'_{rr} = X'_{lr} + X_M$.

Substituting (3.15) into (3.14):

$$\begin{aligned}
\widetilde{V_{as}} &= (v_{qs}^{e} - jv_{ds}^{e}) \\
&= (r_s + jX_{ss})\widetilde{I_{as}} + jX_M \frac{(\psi_{qr}^{'e} - X_M i_{qs}^{e}) - j(\psi_{dr}^{'e} - X_M i_{ds}^{e})}{X'_{rr}} \\
&= (r_s + jX_{ss})\widetilde{I_{as}} + j\frac{X_M}{X'_{rr}}[\psi_{qr}^{'e} - j\psi_{dr}^{'e} - X_M(i_{qs}^{e} - ji_{ds}^{e})] \\
&= (r_s + jX_{ss})\widetilde{I_{as}} + j\frac{X_M}{X'_{rr}}(\psi_{qr}^{'e} - j\psi_{dr}^{'e} - X_M\widetilde{I_{as}}) \\
&= (r_s + jX_{ss} - j\frac{X_M^2}{X'_{rr}})\widetilde{I_{as}} + j\frac{X_M}{X'_{rr}}(\psi_{qr}^{'e} - j\psi_{dr}^{'e}) \\
&= (r_s + jX_{ss} - j\frac{X_M^2}{X'_{rr}})\widetilde{I_{as}} + \frac{X_M}{X'_{rr}}\psi_{dr}^{'e} + j\frac{X_M}{X'_{rr}}\psi_{qr}^{'e}
\end{aligned} \tag{3.16}$$

Defining a phasor variable $\widetilde{E_{as}}$, where

$$\widetilde{E_{as}} = \frac{X_M}{X'_{rr}}\psi_{dr}^{'e} + j\frac{X_M}{X'_{rr}}\psi_{qr}^{'e} \tag{3.17}$$

the voltage can be expressed:

$$\widetilde{V_{as}} = (r_s + jX_{ss} - j\frac{X_M^2}{X'_{rr}})\widetilde{I_{as}} + \widetilde{E_{as}} \tag{3.18}$$

which can be rearranged to express the stator current as:

$$\widetilde{I_{as}} = \frac{1}{r_s + jX_{ss} - j\frac{X_M^2}{X'_{rr}}}[-\widetilde{E_{as}} + \widetilde{V_{as}}] \tag{3.19}$$

So far it has been assumed that positive stator current is defined into the machine. For model implementation, it is useful to define that the current is defined positive out of the machine, similar to the generator. This results in induction machine loads

acting as power sources to the network with a negative power injection. With the direction of positive currents reversed: (3.19) is revised:

$$\widetilde{I_{as}} = \frac{1}{r_s + jX_{ss} - j\frac{X_M^2}{X'_{rr}}}[\widetilde{E_{as}} - \widetilde{V_{as}}] \tag{3.20}$$

From the phasor voltage equations, one can observe that the induction terminal voltage phasor can be calculated as the summation of an internal voltage source and the voltage across a series RL impedance. Defining $Y_s = \frac{1}{r_s + jX_{ss} - j\frac{X_M^2}{X'_{rr}}}$, current can be expressed using the voltage and impedance as:

$$\widetilde{I_{as}} = Y_s(\widetilde{E_{as}} - \widetilde{V_{as}}) \tag{3.21}$$

3.3 Infinite Bus

The infinite bus is a constant voltage source with its $qd0$ voltages fixed. However, as mentioned in detailed model, there exists a small resistance between the infinite bus and the transmission system as shown in Figure 2.21. Thus, by defining the admittance to $\frac{1}{R_{inf}}$, the current phasor out of the infinite bus can be expressed in a form: (3.21):

$$\widetilde{I_{as}} = Y_s(\widetilde{E_{as}} - \widetilde{V_{as}}) \tag{3.22}$$

where $\widetilde{E_{as}}$ is the infinite bus voltage, which is fixed and $\widetilde{V_{as}}$ is the voltage after the small resistance between the infinite bus and the transmission line.

3.4 Simulink Implementation of Reduced-Order System Model

3.4.1 Energy Source/Load General Form

From (3.11), (3.21), and (3.22), all of the components of the microgrid can be integrated to express the stator and network currents in terms of voltages and impedances in a form:

$$\mathbf{I} = \mathbf{Y}_s(\mathbf{S} + \mathbf{E} - \mathbf{V}) \tag{3.23}$$

where $\mathbf{I}$ is a column vector that contains all the phasor currents, $\mathbf{Y_s}$ is a diagonal matrix with corresponding components Y_s, $\mathbf{E}$ is a column vector that contains all the bus $\widetilde{E_{as}}$ term, and $\mathbf{V}$ is a column vector that contains all the bus voltage phasor $\widetilde{V_{as}}$. The $\mathbf{S}$ is also a column vector, whose entry is S if it is a generator bus (3.11), and 0 if it is the induction machine bus or infinite bus. Importantly, the $\mathbf{E}$ matrix entries are the outputs of state models for the generator and the induction machines, or a constant, for the infinite bus. This property allows the system to be simulated without any algebraic loops.

One can express the voltage versus current relationship of the network using an admittance model, as shown in (C.1) in the Appendix. Equating the currents of (C.1) and those of (3.23), results in

$$\mathbf{YV} = \mathbf{Y}_s(\mathbf{S} + \mathbf{E} - \mathbf{V}) \tag{3.24a}$$

$$(\mathbf{Y} + \mathbf{Y}_s)\mathbf{V} = \mathbf{Y}_s(\mathbf{S} + \mathbf{E}) \tag{3.24b}$$

$$\mathbf{V} = (\mathbf{Y} + \mathbf{Y}_s)^{-1}\mathbf{Y}_s(\mathbf{S} + \mathbf{E}) \tag{3.24c}$$

where $\mathbf{Y}$ is the original network admittance matrix.

Plugging (3.24c) into (3.23):

$$\mathbf{I} = \mathbf{Y}_s[I - (\mathbf{Y} + \mathbf{Y}_s)^{-1}\mathbf{Y}_s](\mathbf{S} + \mathbf{E}) \tag{3.25}$$

where I is the identity matrix.

To simplify (3.25), the Woodbury matrix identity is used [15]:

$$(\mathbf{Y} + \mathbf{Y_s})^{-1} = \mathbf{Y}_s^{-1} - \mathbf{Y}_s^{-1}(\mathbf{Y}^{-1} + \mathbf{Y}_s^{-1})^{-1} \tag{3.26}$$

Plugging (3.26) into (3.25)

$$\mathbf{I} = \mathbf{Y}_s(I - I + \mathbf{Y}_s^{-1}(\mathbf{Y}^{-1} + \mathbf{Y}_s^{-1})^{-1})(\mathbf{S} + \mathbf{E}) \tag{3.27a}$$

$$= (\mathbf{Y}^{-1} + \mathbf{Y}_s^{-1})^{-1}(\mathbf{S} + \mathbf{E}) \tag{3.27b}$$

$$= \mathbf{Y}_{new}(\mathbf{S} + \mathbf{E}) \tag{3.27c}$$

In the 5-bus system, since only the infinite bus, the generator and the induction machines are injecting power to the network as described in the previous section, these 4 buses are referred to as energy sources. As a result, the input currents of busses that do not contain energy sources 0. Expanding (C.1) in the Appendix for the 5-bus system:

$$\begin{bmatrix} I_{inf} \\ I_{gen} \\ I_{ind1} \\ \hline I_{ind2} \\ 0 \\ \hline \dots \end{bmatrix} = \left[\begin{array}{cccc|cc} Y_{11} & Y_{12} & Y_{13} & Y_{14} & Y_{15} & \dots \\ Y_{21} & Y_{22} & Y_{23} & Y_{24} & Y_{25} & \dots \\ Y_{31} & Y_{32} & Y_{33} & Y_{34} & Y_{35} & \dots \\ \hline Y_{41} & Y_{42} & Y_{43} & Y_{44} & Y_{45} & \dots \\ \hline Y_{51} & Y_{52} & Y_{53} & Y_{54} & Y_{55} & \dots \\ \dots & \dots & \dots & \dots & \dots & \dots \end{array}\right] \begin{bmatrix} V_{inf} \\ V_{gen} \\ V_{ind1} \\ \hline V_{ind2} \\ V_5 \\ \hline \dots \end{bmatrix} \tag{3.28}$$

and placing it in a simpler form yields:

$$\left[\begin{array}{c} \mathbf{I}_{eng} \\ \hline \mathbf{0} \end{array}\right] = \left[\begin{array}{c|c} \mathbf{A} & \mathbf{B} \\ \hline \mathbf{C} & \mathbf{D} \end{array}\right] \left[\begin{array}{c} \mathbf{V}_{eng} \\ \hline \mathbf{V}_0 \end{array}\right] \tag{3.29}$$

Since the lower part of the $\mathbf{I}$ vector are all 0, it is useful to represent $\mathbf{I_{eng}}$ in the form:

$$\mathbf{I}_{eng} = \mathbf{Y}_{eng}\mathbf{V}_{eng} \tag{3.30}$$

From (3.29), the $\mathbf{Y_{eng}}$ can be solved by first expressing (3.29):

$$\mathbf{I}_{eng} = \mathbf{A}\mathbf{V}_{eng} + \mathbf{B}\mathbf{V}_0 \tag{3.31a}$$

$$\mathbf{0} = \mathbf{C}\mathbf{V}_{eng} + \mathbf{D}\mathbf{V}_0 \tag{3.31b}$$

and then using (3.31b):

$$\mathbf{V}_0 = -\mathbf{D}^{-1}\mathbf{C}\mathbf{V}_{eng} \tag{3.32}$$

Plugging (3.32) into (3.31a):

$$\mathbf{I}_{eng} = \mathbf{A}\mathbf{V}_{eng} - \mathbf{B}\mathbf{D}^{-1}\mathbf{C}\mathbf{V}_{eng} \tag{3.33a}$$

$$\mathbf{I}_{eng} = (\mathbf{A} - \mathbf{B}\mathbf{D}^{-1}\mathbf{C})\mathbf{V}_{eng} \tag{3.33b}$$

Hence, $\mathbf{Y}_{eng} = \mathbf{A} - \mathbf{B}\mathbf{D}^{-1}\mathbf{C}$.

Summarizing, by equating (3.30) and (3.27c), the current phasor of the energy sources can be obtained by first calculating $\mathbf{Y}_{eng}$ from $\mathbf{Y}_{new}$ using the partitioned-matrices $\mathbf{A}$, $\mathbf{B}$, $\mathbf{C}$ and $\mathbf{D}$, and then setting $\mathbf{V}_{eng} = [\mathbf{S} + \mathbf{E}]$. As a result:

$$\mathbf{I}_{eng} = (\mathbf{A} - \mathbf{B}\mathbf{D}^{-1}\mathbf{C})(\mathbf{S} + \mathbf{E}) \tag{3.34}$$

Since the matrix $\mathbf{E}$ is calculated from the states of each energy sources, and derivatives of each of the states are calculated from the q- and d-axis currents of each energy sources, it is convenient to express equation (3.34) in terms of the q- and d-axis currents. To do additional matrices are utilized.

The first matrix is defined as $\mathbf{T}$, which is used to relate the current phasor of the energy sources to the q- and d-axis currents

$$\mathbf{I}_{eng} = \mathbf{T}(\mathbf{I}_q - j\mathbf{I}_d) \tag{3.35a}$$

$$\mathbf{T} = \mathbf{diag}\{e^{j\phi}\} \tag{3.35b}$$

Where $\mathbf{I}_q$ and $\mathbf{I}_q$ are current column vectors for each of the energy source.The matrix is derived in (B.9) and (B.10) in the Appendix.

The next matrix utilized, $\mathbf{S}$, is defined in terms of q-axis currents and machine subtransient reactances as:

$$\mathbf{S} = j\mathbf{S}_x\mathbf{T}\mathbf{I}_q \tag{3.36a}$$

$$\mathbf{S}_x = \mathbf{diag}\{X''_d - X''_q\} \tag{3.36b}$$

where $X_d^{''}$ and X''_q are the wound-rotor synchronous machine subtransient reactances.

Using these matrices, (3.30) can be expressed in term of the q- and d-axis currents:

$$\mathbf{T}(\mathbf{I}_q - j\mathbf{I}_d) = \mathbf{Y}_{eng}(j\mathbf{S}_x\mathbf{T}\mathbf{I}_q + \mathbf{E}) \tag{3.37}$$

After rearranging the terms, (3.37) can be expressed:

$$(I - j\mathbf{Y}_{eng}\mathbf{S}_x)\mathbf{T}\mathbf{I}_q - j\mathbf{T}\mathbf{I}_d = \mathbf{Y}_{gen}\mathbf{E} \tag{3.38}$$

For the convenience of the calculation and implementation, (3.38) is decomposed into real and imaginary parts:

$$(I - j\mathbf{Y}_{eng}\mathbf{S}_x)\mathbf{T} = a + jb \tag{3.39a}$$

$$-j\mathbf{T} = c + jd \tag{3.39b}$$

$$\mathbf{Y}_{eng}\mathbf{E} = e + jf \tag{3.39c}$$

Hence, the currents of each energy source are solved by the linear system:

$$\begin{bmatrix} a & c \\ b & d \end{bmatrix} \begin{bmatrix} \mathbf{I}_q \\ \mathbf{I}_d \end{bmatrix} = \begin{bmatrix} e \\ f \end{bmatrix} \tag{3.40}$$

Once the q- and d-axis currents are solved, they can be used to update the state derivatives. In addition, by using (3.28), the voltages of each buses is obtained.

3.4.2 Block Diagram

The overall Simulink implementation of the reduced-order microgrid model is shown in Figure 3.5. The inputs to the model are the infinite bus voltage, P_o for the generator governor and V_0 generator exciter.

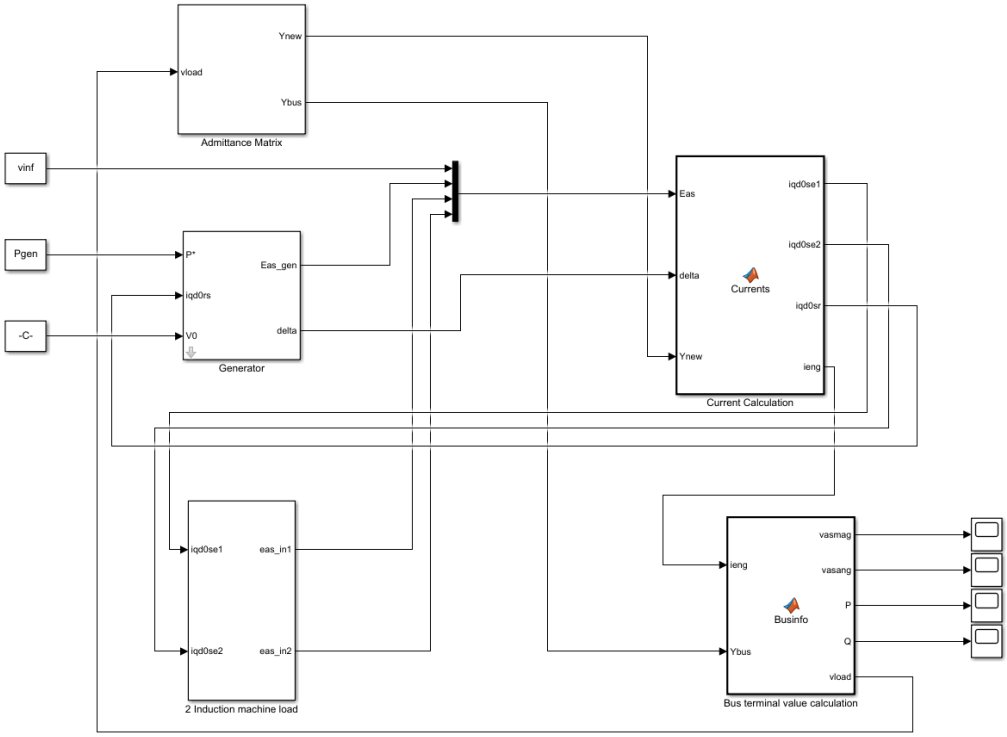

Fig. 3.5.: 5-bus System Reduced-Order Model Implementation

Admittance Matrix

At the top part of Figure 3.5, an **Admittance Matrix** block, detailed in Figure 3.6, is used to calculate the system admittance matrix and the $\mathbf{Y}_{new}$ described above. The admittance matrix are based on the system parameters and the details are explained in the Appendix. Due the existence of the LTC, the admittance can vary once the tap setting changes. Hence the tap-changing mechanism control block described in the Chapter 2 is included.

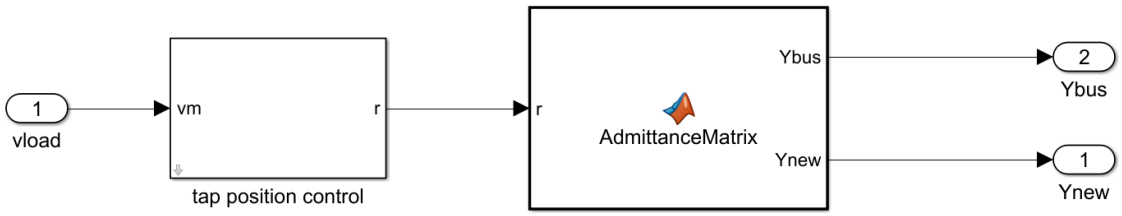

Fig. 3.6.: Reduced-Order Model Admittance Matrix subblock

Generator

Underneath the **Generator** subsystem, the generator reduced-order model is implemented, as shown in Figure 3.7.

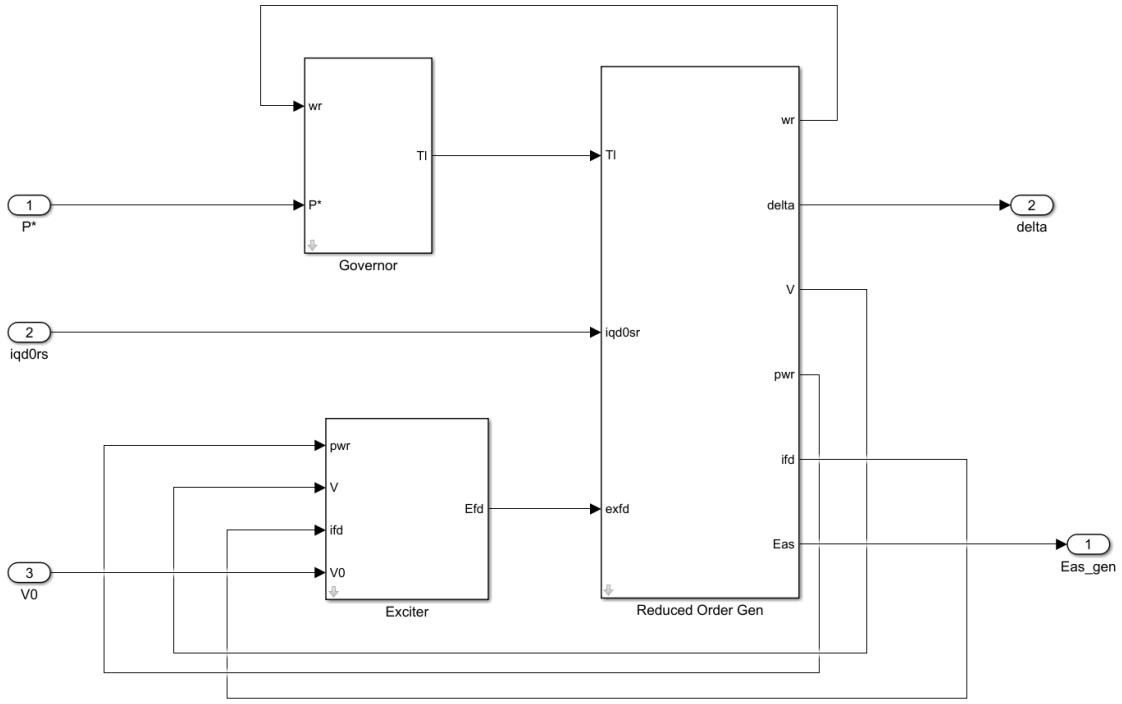

Fig. 3.7.: Generator Reduced-Order Model in 5-bus System

The implementation is similar to the generator/infinite-bus system. The difference is that the model here uses the currents as inputs, whereas in the generator/infinite-

bus system, the model uses the voltage as inputs. Underneath the **Reduced Order Gen** block in Figure 3.7, the machine rotor dynamics are implemented, as shown in Figure 3.8.

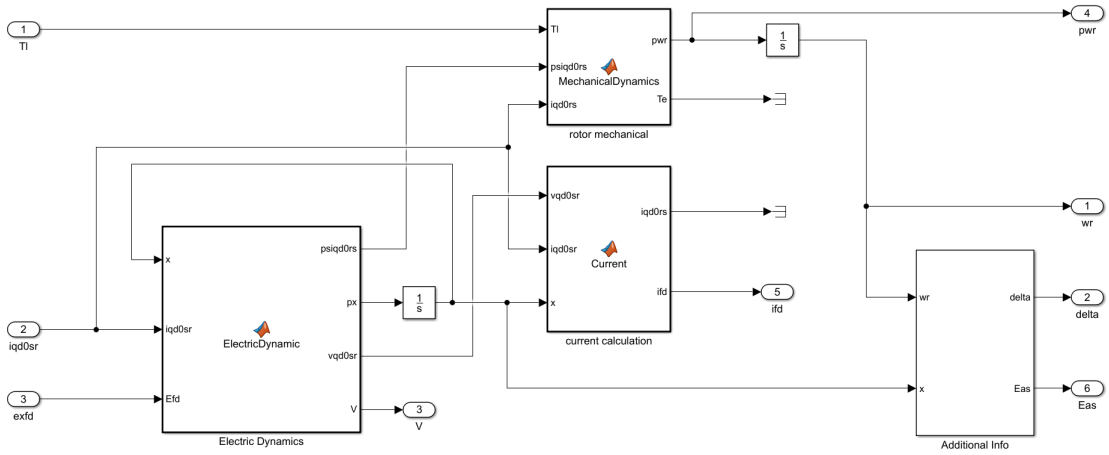

Fig. 3.8.: Reduced-Order Model Generator subblock

The **Additional Info** block in Figure 3.8 is used to calculate the rotor angle δ and the internal voltage E_{as} in (3.11), shown in Figure 3.9.

As can be observed from the block diagram, the inputs to the generator block are generator control inputs P_o and V_0, and the generator stator currents in the rotor reference frame. The outputs of the generator block are the generator internal voltage and the rotor angle.

Induction Machine

There are two induction machines underneath the induction machine load model as described in the 5-bus system. For each of the induction machines, the subsystem is shown in Figure 3.10.

The **dynamics** function block is used to calculate the states for the induction machine in (3.12), the **EasCal** function block calculates the internal voltage of the induction machine, defined in (3.17). The **loadtorque** block calculates the load

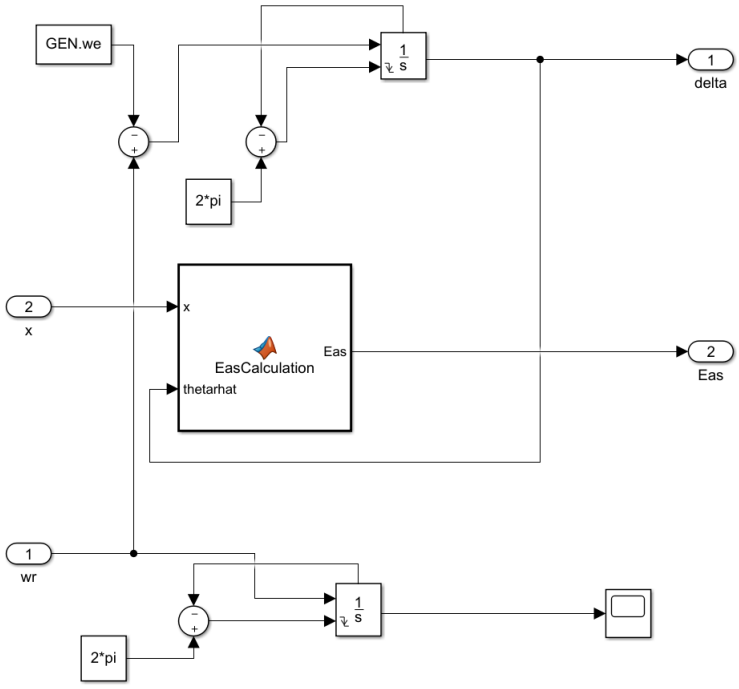

Fig. 3.9.: Reduced-Order Model Generator Addition Info block

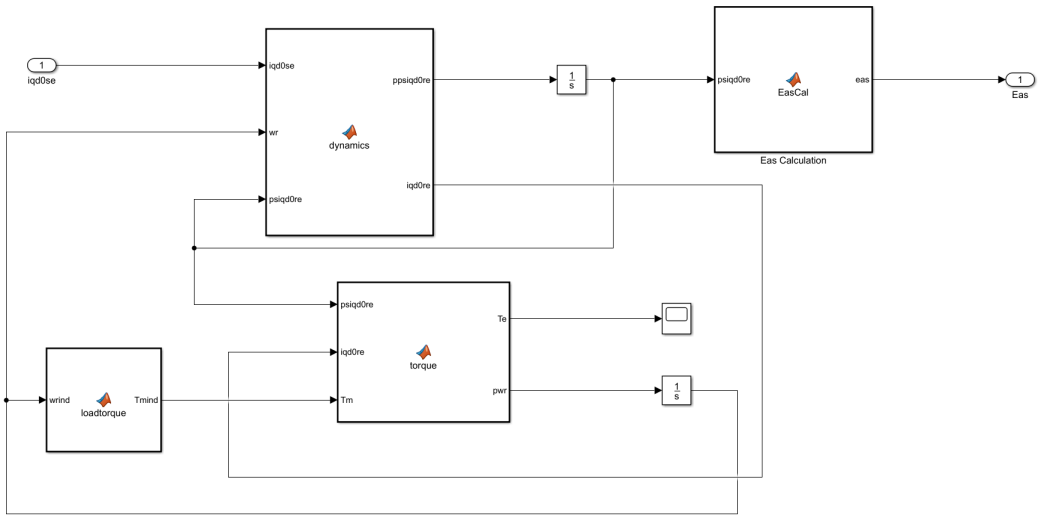

Fig. 3.10.: Reduced-Order Model Induction Machine Simulink Implementation

torque based on the rotor speed characterized by (2.45). The **torque** is used to calculates the rotor electromagnetic torque and the rotor angular velocity. To summarize, similar to the generator model, the inputs to the induction machine are the

stator currents in the synchronous reference frame, and the outputs are the induction machine internal voltage.

Currents Calculation

The **Currents** function block creates all the matrix $\mathbf{S}_x$, $\mathbf{T}$ and $\mathbf{E}$ for the calculation of the energy source currents based on (3.39) and (3.40). The inputs to this function are the internal voltage for each of the energy sources, the rotor angle for the generator and the modified admittance matrix $\mathbf{Y}_{new}$. The outputs are the generator currents in the rotor reference frame, the induction machine currents in the synchronous reference frame, and the currents of the induction machine, generator, and infinite bus in phasor form.

Businfo

With all the currents calculated for the energy sources, the bus information can be calculated. The voltages of each bus can be calculated based on the equation (3.28), and as a results, the complex power can be calculated. Apart from the bus voltages, currents and power calculation, the block output the load bus voltage for the LTC to control the tap setting.

3.4.3 States Initial Conditions

The initial conditions of the states are calculated in a manner similar to the detailed model. This is described in Chapter 2 and thus is not discussed further in this chapter. However, it is noted that since the reduced-order models neglect all stator transient, initial conditions for stator states are not calculated in the reduced-order model.

3.4.4 Representative System Response of Reduced-Order Model

Using the model of the system components and Simulink Implementation described, the study highlighted in Chapter 2 is repeated. Specifically, starting with the system at steady state at the operating point described in the Appendix, with the constant admittance bus drawing 60% of the load power, the two induction machines each drawing 20% of the load power, the commanded power of the generator steps from 0.6 per-unit to 0.4 per-unit at 50s. The the results are shown in Figure 3.11 and Figure 3.12.

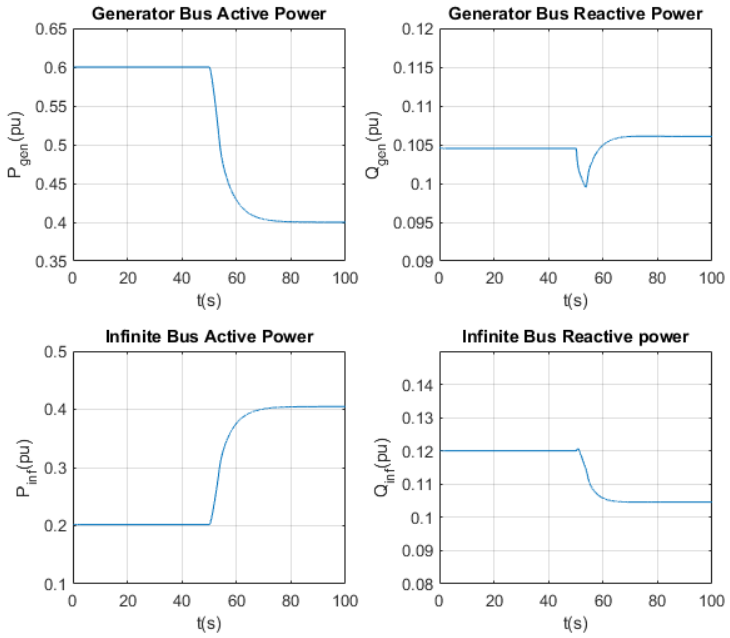

Fig. 3.11.: Reduced-Order Model Simulation Results due to Generator Commanded Power Change(a)

From the responses of the reduced-order model, it can be observed that behavior predicted is almost identical to the ones shown in detailed model, which proves the validity of the reduced-order model. The results shown in the figures again proves the effectiveness of the controls in the governor and LTC. Due to the control in the governor of the generator, the generator active power output tracks the commanded

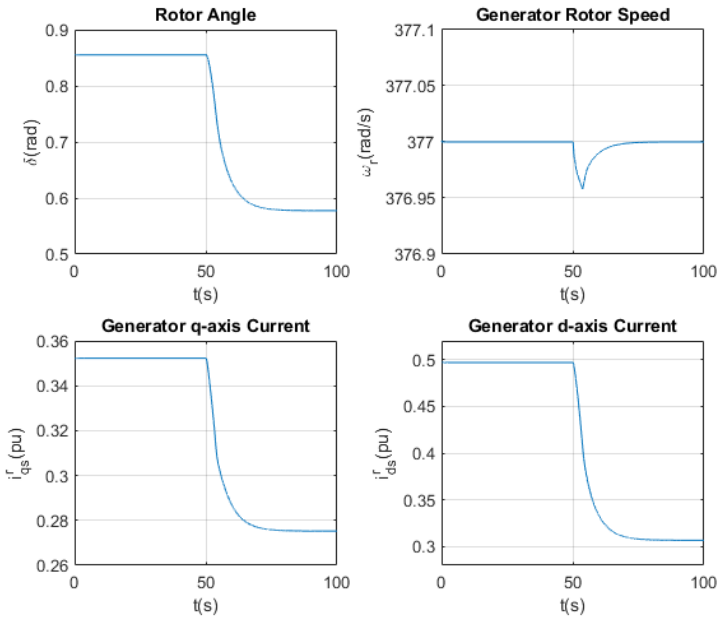

Fig. 3.12.: Reduced-Order Model Simulation Results due to Generator Commanded Power Change(b)

power. Due to the LTC, the induction machine terminal voltage stays within 1 ± 0.01 per-unit so that the load power does not change, which also keeps the total active power output of the infinite bus and generator stays at 0.8 per-unit constantly. Since there is no huge disturbance on the stator voltages in either the generator or the induction machine, there is no fast dynamics related to the stator transients in the simulation response. By using the Simulink variable step solver ODE23tb with maximum time-step 2s, the simulation for the same study in detailed model using the is 8.73s, but the simulation time for reduced-order model is 3.37s. Hence, for the power command changes, reduced-order model can be a great alternative to detailed model. However, as shown in the Figure 3.4, when the machine stator voltages changes, there is a great amount of oscillations with frequency of 60Hz that reduced-order model fails to capture. Therefore, reduced-order model is not useful for control designs or studies that are related to these transient oscillations. Apart from the step changes for the power command and voltage command in the generator, other types

of study can be done by using the reduced-order model. More details of the models can be found in the Chapter 5, where different studies are done and the conclusions are drawn based on the model responses.

4. BEHAVIORAL MODEL

The reduced-order models developed in Chapter 4 are commonly used to model power systems. Further reductions of the models have been explored in order to facilitate their use in model-based control [7], [16]. Specifically, in [7], the researchers have focused on applying singular-perturbation techniques to eliminate some rotor electrical dynamics. In [16], the researchers have placed the models in a structure that is tailored for efficient computation within the algorithms used to solve MPC problems. In this chapter, simplified behavioral models are considered as an alternative to the those based upon traditional electric machine models. Specifically, for the generator a goal is to consider whether the dynamics of the machine, governor, and exciter can be accurately described in an aggregate sense using simplified first-order models in tandem with corresponding limits and rate-of-change limits. To do so, the behavioral model of the generator system is structured to utilize real and reactive power as states. In the case of the induction machine, a behavioral model is considered in which the real and reactive power are estimated using a steady-state equivalent circuit with the rotor slip selected as a state variable. In this chapter, both models, and the means to couple them to the network model, are derived.

4.1 Generation System

As mentioned in previous chapters, the generation system has two control inputs, the P_o to the governor and the V_0 to the exciter. To derive the behavioral model of the generation system, the generator/infinite bus system is used. The response of the active and reactive power step to changes P_o and V_0, were observed. Example responses, where the P_o was stepped from 0.6 per-unit to 0.7 per-unit, and V_0 was stepped from 1.023 per-unit to 1.033 per-unit are shown in Figures 4.1 and Figure 4.2, respectively.

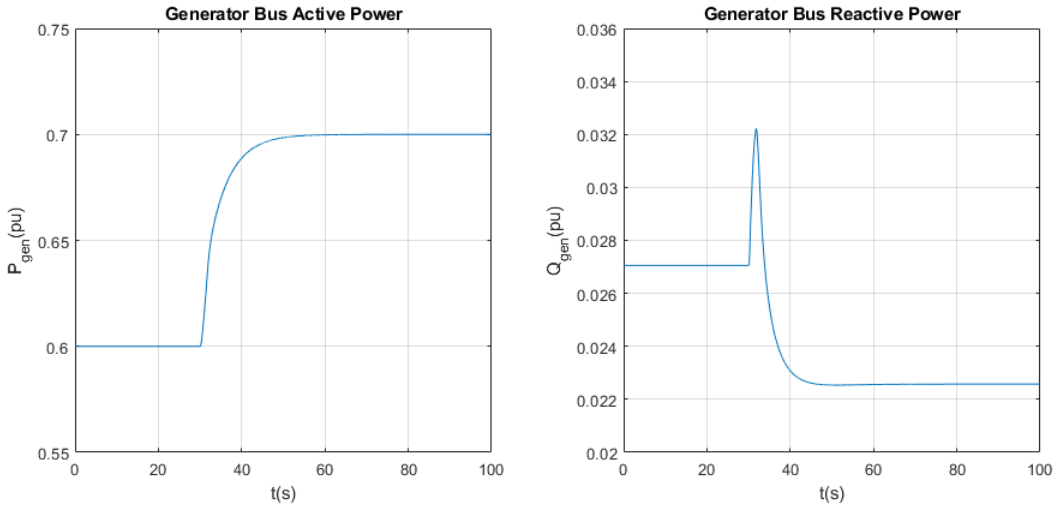

Fig. 4.1.: PQ step response to P_o

From Figure 4.1, one can observe that the real power out of the generator has the characteristics of a first-order response to P_o. Exploring the time-constant of the response, it is consistent with that of the reheater in the governor, T_r. From Figure 4.2, one can observe that the real power out of the generator changes with a step in V_o. However, considering the overall change in power level, it is relatively minor. In addition, the response is consistent with the fast stator dynamics, which are typically ignored in power system models. Moreover, the change in V_o does not create a change

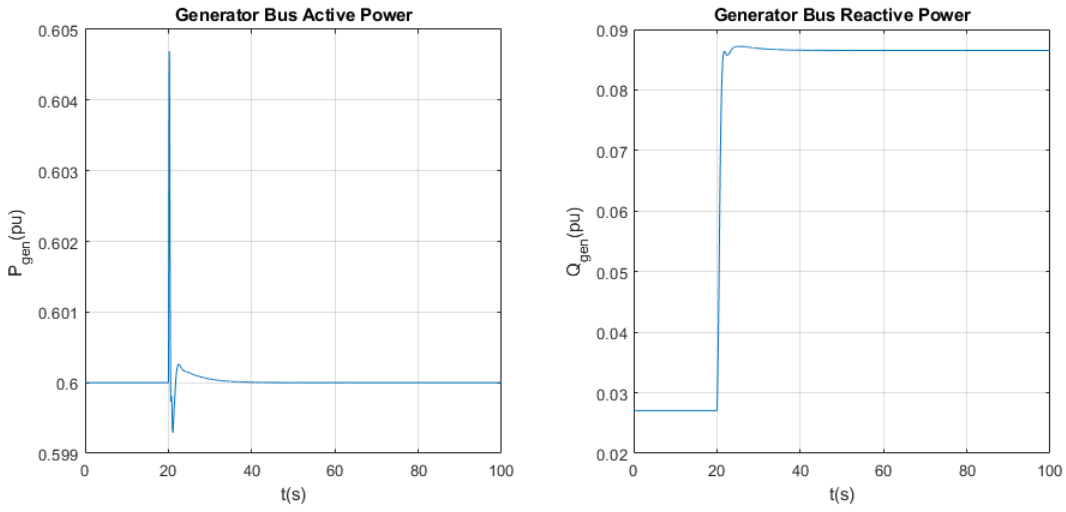

Fig. 4.2.: PQ step response to V_0

in steady-state power. From these observations, a behavioral transfer function of the real power out of the generator is expressed:

$$P^g_{beh} = \frac{P_o}{1 + T_r s} \tag{4.1a}$$

Further investigations have shown that this model is reasonable, provided one does not exceed the slew rate limits that are present in the governor.

Considering the reactive power, shown in Figure 4.1, one can see that it indeed changes with the commanded P_o. Here, one notes that the reactive power initially increases prior to decreasing in a manner consistent with a first-order response on a time-scale of T_r to a new steady-state. This behavior appears as a non-minimum phase-type response. Considering the reactive power response to the step in V_o , one can see there is a relatively rapid step to a new steady state.This dynamic is approximated as a first-order transfer function with a time constant consistent with

the d-axis transient time constant. Combining the responses, a transfer function relating reactive power to system inputs is expressed:

$$Q^g_{beh} = \frac{Q^g_{ss}}{1 + T'_{do}s} + \frac{sP^g_{beh}}{1 + T_r s} \tag{4.2a}$$

In 4.2, Q^g_{ss} is the steady-state reactive power. It provides the relationship between the reactive power and V_o. Specifically, to obtain Q^g_{ss}, the expression for reactive power in terms of qd variables, (2.5) in Chapter 2, is used. In per unit, assuming steady state the relationship between reactive power, stator current, and field voltage is expressed:

$$Q^g_{ss} = -X_q {I^r_{qs}}^2 - X_d {I^r_{ds}}^2 + I^r_{ds} E'_{fd} \tag{4.3}$$

where I^r_{qs} and I^r_{ds} are the machine stator currents. Considering the exciter model expressed in Chapter 2, if one neglects the PSS and OEL blocks, E'_{fd} can be expressed as a first-order transfer function

$$E'_{fd} = \frac{G(V_{gen} - V_0)}{1 + T_e s} \tag{4.4}$$

The missing parts of (4.3) and (4.4) are the generator terminal voltage and stator currents, which will be calculated based on a restructuring of the network equations to accept generator real and reactive power.

4.1.1 Generator Terminal Voltages and Currents Calculation

To compute the generator terminal voltage and stator current, the power flow model of the network described in Chapter 3 is reconfigured to accept real and reactive power as inputs. Specifically, the generator is represented as a 'PQ' bus, similar to that of a load. The details of the power flow model are in the Appendix.

To implement within the simulation, this is performed by coupling the machine model in Simulink with the network model, which is implemented in Matpower. It is noted is that in a typical PQ bus, which normally is a load drawing power from the

grid, the input to the Matpower is the positive power consumed by the load. However, in the behavioral model of the generation system, the generation bus provides power to the system; thus, the input power to Matpower is the negative value of the power generated by the generator bus.

By using the Matpower described above, the generator terminal voltage phasor can be calculated, which is used in the exciter behavioral representation in (4.4), where the V_{gen} is the magnitude of the phasor. At the same time, using the terminal voltage phasor and the machine complex power, the current phasor at the generator terminal is obtained by

$$\widetilde{I_{as}} = (\frac{P + jQ}{\widetilde{I_{as}}})^* \tag{4.5}$$

Where the $*$ is the complex conjugate operator.

Using the bus information of the power, voltage, and current, the machine rotor angle δ is calculated using:

$$\widetilde{\delta} = angle(\widetilde{V_{as}} + (r_s + jX_q)\widetilde{I_{as}}) \tag{4.6}$$

.

Using reference-frame theory, the current phasor is expressed in terms of q- and d-axis currents in the synchronous reference frame, using (B.9) in the Appendix:

$$\widetilde{I_{as}} = |\widetilde{I_{as}}|\angle\theta_i = I^e_{qs} - jI^e_{ds} \tag{4.7}$$

Transforming to the rotor reference frame, the respective currents are calculated using:

$$I^r_{qs} = I^e_{qs}\cos\delta - I^e_{ds}\sin\delta \tag{4.8a}$$

$$I^r_{ds} = I^e_{qs}\sin\delta + I^e_{ds}\cos\delta \tag{4.8b}$$

These currents are used in (4.3) to calculate the generator steady-state reactive power.

To summarize, the generation system behavioral has only four states representing the transfer function of the active power, reactive power, and the field excitation voltage. Compared with the detailed- or reduced-order model described in the previous chapters, the number of states is significantly reduced.

4.1.2 Behavioral Model Generator/Infinite Bus Implementation

The generator/infinite-bus system is modeled using the transfer function described above, and the simulink implementation of the system is shown in Figure 4.3.

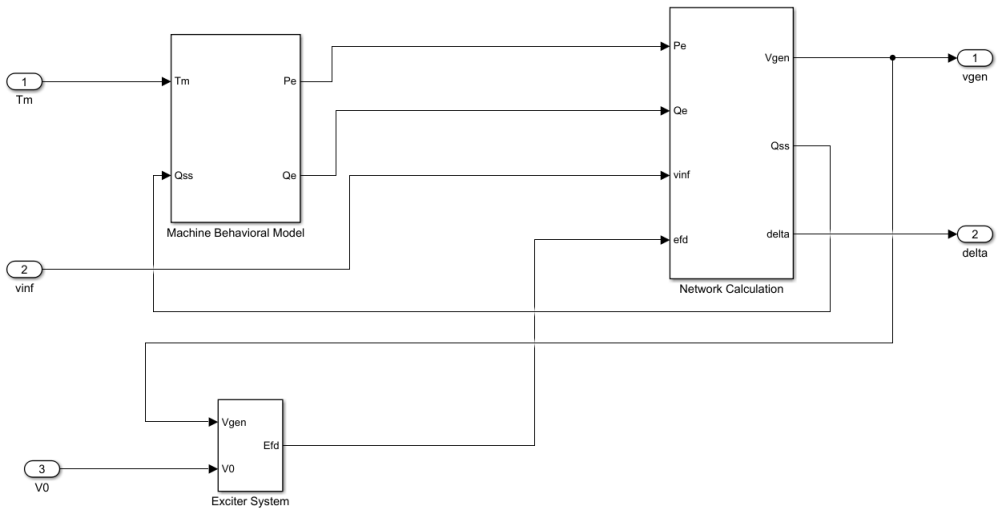

Fig. 4.3.: Behavioral Model Generator/Infinite Bus Implementation

In the **Machine Behavioral Model** block, the transfer functions for the active and reactive power are implemented in as state models. Details of the blocks are shown in Figure 4.4. After the calculation of the active power derivative, a slew rate limiter is used to limit the rate of change of the active power. The slew rate is set to the slew rate of the valve opening control in the governor. In the **Network Calculation** block, the generator bus terminal voltage, the steady-state reactive power, and the rotor angle are all calculated. The Simulink diagram is shown in Figure 4.5.

In Figure 4.5, the **Network** function block uses Matpower to solve for the bus voltages. The **iascal** function block is used to calculate the bus current magnitude

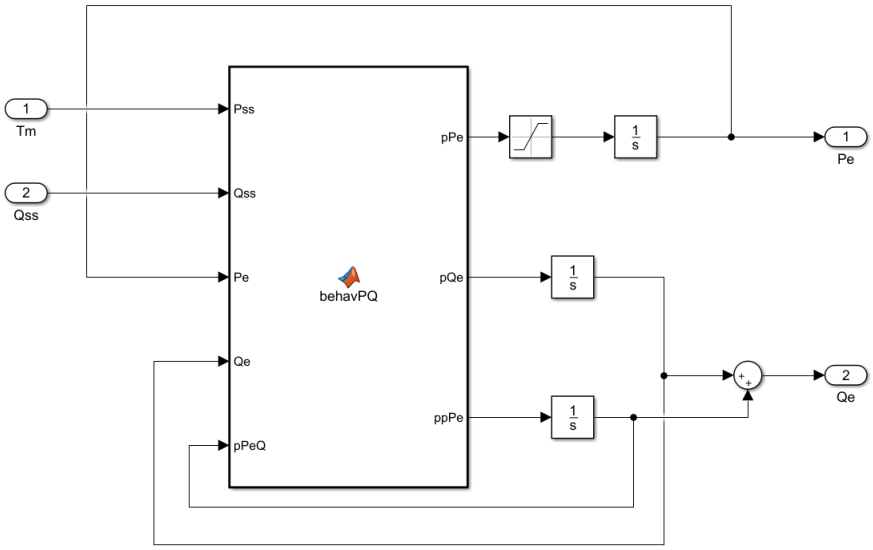

Fig. 4.4.: Generator Behavioral Model Implementation

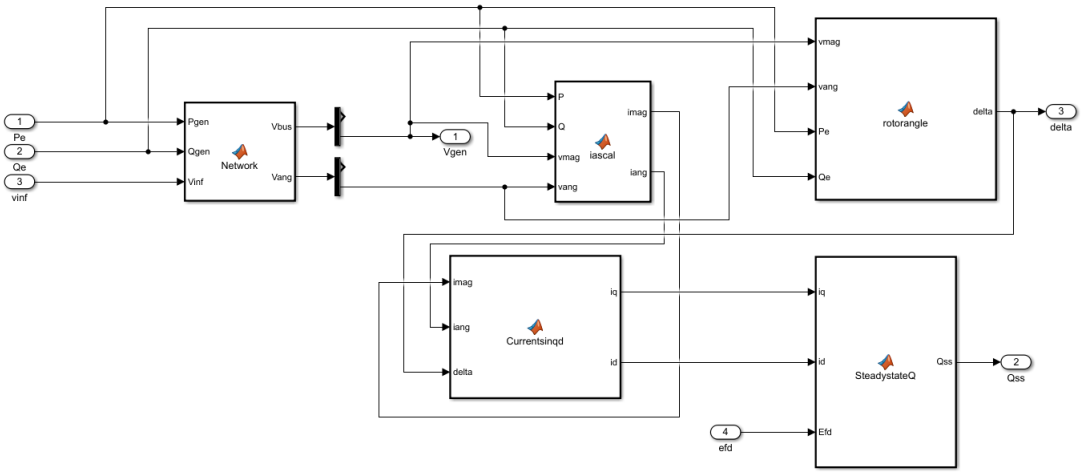

Fig. 4.5.: Behavioral Model Network Calculation Implementation

and angle. The **rotorangle** function block calculates the rotor angle. In the **Currentsinqd** function block, the q- and d-axis currents of the generator in the rotor reference frame are calculated so that the steady-state reactive power can be calculated.

In Figure 4.3, the exciter system block calculates the field voltage to the generator. The implementation is shown in Figure 4.4.

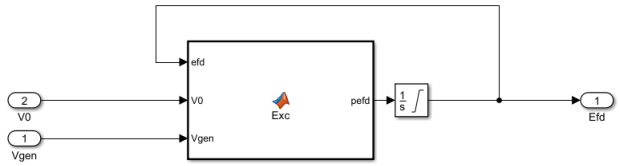

Fig. 4.6.: Behavioral Model Exciter Implementation

Based on the Simulink model described above, a study has been done to observe the predictions of the behavioral model and compare them to the reduced-order model. The study performed is similar to that shown in Chapter 3 where several step changes are made: the infinite bus voltage magnitude drops from 1 per-unit to 0.7 per-unit at 50s and returns to 1 per-unit at 70s; the V_0 increases 0.1 per-unit at 100s; and finally, the P_o steps from 1 per-unit to 0.6 per-unit at 200s. The results of the reduced-order model and behavioral model are shown in Figure 4.7, where the blue lines are the reduced-order model predictions.

Considering the response, the shape of the behavioral model agrees with the reduced-order model. There is some difference, as the behavioral model does not include some of the the faster dynamics shown in the reduced-order model. This is expected since the behavioral model is a further model reduction from the reduced-order model. Comparing the simulation speed, the reduced-order model requires 10.14 seconds to simulate the 300s study using the Simulink variable step solver ODE23tb with a maximum time-step of 5s. The behavioral model requires only 3.32s using the same solver.

Based on the results, it is shown that the behavioral model represents the power output of the generator, the bus voltage, and the rotor angle reasonably well with appreciable improvement in the simulation speed. This is achieved by directly char-

acterizing the transfer function representing the power output based on the machine inputs without considering the machine internal dynamics.

Historically, a common generator study is to consider a fault response and evaluate the potential instability using simulation and analytical techniques such as the equal-area criterion [12]. The equal-area criterion is an old graphical method to predict the critical fault clearing time, which is the time required to keep the generator from losing synchronism (pole slipping). Specifically, when there is a fault that causes the synchronous machine terminal voltage to drop so that the electrical torque of the generator is less than the load torque in the governor, the rotor starts to accelerate. If the fault is not cleared in time, the rotor cannot come back to synchronous speed once the fault is removed. To further consider the behavioral model, a second study is done to check to evaluate the behavioral model predictions in such a large transient. In the study, a fault in simulated by setting the infinite bus voltage magnitude to 0.1 per-unit at 20s and subsequently removing the fault by restoring the bus voltage to 1 per-unit at 20.3s. The results are shown in Figure 4.8. From the results, it can be observed that, after the fault, the reduced-order model predicts sustained oscillations, which means that the system is not stable after the fault. Further, Figure 4.9, it can be observed that the machine loses synchronism. In this case, one can observe that after the fault the behavioral model does predict significant oscillations in the rotor angle, but eventually returns to a pre-fault value. Thus, it fails to predict the correct system response. This is not unexpected as behavioral model was characterized with disturbances in which the rotor speed stayed nearly constant. In addition, the rotor dynamics are not represented within the behavioral model. Thus, from this and subsequent studies it is found that model accuracy degrades as the rotor speed varies appreciably from synchronous.Here, the variable ω_r may be a means to gauge model accuracy.

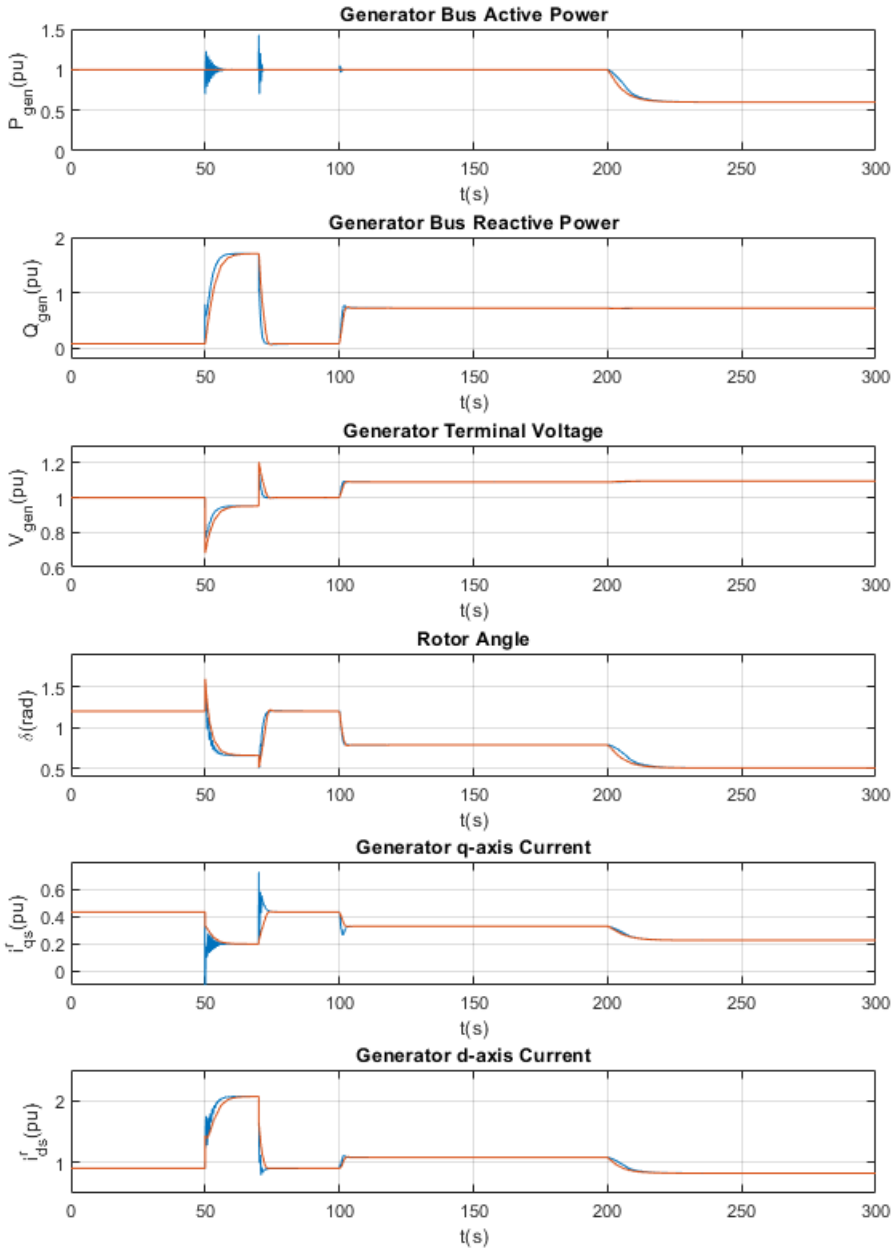

Fig. 4.7.: Generator/Infinite Bus Model Comparison for Detailed and Behavioral Model, blue lines are reduced-order model results and red lines are behavioral model results

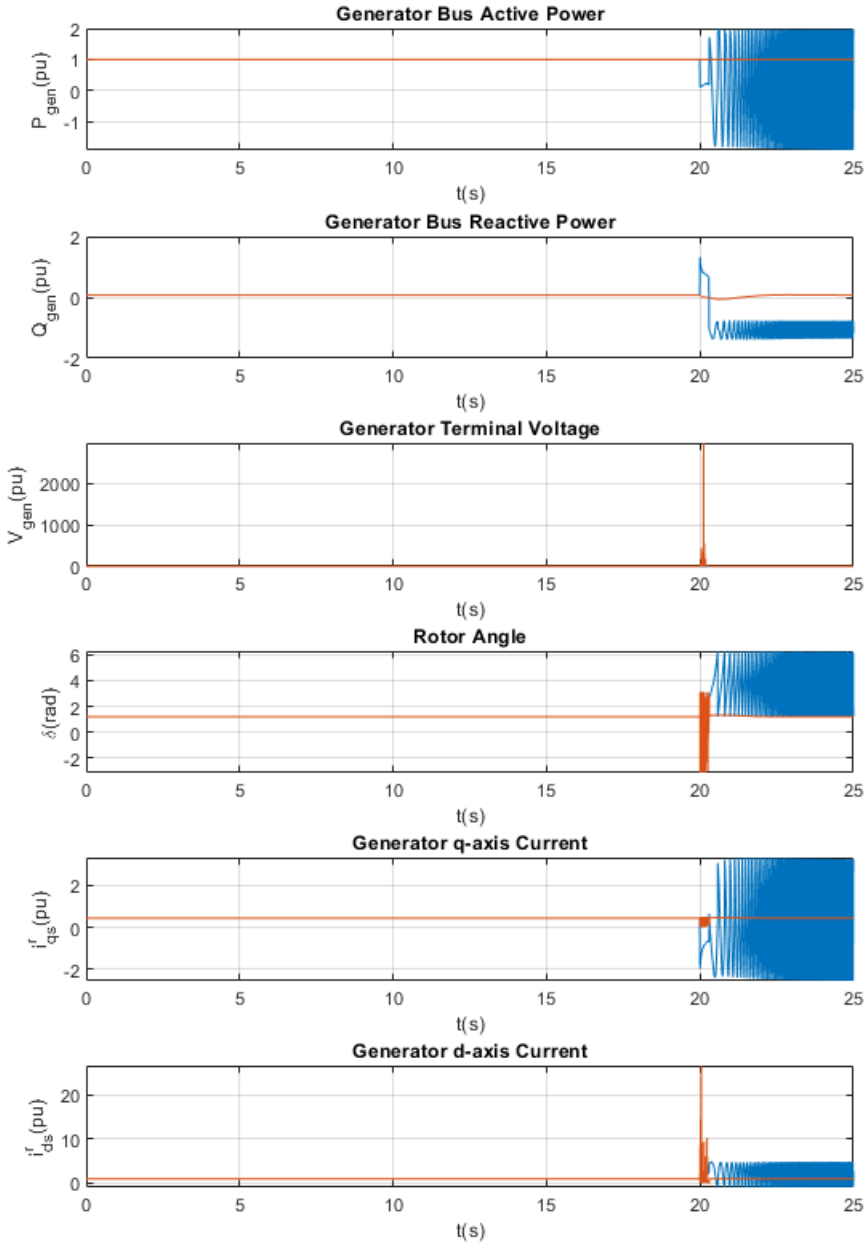

Fig. 4.8.: Generator/Infinite Bus Model Comparison for Detailed and Behavioral Model, blue lines are reduced-order model results and red lines are behavioral model results

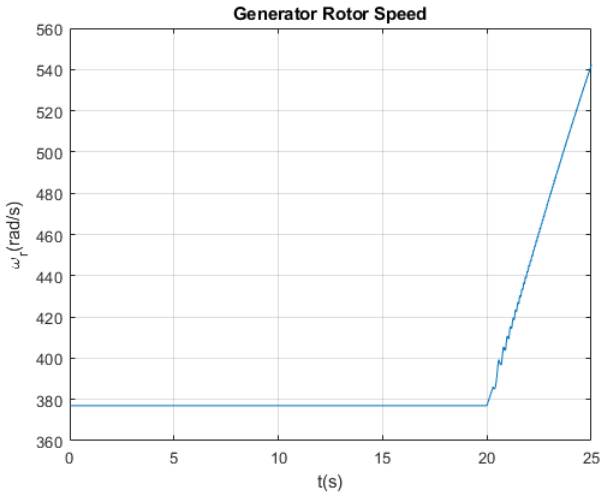

Fig. 4.9.: Generator Rotor Speed

4.2 Induction Machine

For the induction machine, a similar concept, to represent its active and reactive power behavior is considered. The difference in developing the model is that the power dynamics of the machine are not characterized using a set of dynamic studies. Rather, the steady-state equivalent circuit, in tandem with the rotor mechanical dynamics, are used to predict the power behavior. This is partially justified by the fact that the induction machine does not have the ancillary equipment (governor, exciter) of the generator. The behavioral model is based upon models considered in [11] and is derived from the induction machine steady-state circuit shown in Figure 2.83. Within

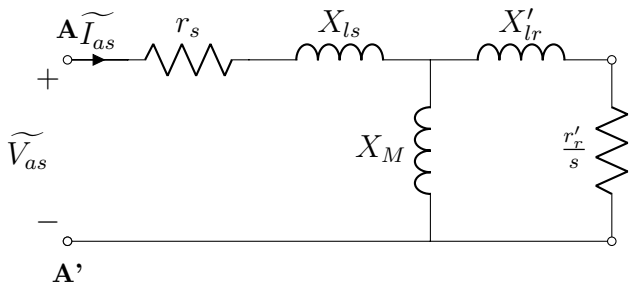

Fig. 4.10.: Induction Machine Steady-State Equivalent Circuit

the circuit, r_s and r'_r are the stator and rotor resistances, X_{ls} and X'_{lr} are the stator and rotor leakage reactances, X_M is the magnetizing reactance and s is the slip defined in (2.82).

From the Figure 4.10, a Thevenin equivalent circuit can be obtained from **AA'**, which is shown in Figure 4.11. In Figure 4.11, the impedance of r_e and X_e in steady state are dependant on s and their sum is expressed as:

$$r_e(s) + jX_e(s) = \frac{jX_M(\frac{r'_r}{s} + jX'_{lr})}{\frac{r'_r}{s} + j(X_M + X'_{lr})} \tag{4.9}$$

Furthermore, the stator current versus terminal voltage relationship is expressed:

$$\widetilde{I_{as}} = \frac{\widetilde{V_{as}}}{[r_s + r_e(s)] + j[X_M + X_e(s)]} \tag{4.10}$$

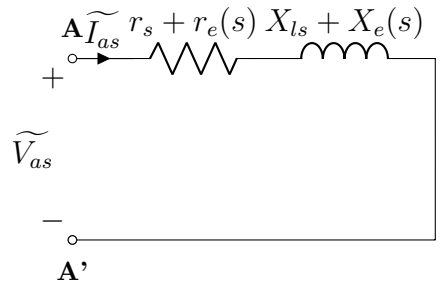

Fig. 4.11.: Thevenin Equivalent circuit seen from **AA'**

Using the steady-state circuit model, all of the electrical dynamics are neglected in the behavioral model. The only state used is slip, with a state representation:

$$ps = \frac{T_l - T_e}{2H} \tag{4.11}$$

Where p is the $\frac{d}{dt}$ operator; s is the slip; T_l is the load torque and T_e is the electromagnetic torque. The electromagnetic torque is calculated using the steady-state equation for torque (2.83) in Chapter 2 .

Using (4.10) and (C.2), the complex power of the induction machine is calculated. After equating the real part and the imaginary part of the complex power, the active and reactive power is found using:

$$P = \frac{[r_s + r_e(s)]|\widetilde{V_{as}}|^2}{[r_s + r_e(s)]^2 + [X_s + X_e(s)]^2} \tag{4.12a}$$

$$Q = \frac{[X_s + X_e(s)]|\widetilde{V_{as}}|^2}{[r_s + r_e(s)]^2 + [X_s + X_e(s)]^2} \tag{4.12b}$$

To summarize, the main equations governing the behavioral model of an induction machine are given in (4.11) and (4.12). With the system model, the active and reactive power of the induction machine are input to the network for the calculation of the bus voltages.

Direct Online Start

To validate the behavioral model, a study of an induction machine is performed. Within the study the initial rotor speed is 0 rad/s when the stator terminals are connected to the voltage source. Once the machine reaches a steady-state, the magnitude of the bus voltage is reduced from 1 to 0.9 pu. The Simulink Model for the study is shown in Figure 4.12. The parameters used are those of induction machine 1 in the Appendix. The results are shown, along with those predicted using the reduced-order model in Figure 4.13.

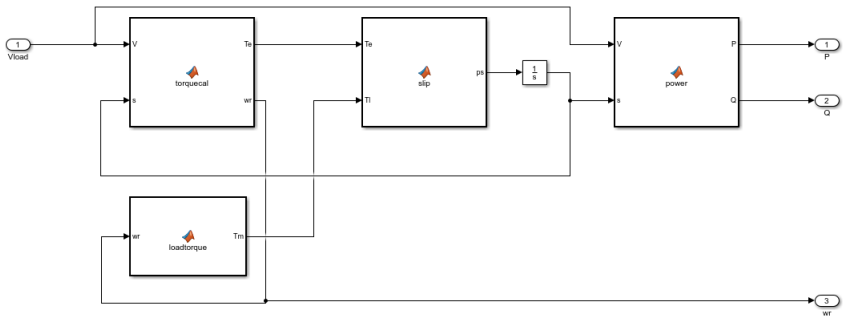

Fig. 4.12.: Induction Machine Direct Online Startup Simulink Implementation

Comparing responses, it is clear that the power predicted by the behavioral model closely matches that of the reduced-order model and startup and the bus voltage disturbance.

Using ODE23tb solver, with a maximum time-step of 0.5s, the simulation time for the reduced-order model is 0.97s and for the behavioral model is 0.88s by using the same solver with same maximum time-step setting. Although there is not significant difference between the simulation speed of behavioral model and the reduced-order model, this difference can be amplified if there are multiple machines.

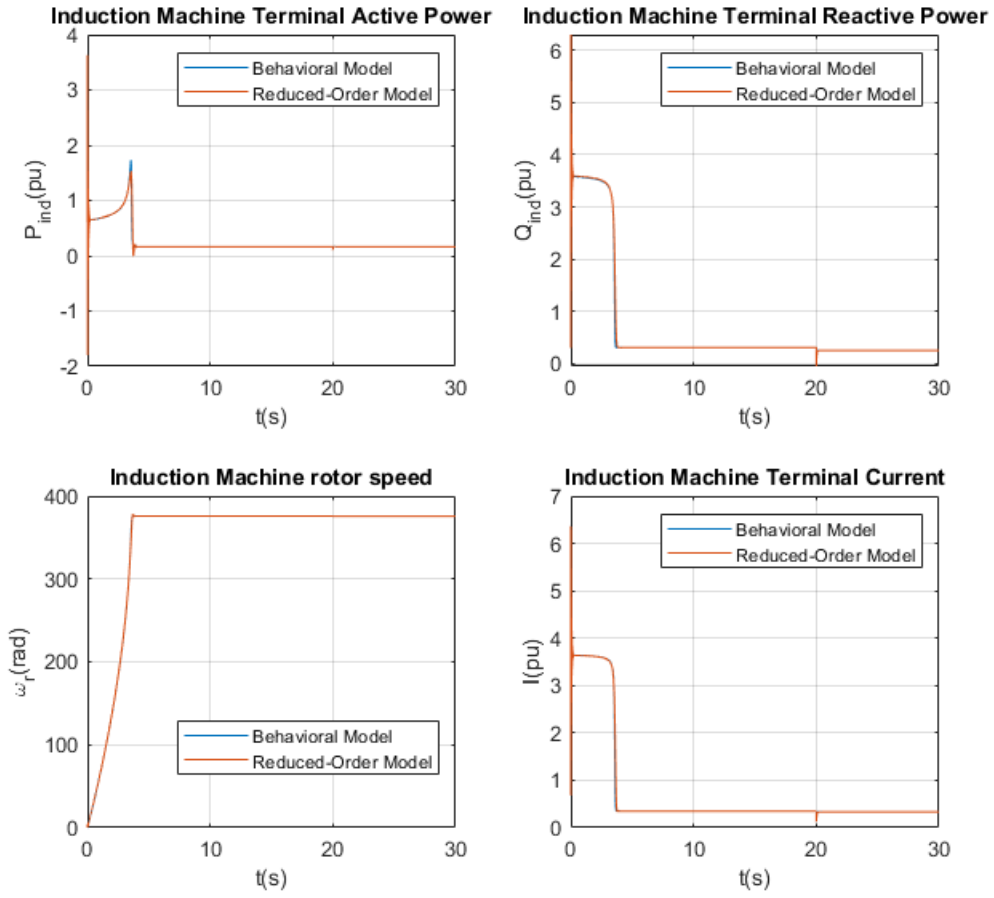

Fig. 4.13.: Induction Machine Direct Online Startup Comparison

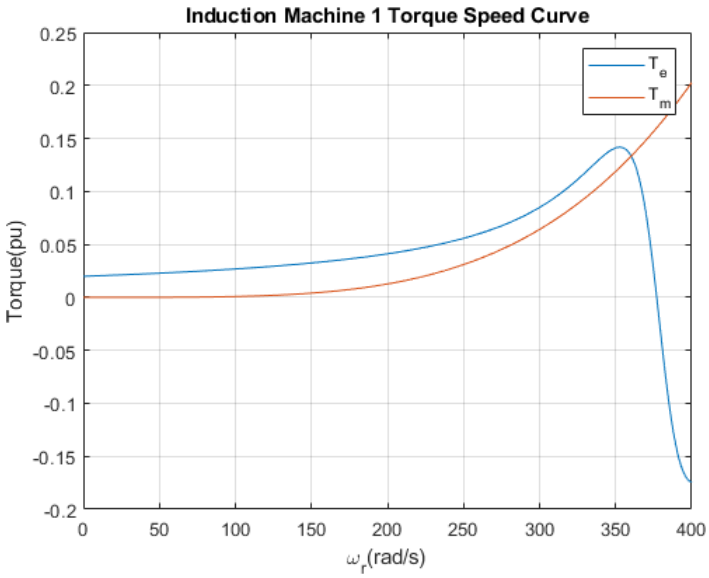

Fig. 4.14.: Induction Machine Torque Speed Curve

4.3 Simulink Implementation

4.3.1 Block Diagram

The Simulink Block diagram of the behavioral model of the overall system is shown in Figure 4.15.

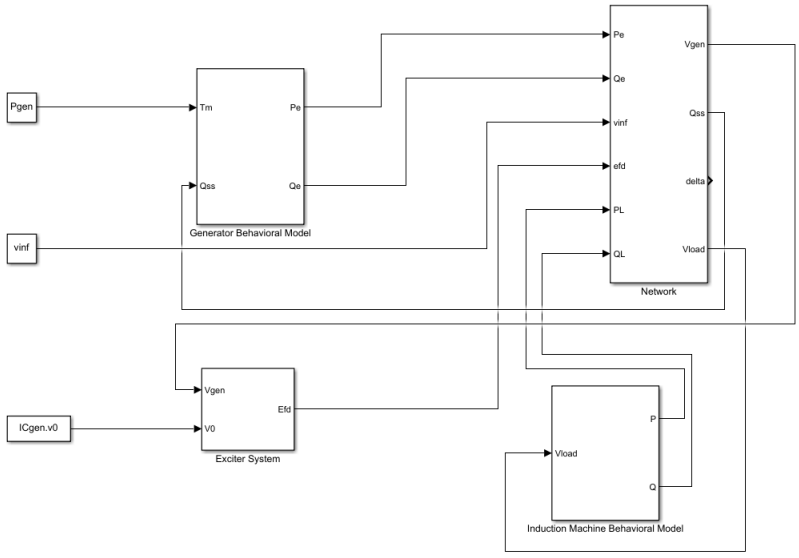

Fig. 4.15.: Behavioral Model for 5-bus System Simulink Implementation

The **Generator Behavioral Model** block is the same as shown in Figure 4.4 and the **Induction Machine Behavioral Model** block is the same as shown in Figure 4.12. In the **Network** block is shown in Figure 4.16. The inputs to the **Network** block are the power inputs from the generator and the induction machines, and the induction machine terminal voltage used for the LTC tap setting. The outputs for the block is the rotor angle, generator terminal voltage and the steady-state reactive power for the generator.

4.3.2 States Initial Conditions

Since the number of states included in behavioral model is greatly reduced, the calculation of the initial condition is simplified. For the generation system, the states

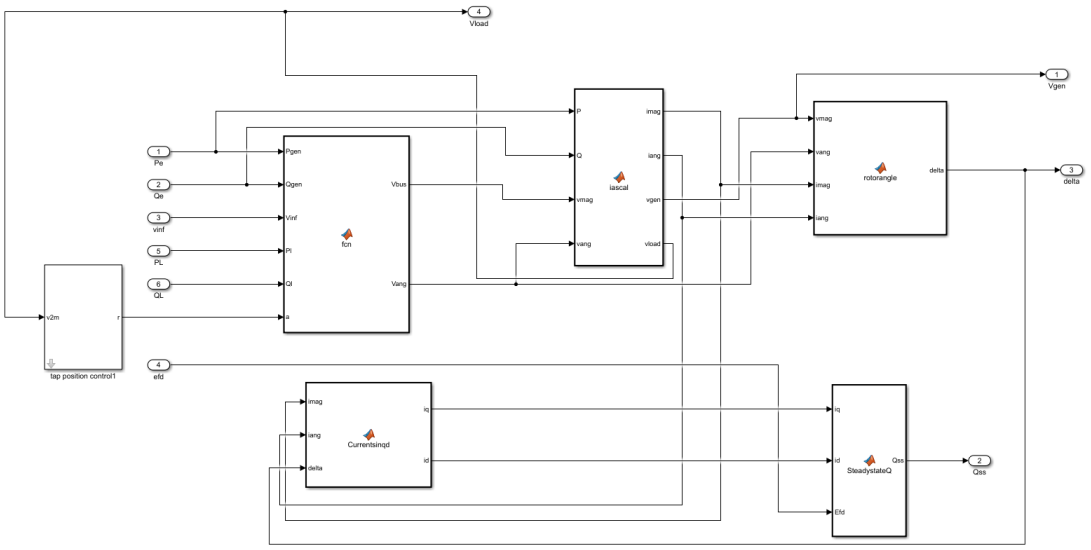

Fig. 4.16.: Behavioral Model for 5-bus System Network Sub-block

are generator active and reactive power, the change of the machine active power and the field voltage E'_{fd}. The active power initial condition is calculated based on the commanded power; and the reactive power is from the power flow solution. The change of the active power initial condition is 0 and the E'_{fd} initial condition is calculated following the same procedure described in the Chapter 2. For the induction machine, the only state is the slip of the machine, which is also described in the Chapter 2; hence it is not discussed further in this chapter.

4.3.3 Sample Response

With the mathematical model of the system components and Simulink Implementation described, a sample study is performed. The study is the same as as that shown in Chapters 2 and 3. The results are shown in Figure 3.11 and Figure 3.12.

From the responses of behavioral model, it can be observed that they are almost identical to the responses shown in the detailed model and reduced-order models, which provides some validation of the approach. The simulation time for the behavioral model using a Simulink variable step solver ODE23tb with maximum time-step

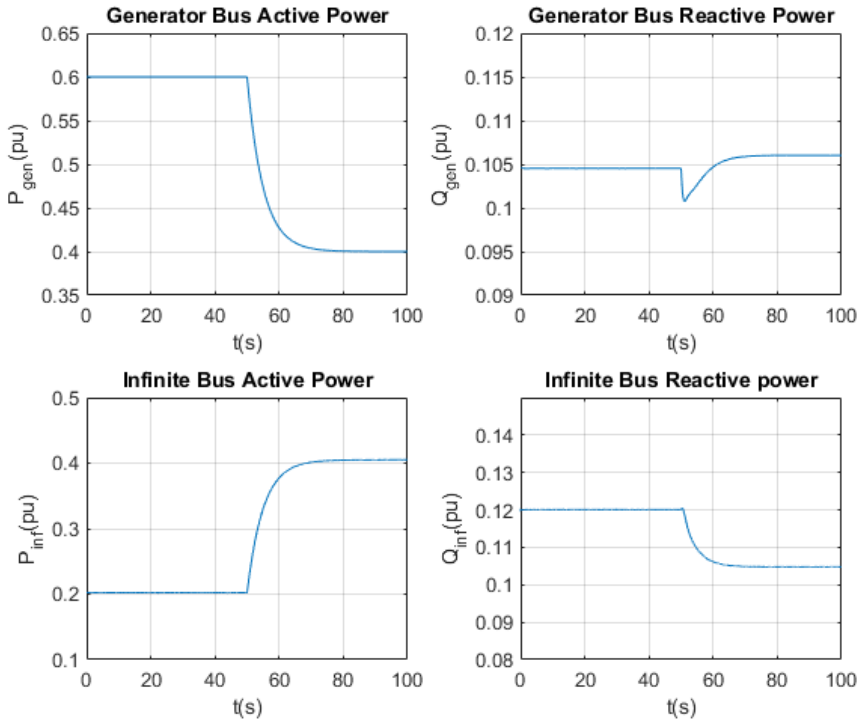

Fig. 4.17.: Behavioral Model Simulation Results to Generator Commanded Power Step(a)

2s requires 1.02s, which is less than the 8.73s and 3.37s for the detailed- and reduced-order models using the same solver. Further assessment of the behavioral model is provided in the following chapter.

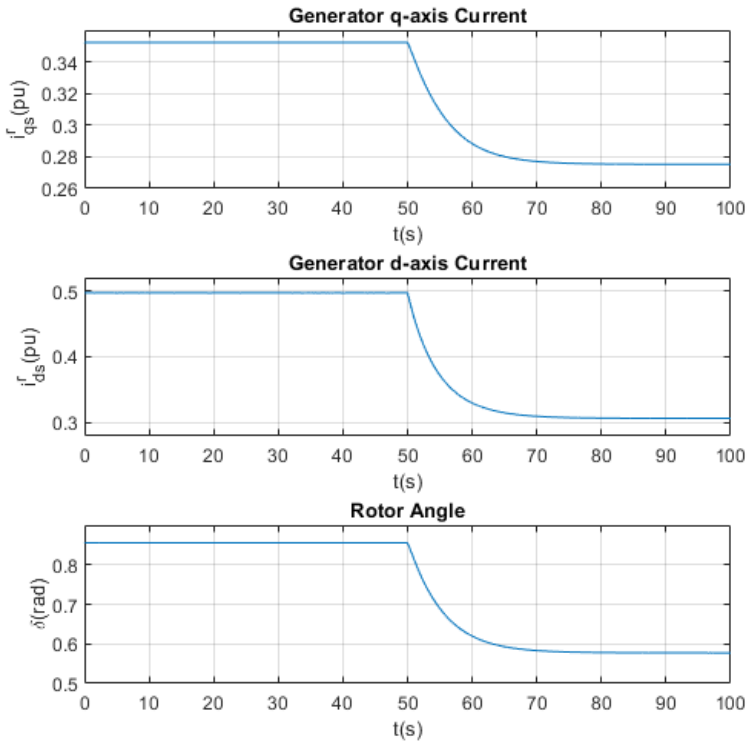

Fig. 4.18.: Behavioral Model Simulation Results to Generator Commanded Power Step(b)

5. SIMULATION RESULTS

5.1 Model Comparison

In this research, three models are derived for a 5-bus power system microgrid. The most complicated model is a detailed model, which includes all stator and rotor states of the generator and induction machines. The total number of states is 48. In the reduced-order model, the stator transients of the induction machines, the generators, and the network are all neglected based on utilizing a mathematical technique referred to as singular perturbation theory. In the reduced-order model, only the rotor dynamics and the generator governor and exciter dynamics are included, which results in a reduction to 18 states for the system. In the last model proposed, the dynamics of the real and reactive power of the generator and induction machine are included, which reduces the number of states to six. In this chapter, the responses of the models to several system perturbations are compared. Prior to comparing, it is noted that some abbreviations are used to simplify descriptions: FD stands for the detailed model, RO stands for the reduced-order model and BH is the behavioral model.

5.2 Results Comparison

5.2.1 Study 1: Step Changes in Generator Inputs

In the first study, the system is operated in a steady state with load drawing 0.6 per-unit active, 0.106 per-unit reactive power, and P_o set to 0.6 pu and the voltage V_o set to 1 pu. The commanded power is then stepped from 0.6 per-unit to 0.4 per-unit at 30s, and the V_0 is increased by 0.01 per-unit. The results of the study are shown in Figure 5.1 and Figure 5.2. Simulation is performed by using the Simulink built-in variable step solver ODE23tb with maximum time-step 2s for all the models.

From the results it is shown that all the models begin and end at the same steady state, which means the initial-value calculations in each model are correct. At 50s, when the commanded power of the generator drops, the generator bus active power starts to drop to the commanded value, which shows the control in the governor is effective. Moreover, since the generator power drops, to ensure the power balance of the system, the infinite bus active power increases. Furthermore, due to the control of LTC, the induction machine is not affected by the power step change so that the power generated by the induction machine stays at its original value. In the Figure 5.2, some quantities of the generator are also plotted. As the commanded power drops, the generator rotor speed reduces down until the electrical torque of the generator equals the mechanical torque from the governor, which also leads to a decrease in the rotor angle. The q- and d-axis currents of the generator all drop to reduce the output active power. At 80s, the voltage control signal in the exciter V_0 increases, which results is an increase in the excitation voltage E'_{fd}. Based on (2.71a), the q-axis voltage also increases. However, as shown in Figure 5.2, the generator terminal voltage does not vary significantly, so that the d-axis voltage must decrease as a result. Based on (2.71b), the q-axis current would decrease. To keep the generator output active power stays at the commanded value, the d-axis current must increase. All the description here agrees with the responses shown in Figure 5.1 and in Figure 5.2. In addition, the three models have similar shapes, but the FD and RO do possess some

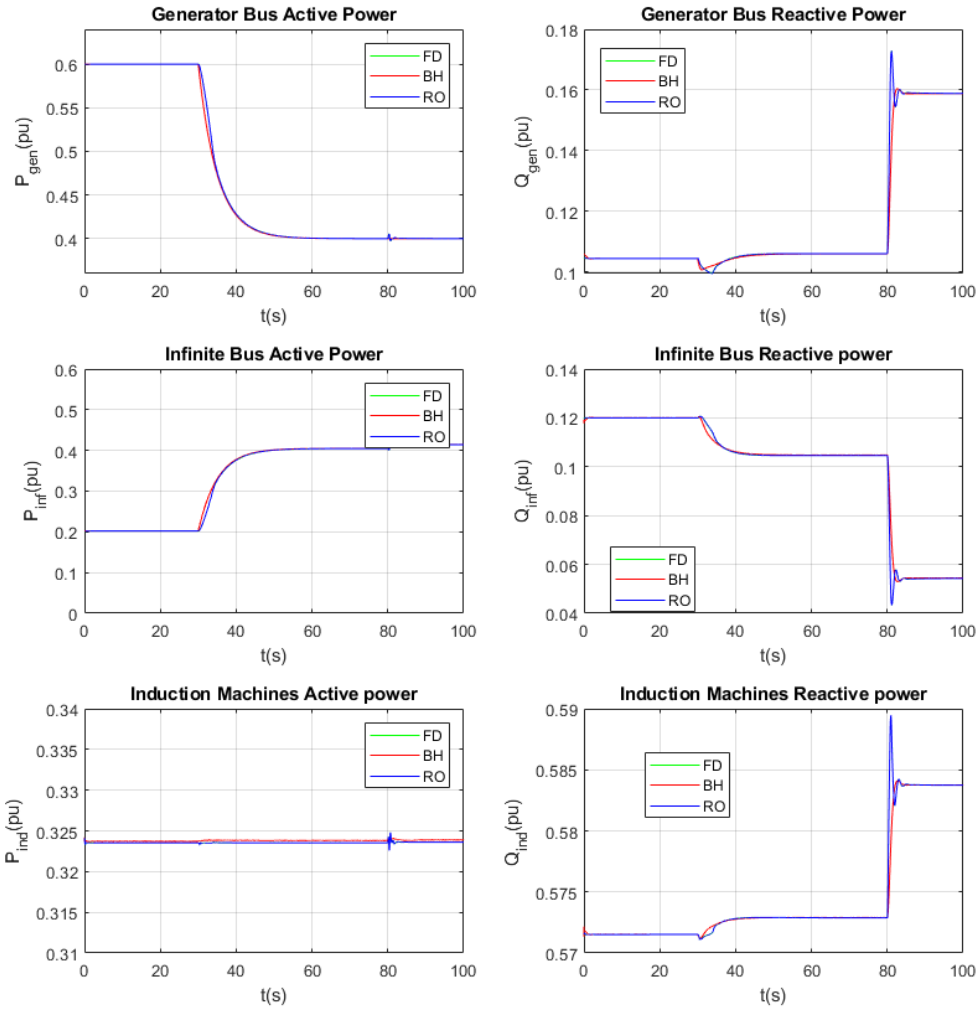

Fig. 5.1.: 5-Bus System Inputs Step Responses(Part a)

higher order dynamics compared to the BH. In this study, the FD requires 33.23s to complete the 100s simulation, while RO requires 3.67s, and BH requires 1.29s.

5.2.2 Study 2: Induction Machines Startup Response

In the BH chapter, a single machine startup response is shown in the representative system study. Therein a single machine is connected to the infinite bus. Here, a

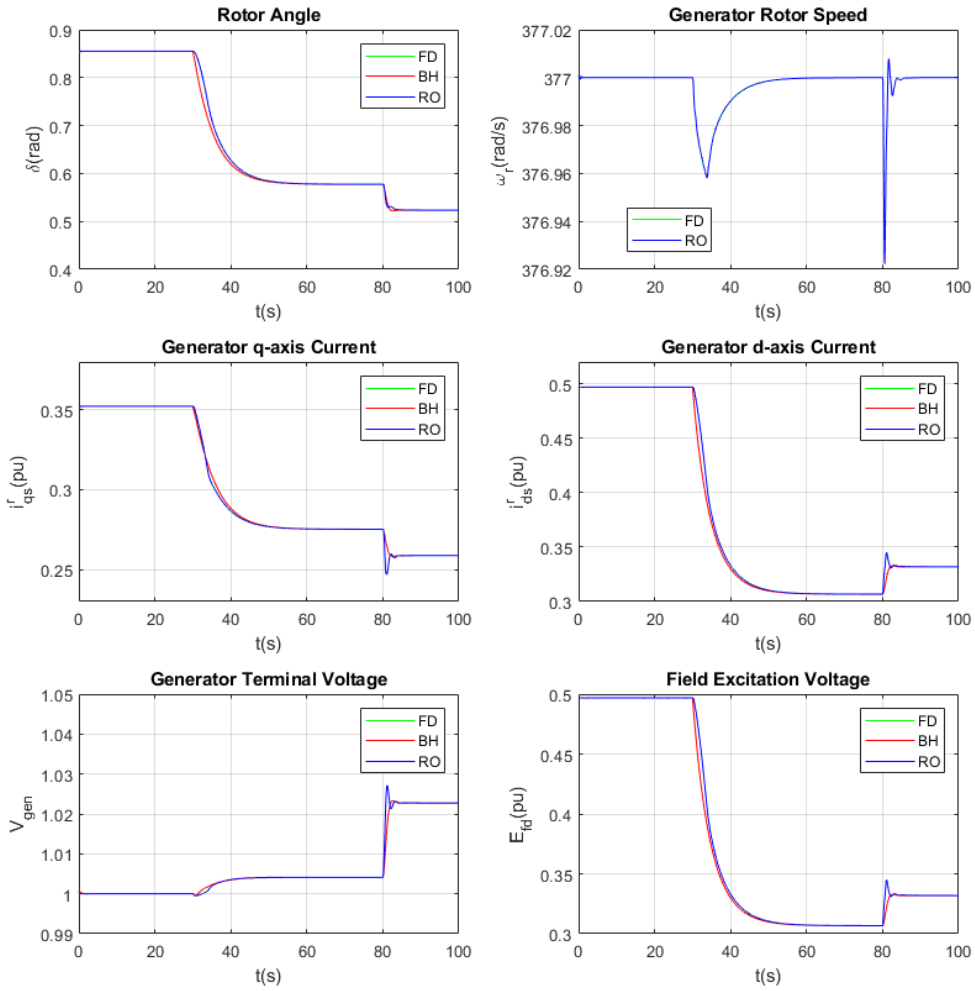

Fig. 5.2.: 5-Bus System Inputs Step Responses(Part b)

study is performed for the full system in which both machines undergo a startup at the load bus. The predicted performance of the three models are shown in Figure 5.3 and Figure 5.4. Simulation is performed by using the Simulink built-in variable step solver ODE23tb with maximum time-step 5s for all the models.

The results in both figures show that all the models predict similar dynamics. In Figure 5.3, the induction machines reach their final steady states at 50s and 170s; at the same time, the total active power of the induction machine shows two small

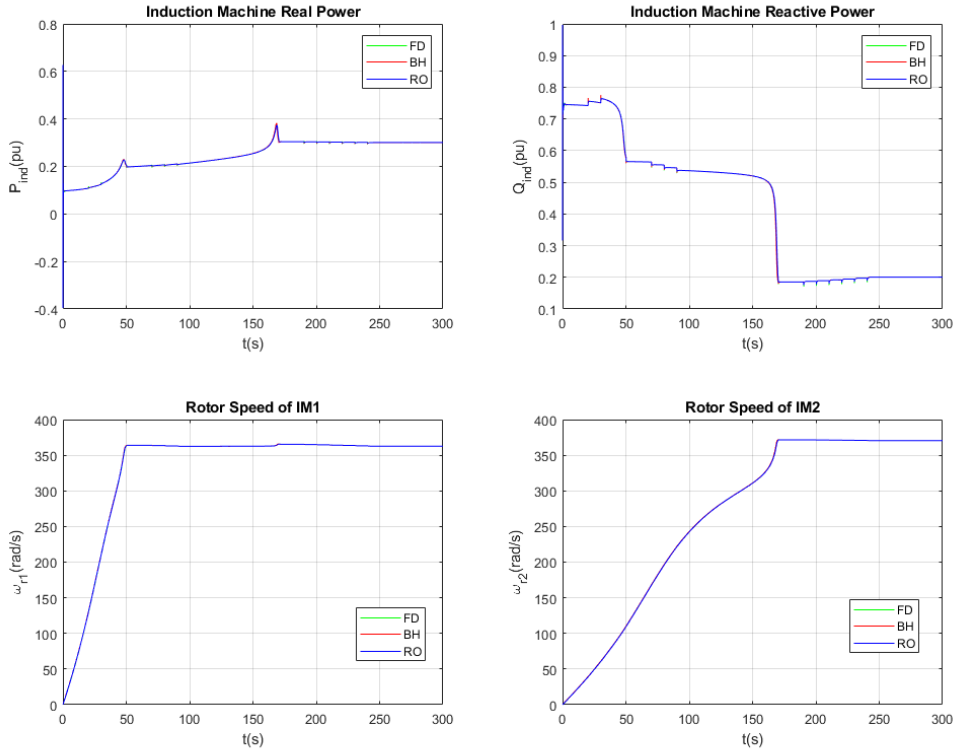

Fig. 5.3.: Induction Machine System Startup responses (Part a)

transients as they exceed the breakpoint torque and approach synchronous speed. In the results shown, there are staircase-shape responses in the induction machine terminal voltage, which shows that the controls in the LTC are changing its turn-ratio to regulate the load voltage within 1 ± 0.01 per-unit. For the study, the FD requires 106.46s to run the 300 simulation, the RO requires 40.63s and the BH requires 26.55s.

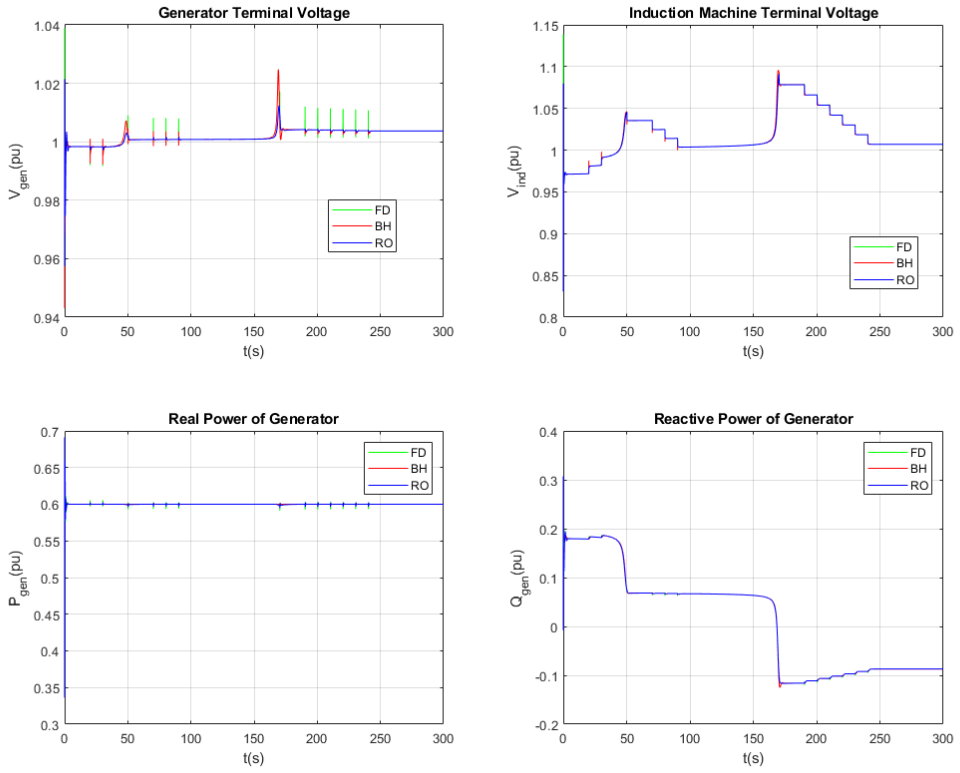

Fig. 5.4.: Induction Machine System Startup responses (Part b)

5.2.3 Study 3: Line Fault

A line fault study is performed to further examine the models. Within the study, one of the lines, shown in Figure 1.1 between bus 3 and bus 4, is opened. For the FD model, the opening is performed by changing the parameters of the line inductor, resistor and the shunt capacitor in the corresponding states equations. For the RO and BH, the admittance matrix of the system are modified accordingly. The results are shown in Figure 5.5 and Figure 5.6. Simulations is performed by using the Simulink built-in variable step solver ODE23tb with maximum time-step 0.5s for all the models.

As shown, although all three models reach the same steady state post disturbance, there are differences in their transient responses. For example, in the real and reactive

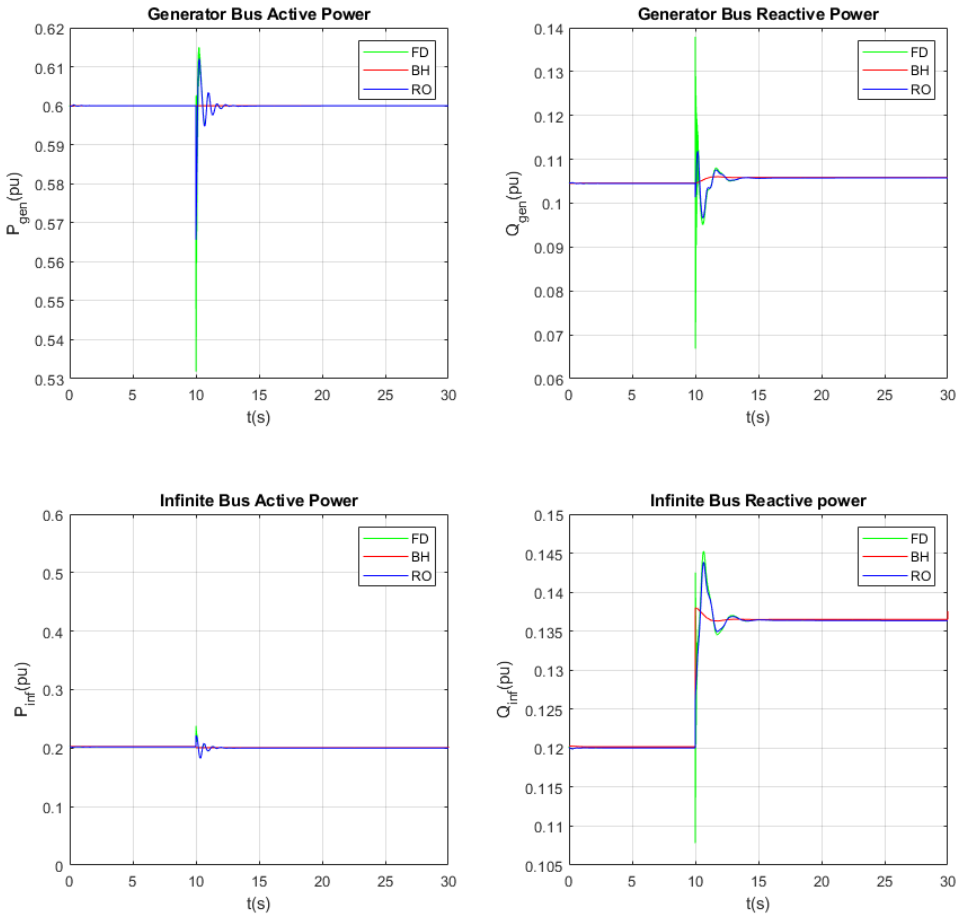

Fig. 5.5.: 5-Bus System Line Fault Responses (Part a)

power of the generator, there is a transient oscillation predicted by both the FD and RO models that is not predicted by the BH. Similarly, there are oscillations in the rotor angle and the q- and d-axis currents not captured by the BH. Close inspection reveals that the scale of the difference between models is relatively modest. For example, the change in rotor angle over the transient is less than 2 percent. Thus, although different, the difference between models is modest. The simulation time for the FD was 11.92s, 1.32s for the RO and 0.89s for the BH.

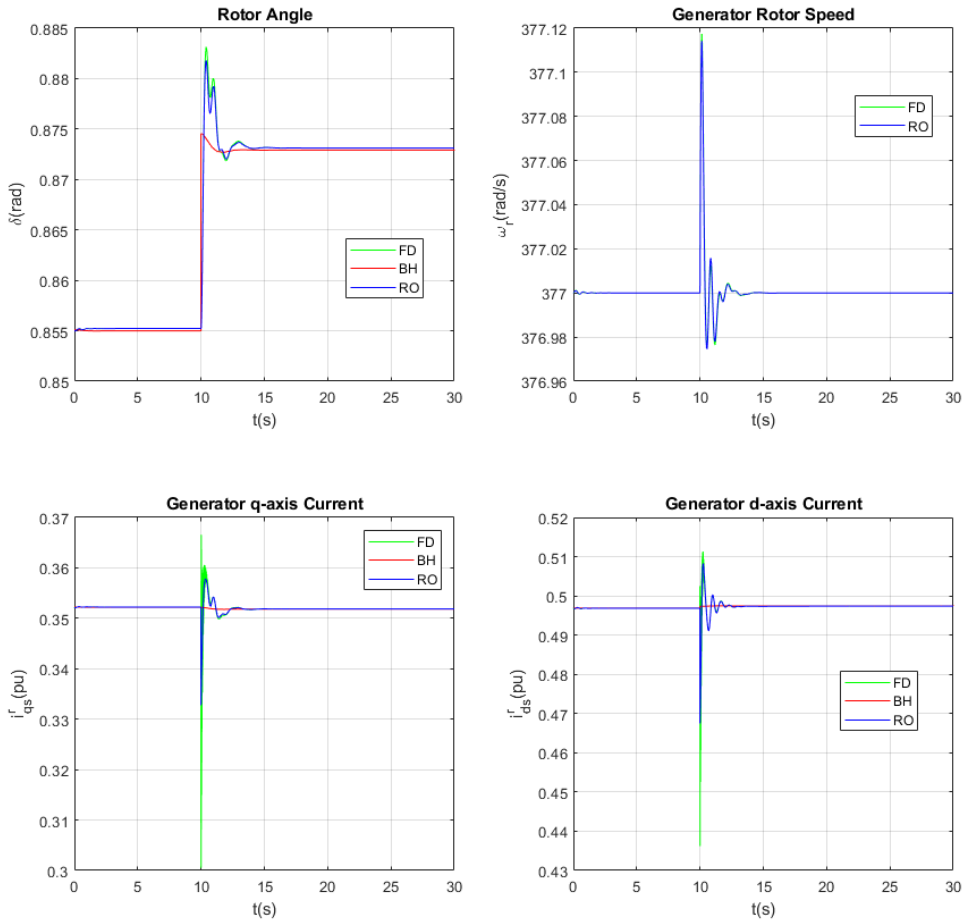

Fig. 5.6.: 5-Bus System Line Fault Responses (Part b)

5.2.4 Study 4: Rotor Transient Stability

The last study performed is one in which a fault is placed on the infinite bus and subsequently cleared. The study is performed twice. In the first case, a fault is placed on the system and cleared after 10 electrical cycles. In the second, a fault is placed on the system and cleared after 100 cycles. When the fault is cleared after 10 cycles, the system recovers back to its initial steady-state. When cleared after 100 cycles, the system does not recover as the generator is not able to return to synchronous speed. Simulations are performed by using the Simulink built-in variable step solver

ODE23tb with maximum time-step 0.5s for all the models.The results of the 10 cycle clearing are shown in Figure 5.7 and Figure 5.8.

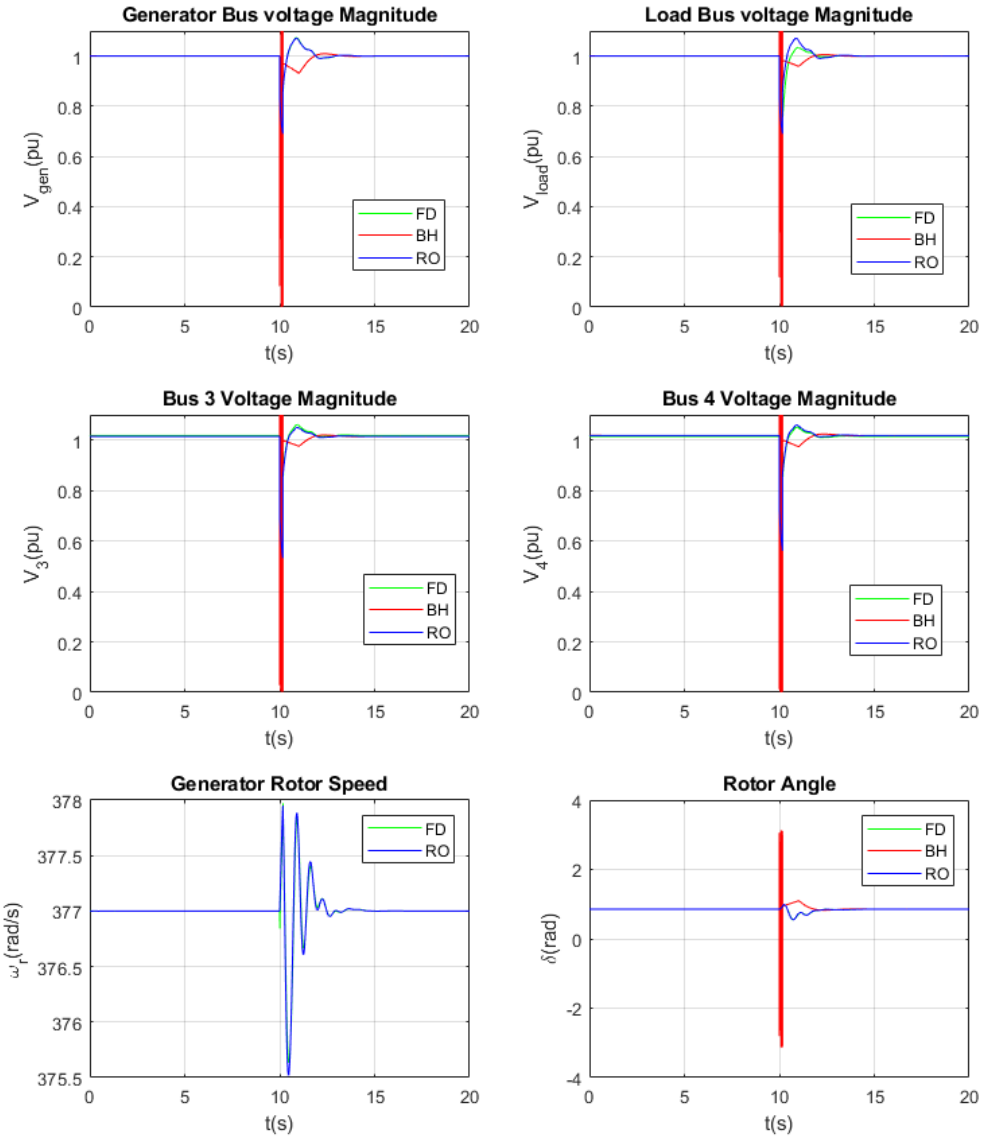

Fig. 5.7.: 5-Bus System Transient Study 1 (Part a)

The results of the 100 cycle clearing are shown in Figure 5.9 and Figure 5.10.

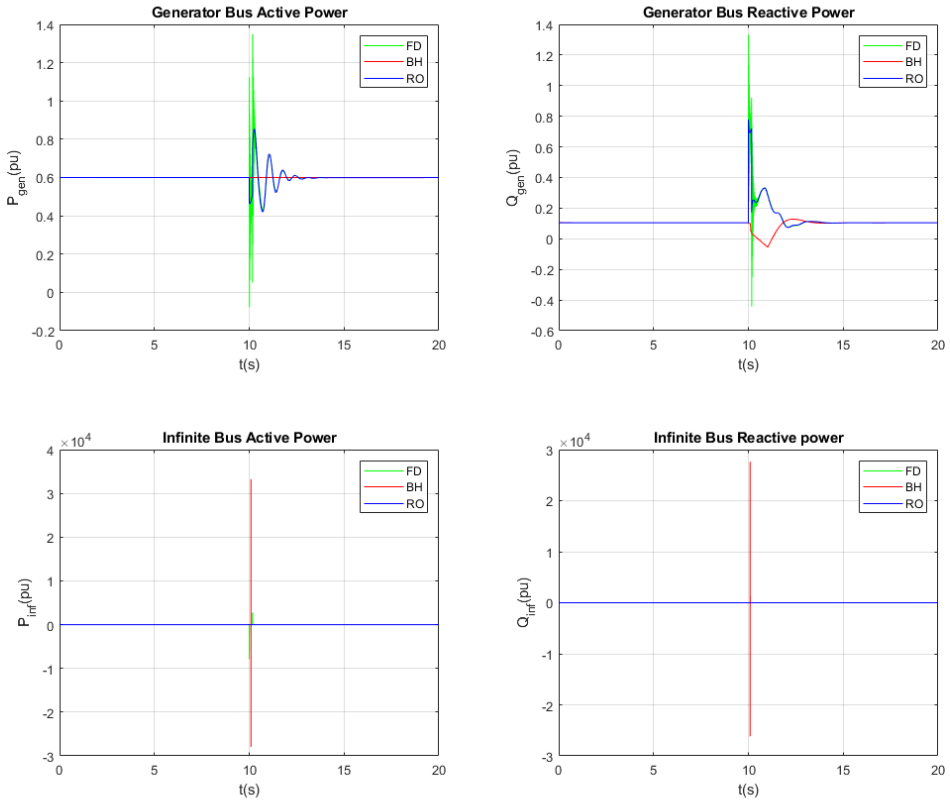

Fig. 5.8.: 5-Bus System Transient Study 1 (Part b)

Based on the observations of the results shown from Figure 5.7 to 5.10, the BH responses in both cases differ from the FD and RO models. For the 10 cycle study, the values predicted during the transient interval do not match, but the final steady-state values are in agreement. The BH model predicts a return to a pre-fault steady state. For the 100 cycle study, the BH fails to capture the transient dynamics and also fails to predict that the system will not return to steady-state as the machine fails to return to synchronization.This inability to capture the dynamics under this large disturbance results from the inability of the model to capture internal dynamics of the machine. As mentioned in Chapter 4, the BH is characterized assuming a small change in angular velocity and does not include speed dynamics as a state. Comparing computational performance, for the 10 cycle case, the FD requires 11.35s, RO 1.66s

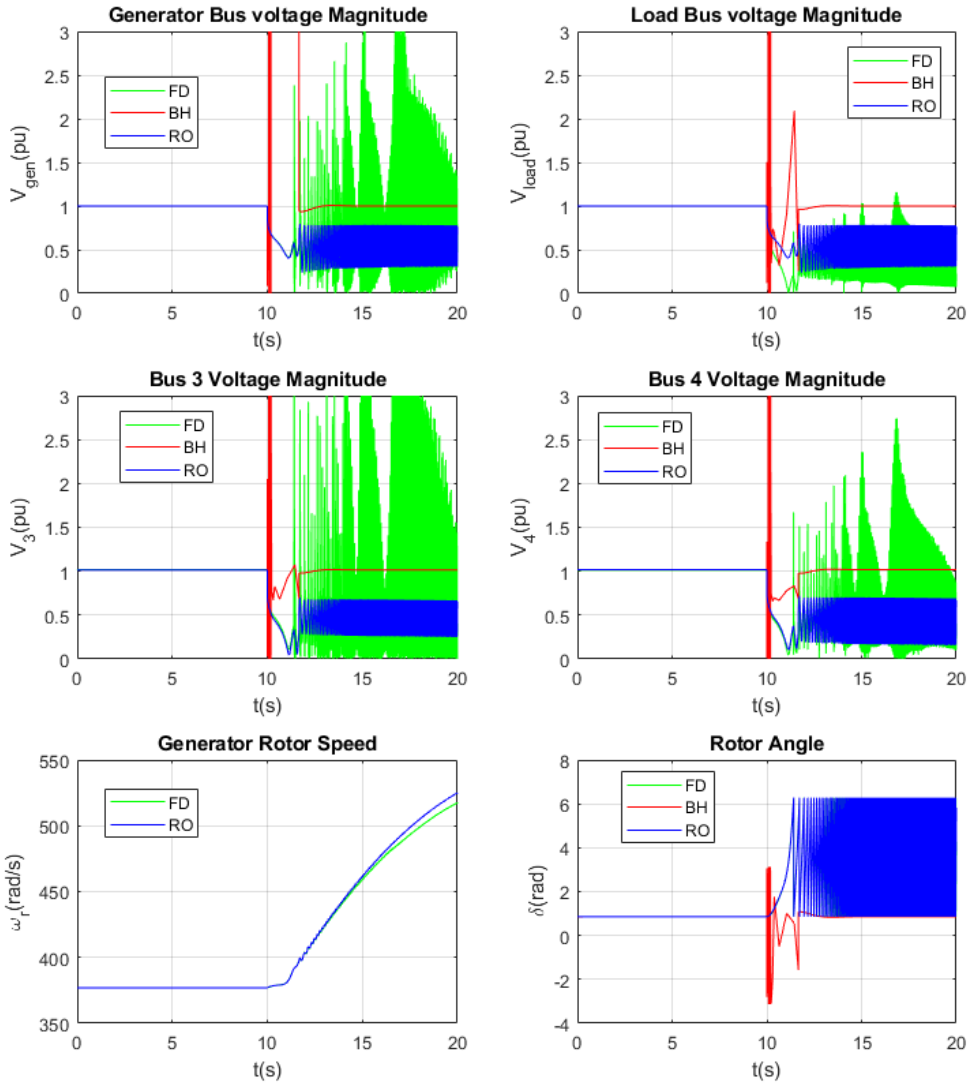

Fig. 5.9.: 5-Bus System Transient Study 2 (Part a)

and the BH takes 22.10s. For the 100 cycle case, the FD requires 172.21s, RO requires 2.23s and BH 25.76s. The BH requires more time due to the fact that when solving the network system, the input power and voltage have very large excursions, as shown in Figure 5.10. During these large changes, the algorithm requires many iterations to converge, which results in an additional computational time. This again shows

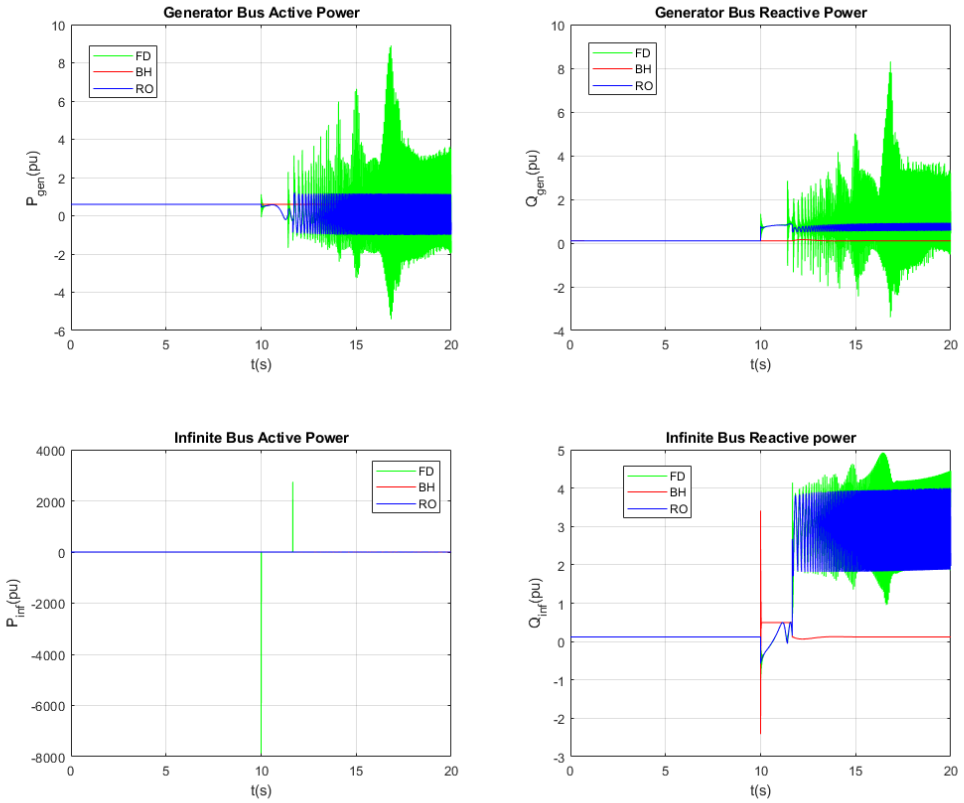

Fig. 5.10.: 5-Bus System Transient Study 2 (Part b)

that BH is not a suitable representation for cases in which the rotor angualr velocity changes appreciably.

5.3 Conclusions

A summary of the models described in this work is shown in table (5.1).

Table 5.1.: Model Summary

	FD	RO	BH
Stator Transient	Yes	No	No
Rotor Transient	Yes	Yes	No
Network Transient	Yes	No	No
# of states for Generator	17	14	4
# of states for Induction Machine	7	4	1
# of states in the 5-bus system	48	18	6

Based on the results provided in the previous sections, some conclusions can be drawn. First of all, FD is useful in all the studies mentioned, and it provides the most details of the power system components. However, the disadvantage of FD is the computational efficiency. Since FD contains all of the dynamics of the components in the power system, it takes a lot efforts to solve and simulate all the ODEs. The alternative to FD is the RO, which ignore the stator transient of the machines and the transient of the network components (transmission lines and transformers) and it is based on the singular perturbation theory. Based on the results shown in previous section, RO shows a great improvement in the computational speed with a small sacrifice in the some fast transient, and it is valid in all the studies mentioned.

However, both of the aforementioned models require a significant number of parameters, which can be difficult to obtain and it is often useful to have the ability to further reduce computational effort when attempting to model performance in real time. As a results, the BH models are is derived and discussed. After a closer look of the responses of BH in study 1,3 and 4, it can be observed that the responses of BH is reasonably accurate if the rotor speed of the generator does not vary an appreciable amount.

5.4 Future Recommendations

5.4.1 Components Model Improvements

For the generation system, the governor and exciter used in this work are from [11]. Hence, to improve the model generality, other types of exciter, examples are in [9], and governors, examples are in [17] and [18], should be considered. In addition, in all three models, saturation of the synchronous generator and the induction machine are not included. Therefore, in order to simulate power system responses under the condition that the machine is saturated, the models can be improved to include this nonlinear behavior. Furthermore, the transmission lines models used are only the π-equivalent circuit. However, to model the medium and long transmission lines, the propagation constant of the transmission lines should be included, the details can be found in [12]. For the transformer, since the model for the transformer used is only the lumped leakage reactance of the transformer, the magnetizing components of the transformer can be included for further fidelity. Similarly for the LTC, the model used is an ideal device, whose tap setting can be changed instantaneously. However, more details can be modeled based on the LTC mechanical geometry.

5.4.2 System Model Improvements

Apart from detailed model and the reduced-order model, other types of models of the power system components can be developed. For example, in [14], three more models of the generator/infinite bus system are developed based on different mathematical techniques. Moreover, as mentioned in the previous section, the behavioral model is not suitable for the rotor transient stability studies. Hence, one potential improvement is to include the rotor dynamics in the behavioral model for the generator. In addition, currently the network algebraic equation are solved by using the Matpower, which is a multi-function package in MATLAB. However, since in the network

calculation in behavioral model, only the network bus voltages are calculated, a faster solver with this specific target can be written to improve the simulation efficiency.

5.4.3 Model Potential Application

The studies using the models developed in this work only show the models' functionality of simulating different disturbances or operating points. However, an eventual goal of the modeling effort is to support research related to power system control designs. In our current research group, some promising progresses has been made by using the reduced-order model as the MPC prediction model to control the plant. Ongoing research is to consider the use of the behavioral models as the prediction model.

REFERENCES

REFERENCES

[1] A. Bonfiglio, A. Oliveri, R. Procopio, F. Delfino, G. B. Denegr, M. Invernizzi, and M. Storace, "Improving power grids transient stability via model predictive control," in *2014 Power Systems Computation Conference*, 2014, pp. 1–7.

[2] A. Bonfiglio, F. Cantoni, A. Oliveri, R. Procopio, A. Rosini, M. Invernizzi, and M. Storace, "An mpc-based approach for emergency control ensuring transient stability in power grids with steam plants," *IEEE Transactions on Industrial Electronics*, vol. 66, no. 7, pp. 5412–5422, 2019.

[3] A. Bonfiglio and M. Invernizzi, "Model predictive control application for the control of a grid-connected synchronous generator," in *2018 International Electrical Engineering Congress (iEECON)*, 2018, pp. 1–4.

[4] J. Martin and I. Hiskens, "Corrective model-predictive control in large electric power systems," in *2017 IEEE Power Energy Society General Meeting*, 2017, pp. 1–1.

[5] X. Miao and M. D. Ili, "Distributed model predictive control of synchronous machines for stabilizing microgrids," in *2017 North American Power Symposium (NAPS)*, 2017, pp. 1–6.

[6] T. Van Cutsem, "Tvc's web page," 2019. [Online]. Available: http://www.montefiore.ulg.ac.be/ vct/software.html

[7] P. Sauer and M. Pai, *Power system dynamics and stability*. Prentice Hall, 1998.

[8] S. Paul Krause, Oleg Wasynczuk and Steven Pekarek, *Analysis of Electric Machinery and Drive Systems,3rd Edition*. Wiley, 2013.

[9] "Ieee recommended practice for excitation system models for power system stability studies," *IEEE Std 421.5-2016 (Revision of IEEE Std 421.5-2005)*, pp. 1–207, 2016.

[10] J. V. Milanovic, K. Yamashita, S. Martnez Villanueva, S. . Djokic, and L. M. Korunovi, "International industry practice on power system load modeling," *IEEE Transactions on Power Systems*, vol. 28, no. 3, pp. 3038–3046, 2013.

[11] T. van Cutsem, *Voltage Stability of Electric Power Systems*. Springer (previously Kluwer Academic Publishers), 1998.

[12] J. Grainger and W. Stevenson, *Power system analysis*, ser. McGraw-Hill series in electrical and computer engineering: Power and energy. McGraw-Hill, 1994. [Online]. Available: https://books.google.com/books?id=NBIoAQAAMAAJ

[13] M. S. Calovic, "Modeling and analysis of under-load tap-changing transformer control systems," *IEEE Transactions on Power Apparatus and Systems*, vol. PAS-103, no. 7, pp. 1909–1915, 1984.

[14] O. Ajala, A. Dominguez-garcia, P. Sauer, and D. Liberzon, "A library of second-order models for synchronous machines," 03 2018.

[15] W. W. Hager, "Updating the inverse of a matrix," *SIAM review*, vol. 31, no. 2, pp. 221–239, 1989.

[16] J. Marija D Ilic, *Dynamics and Control of Large Electric Power Systems*. Wiley, 2000.

[17] "Ieee recommended practice for functional and performance characteristics of control systems for steam turbine-generator units," *IEEE Std 122-1991*, pp. 1–28, 1992.

[18] "Ieee recommended practice for preparation of equipment specifications for speed-governing of hydraulic turbines intended to drive electric generators," *IEEE Std 125-2007 (Revision of IEEE Std 125-1988)*, pp. 1–55, 2007.

[19] R. D. Zimmerman, C. E. Murillo-Snchez, and R. J. Thomas, "Matpower: Steady-state operations, planning, and analysis tools for power systems research and education," *IEEE Transactions on Power Systems*, vol. 26, no. 1, pp. 12–19, 2011.

[20] C. E. M.-S. Ray D. Zimmerman, *MATPOWER user's manual*, Power Systems Engineering Research Center (PSerc).

APPENDICES

A. PARAMETERS & SAMPLE OPERATING POINT

Model Parameter

The parameter used in this work is also from [6]. The parameters of the synchronous generator machine, exciter, governor and induction machine are shown in tables below. All the parameter below are in per-unit(pu), with the power base 500 MVA for the generator and 50MVA for the induction machine. The voltage base is 15KV for the generator and 20KV for induction machines. The parameters of the transmission lines and transformers are shown in Figure 1.1.

Table A.1.: Synchronous Machine Parameters

Parameter	Value
r_s	0pu
X_{ls}	0.15pu
X_q	2.00pu
X_d	2.20pu
X'_q	0.40pu
X'_d	0.30pu
X''_q	0.20pu
X''_q	0.20pu
T'_{do}	7.00pu
T''_{do}	0.05pu
T'_{qo}	1.50pu
T''_{qo}	0.05pu
H	4s

Table A.2.: Steam Governor Parameters

Parameter	Value
σ	0.04
T_{mes}	0.1s
T_{sm}	0.4s
$\dot{z}_{min}$	-0.05 pu/s
$\dot{z}_{max}$	0.05 pu/s
z_{min}	0 pu
z_{max}	1 pu
T_{hp}	0.3s
f_{hp}	0.4
T_r	5s
f_{mp}	0.3
T_{lp}	0.3s
ivo	1

Table A.3.: Induction Machine Parameters

Parameter	Machine 1	Machine 2
r_s	0.031pu	0.013pu
X_{ls}	0.1pu	0.067pu
X'_{lr}	0.18pu	0.17pu
X_M	3.2pu	3.8pu
r'_r	0.018pu	0.009pu
H	0.7s	1.5s

Table A.4.: Exciter Parameters

Parameter	Value	Parameter	value
G	70	C	0.06pu
$T_a = T_b$	1s	i_{f1}^{lim}	2.9pu
T_e	0.4s	i_{f2}^{lim}	1.0pu
v_f^{min}	0	T_{oel}	8s
v_f^{max}	5pu	K_{oel}	2.0
K_{pss}	50	L_1	-1.1
T_w	5s	L_2	0.1
$T_1 = T_3$	0.323s	L_3	0.2
$T_2 = T_4$	0.0138s		

Table A.5.: LTC Tap-Setting Parameters

Parameter	value	Parameter	value
N_{tap}	33	t_s	5s
r_{min}	0.88	t_{d1}	20s
r_{max}	1.2	t_{d2}	10s
V_d	0.01pu	V_o	1pu

Representative Operating Point

The representative operating point used in this work is also from [6], which is shown in Figure A.1.

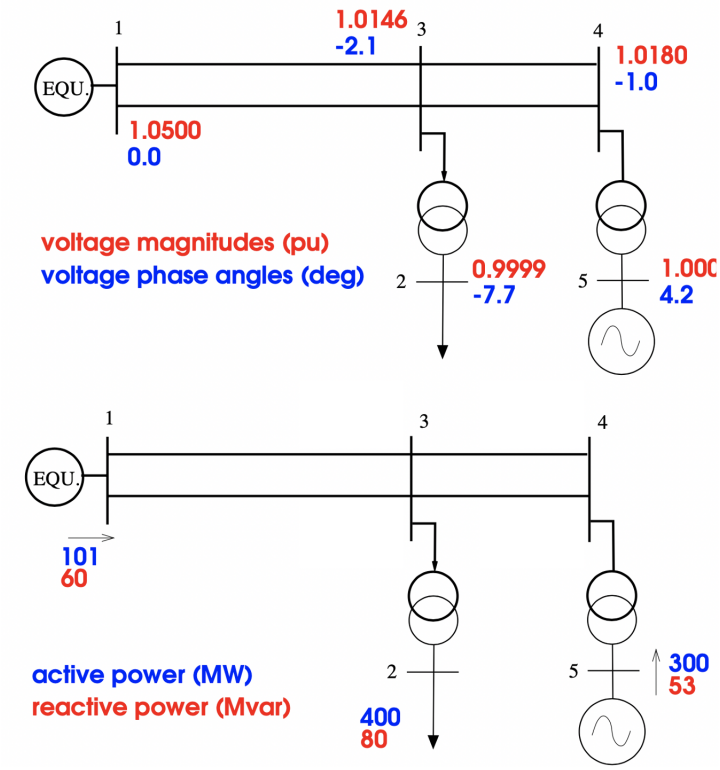

Fig. A.1.: Sample Operating Point

This operating in the figure shows an infinite bus voltage 1.05 per-unit, and the load voltage is fixed at 1 per-unit by the LTC and the voltage at the generator is 1 per-unit as well. On the power side, the load active power consumption is 400MW and the reactive power is 80 Mvar. The generator active power is 300MW and the reactive power is 53 Mvar. Based on the Figure 1.1, the operating tap-setting is 0.99 for the LTC, which will can be altered if a different operating point is chosen. However, for the transformer, the turns ratio setting is fixed at 1.03.

B. REFERENCE-FRAME THEORY

Reference Frame Variable Transformation

The reference-frame theory is used throughout the whole thesis, which allows change of variables including voltages, currents and flux linkages from the three phase *abc* variables to *qd*0 variables. The reference-frame theory allows the AC quantities to transform to DC quantities when analysis is performed. The way the change of variables is performed is by referring the variable to a frame of reference. The transformation can be expressed in the equation (B.1).

$$\mathbf{f}_{qd0s} = \mathbf{K}_s \mathbf{f}_{abcs} \tag{B.1}$$

Where

$$\mathbf{f}_{qd0s} = \begin{bmatrix} f_{qs} & f_{qs} & f_{qs} \end{bmatrix}^T \tag{B.2a}$$

$$\mathbf{f}_{abcs} = \begin{bmatrix} f_{as} & f_{bs} & f_{cs} \end{bmatrix}^T \tag{B.2b}$$

$$\mathbf{K}_s = \frac{2}{3} \begin{bmatrix} \cos\theta & \cos\left(\theta - \frac{2\pi}{3}\right) & \cos\left(\theta + \frac{2\pi}{3}\right) \\ \sin\theta & \sin\left(\theta - \frac{2\pi}{3}\right) & \sin\left(\theta + \frac{2\pi}{3}\right) \\ \frac{1}{2} & \frac{1}{2} & \frac{1}{2} \end{bmatrix} \tag{B.2c}$$

In the detailed model, quantities like currents, voltages and flux linkages of the transmission line, LTC, transformer, induction machines, constant RC load and the infinite bus all calculated in the global synchronous reference frame, which has the frequency defined by the infinite bus ω_e, and $\theta = \omega_e t$. However, in the synchronous generator, all the quantities are in the synchronous machine rotor reference frame, where $\theta = \omega_r t$.

Similarly, the reverse transformation can be done by using equation (B.3)

$$\mathbf{f}_{abcs} = (\mathbf{K}_s)^{-1}\mathbf{f}_{qd0s} \tag{B.3}$$

Where

$$(\mathbf{K}_s)^{-1} = \begin{bmatrix} \cos\theta & \sin\theta & 1 \\ \cos(\theta - \frac{2\pi}{3}) & \sin(\theta - \frac{2\pi}{3}) & 1 \\ \cos(\theta + \frac{2\pi}{3}) & \sin(\theta + \frac{2\pi}{3}) & 1 \end{bmatrix} \tag{B.4}$$

Change Between Two Reference Frame

One more important relationship to be used in the models in this document is about the variables change between different reference frames. As mentioned above, the synchronous generator is modelled in the rotor reference frame. It is important to change the quantities in the synchronous machine rotor reference frame to the global synchronous reference frame for the calculation globally. In general, based on the reference frame angle difference $\theta_{xy} = \theta_y - \theta_x$, a transformation from the x reference frame to y reference frame is done by using the equation:

$$\mathbf{f}^y_{qd0s} = \mathbf{K}^{xy}_s \mathbf{f}^x_{abcs} \tag{B.5}$$

Where

$$\mathbf{f}^y_{qd0s} = \mathbf{K}^{xy}_s \mathbf{f}^x_{qd0s} \tag{B.6}$$

$$\mathbf{K}^{xy}_s = \begin{bmatrix} \cos\theta_{xy} & -\sin\theta_{xy} & 0 \\ \sin\theta_{xy} & \cos\theta_{xy} & 0 \\ 0 & 0 & 1 \end{bmatrix} \tag{B.7}$$

Steady-State Relations

The reference frame theory is also used when the steady-state values are calculated for voltage and current. The complete derivation of the relation between the phasor representation and the synchronous reference frame representation of a balance set of voltages and current can be found in the chapter 3 of [8]. In the thesis, some key relations are used as described below.

For each phasor $\widetilde{f_{as}}$ in per-unit:

$$\widetilde{F_{ai}} = |\widetilde{F_{ai}}|\underline{/\theta_{Fai}} = |\widetilde{F_{ai}}|(\cos\theta_{Fai} + j\sin\theta_{Fai}) \tag{B.8}$$

Where f is either the voltages or the currents. The i represents bus number. The voltage and current calculated is the quantity in phase a. The equation above is the phasor in per-unit for the phase a quantities since all the components in this document is assumed to be symmetrical, with phase b and phase c 120 degrees lagging and leading, respectively.

The main relation used in this work is that in the per-unit quantities:

$$\widetilde{F_{ai}} = F^e_{qi} - jF^e_{di} \tag{B.9}$$

The equation (B.9) is very useful for the initial condition calculation of the states for all the models.

The other important relation between the phasor and the reference frame angle is also from [8], chapter 5, and the details can be found in starting from page 160. It is used in the analysis of the synchronous machine in thesis. Since the rotor angle δ is important for the machine analysis, and it is used to represent the steady-state phsor quantities in terms of the rotor reference frame as well, it is convenient to express

the phasor representation of the currents and voltages in term of quantities in rotor reference frame and the rotor angle δ:

$$\widetilde{F_{ai}} = (F_{qi}^r - jF_{di}^r)e^{j\delta} \tag{B.10}$$

One important thing about the equations above is that the angle δ is the angle between the rotor angle of the machine θ_r and the synchronous reference frame θ_e. Hence, by using the equation (B.8) and equation (B.10), the q- and d-axis quantites in the synchronous machine rotor reference frame can be calculated:

$$F_{qi}^r = |\widetilde{F_{as}}| \cos(\theta_{Fai} - \delta) \tag{B.11a}$$

$$F_{di}^r = -|\widetilde{F_{as}}| \sin(\theta_{Fai} - \delta) \tag{B.11b}$$

$$F_{0i} = 0 \tag{B.11c}$$

The equation (B.11) and equation (B.10) are used in the initial condition calculation in the synchronous machine in the detailed and reduced-order model, and they are also used heavily in behavioral for the synchronous machine algebraic calculations described in chapter (4).

C. POWER FLOW BY MATPOWER

Problem Formulation

The main objective of the power flow problem is to obtain per-unit voltages phase a phasor of each bus in a power system network based on given information about each bus. Since, again, a balanced set of three phase voltages are assumed in each bus, once phase a voltages are obtained, phase b and phase c voltage can be calculated easily. Hence, in all the description in this section, it is assumed that the phasor are all in phase a. Due to the non-linearity of the phasor, it is difficult to find a analytical solution for the problem. However, several numerical approaches are used to find the final solution within an desired tolerance. In general, there are three kinds of buses in a power flow study. In all the generator buses, typically the one generator with the highest power level rating are treated as a slack bus, where the voltage magnitude and angle are known. In the 5 bus system, it is the infinite bus at bus 1. However, all the other generator buses are treated as a PV bus, where the active power and the voltage magnitude are known, and the unknowns are the voltage angle. The reason why the active power and the voltage magnitude are known is that two inputs to the generation system is the commanded power P_o in the governor, and AVR input V_0 in the exciter. The third kind of buses are the load buses, where the active and reactive power(P and Q) consumption are known, and the unknowns are the voltage magnitude and angle. Hence, the load buses are called PQ buses. To solve these unknowns, the power balance equations at each buses are used. The power balance means that all the active power and reactive power go into each bus i must be consumed by the bus i or that all the active power and reactive power come out of each bus i must be generated by the bus i. On a system level, the power balance

means all the active and reactive power generated by the generator buses or the slack bus must be consumed by the load buses and the loss on the transmission line.

In the power system study, the bus voltages phasor of each buses are calculated.The relationship between the voltage and the currents are:

$$\mathbf{I} = \mathbf{YV} \tag{C.1}$$

Where $\mathbf{I}$ is a column vector contains all the bus current phasor, $\mathbf{Y}$ is the admittance matrix of the network, and $\mathbf{V}$ is a column vector contains all the bus voltage phasor.

The complex power generated/consumed at each bus are calculated based on the equation:

$$\widetilde{S}_i = \widetilde{V}_i \widetilde{I}_i^* \tag{C.2}$$

Where the $*$ is the conjugate operator of a complex number.

With the complex power equation illustrated, for a system with number of N buses with number of G generators, the number of unknowns are G of the generator voltage angles plus $2(N-G-1)$ of load voltage magnitude and angles; hence, the number of unknowns are $2N-G-2$. For each generator buses, there are G equations for the active power balance; for each of the load buses, there are $2(N-G-1)$ equations for the active and reactive power balances; hence a number of $2N-G-2$ equations can be used to solve all the unknowns.

Admittance Matrix

The admittance matrix is a size $N \times N$ square matrix, built based on the admittance between each buses, where N is the number of buses. The entries in the admittance matrix are based on the transmission lines and the transformers connecting two buses.

For transmission lines, the model used is the per-phase nominal-π model, shown in Figure 1.2 from [12]. Between bus i and bus j, the relationship between the voltage phase phasor and the current phasor is:

$$\widetilde{I}_i = (\widetilde{V}_i - \widetilde{V}_j)\frac{1}{R_l + jX_l} + \widetilde{V}_i jb_l \tag{C.3}$$

Where the $\widetilde{I}_i$ is the current bus i injects to the power system network; $\widetilde{V}_i$ and $\widetilde{V}_j$ are the voltage at bus i and bus j; $\frac{1}{R_l+jX_l}$ are the admittance of the line connecting the bus i and bus j; and jb_l is the admittance of the shunt capacitor of the line. Even though the equation (C.3) only represents the relationship of voltage and current between two buses on one line, a more general form of $\mathbf{Y}$ can be derived. The entry at row i, column j is:

$$\mathbf{Y}_{ij} = \begin{cases} \sum_{k=1,2,\ldots,N;k\neq i} Y_{ik}, & \text{if } i = j \\ -Y_{ij}, & \text{if } i \neq j \end{cases} \tag{C.4}$$

Where y_{ik} are the admittance of the shunt capacitors of all the transmission lines connected to the bus i; y_{ij} is the admittance of the transmission line connecting the bus i and bus j.

For the transformer, the model used is the simplified per-phase nominal reactance shown in Figure 1.3. The nominal turns ratio $\frac{N_1}{N_2}$ of the transformer is 1. However, to incorporate the voltage regulator on the left side of the Figure 1.3 into the form of the equation (C.12) when the turn's ratio is not 1, some modifications are made to the model. The input complex power and the output complex power of the voltage regulator are calculated based on:

$$\widetilde{S}_i = \widetilde{V}_i \widetilde{I}_i^* \tag{C.5a}$$

$$\widetilde{S}_t = \widetilde{V}_t \widetilde{I}_t^* \tag{C.5b}$$

Where

$$\widetilde{V}_t = \frac{N_2}{N_1}\widetilde{V}_i \tag{C.6a}$$

$$\widetilde{I}_t = -\widetilde{I}_j \tag{C.6b}$$

Since the voltage regulator is assumed to be ideal. i.e., no power loss: $\widetilde{S}_i = \widetilde{S}_t$. Let $r = \frac{N_1}{N_2}$, and r will be a real number based on the turns ratio. A relation between the input currents and output current can be obtained based on equations (C.5) and equation (C.6):

$$\widetilde{I}_j = -r\widetilde{I}_i \tag{C.7}$$

Another equation can also be used to calculate the output current based on the voltage after the voltage regulator:

$$\widetilde{I}_j = (\widetilde{V}_j - \frac{\widetilde{V}_i}{r})Y_l = -\widetilde{V}_i\frac{Y_l}{r} + \widetilde{V}_j Y_l \tag{C.8}$$

Where $Y_l = \frac{1}{jX_l}$.

Plug equation (C.7) into equation (C.8):

$$\widetilde{I}_i = \widetilde{V}_i\frac{Y_l}{r^2} - \widetilde{V}_j\frac{Y_l}{r} \tag{C.9}$$

According to the equation (C.9) and equation (C.8):

$$\begin{bmatrix}\widetilde{I}_i \\ \widetilde{I}_j\end{bmatrix} = \begin{bmatrix}\frac{Y_l}{r^2} & -\frac{Y_l}{r} \\ -\frac{Y_l}{r} & Y_l\end{bmatrix}\begin{bmatrix}\widetilde{V}_i \\ \widetilde{V}_j\end{bmatrix} \tag{C.10}$$

Based on the equation (C.10), the π-equivalent circuit can be obtained:

With the modified transformer π-equivalent circuit, the LTC transformer can be updated in the admittance matrix in the same fashion as the transmission line π-equivalent circuit described previously, and corresponding entries to the admittance matrix can be expressed in the same form as shown in equation (C.4).

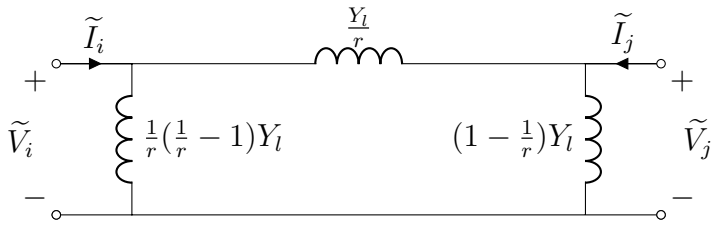

Fig. C.1.: Transformer π-Equivalent Circuit

The constant admittance at one bus can also be included in the admittance matrix. Since the constant admittance are connected to the grounded directly, it is similar to the shunt admittance of the transmission lines and transformers, which can be described by:

$$\widetilde{I}_i = \widetilde{V}_i Y_i \tag{C.11}$$

Where Y_i is the admittance at bus i connected to the ground.

After adding the influence of the constant admittance at the bus i from equation (C.11), the admittance matrix can be calculated based on:

$$\mathbf{Y}_{ij} = \begin{cases} Y_i + \sum_{k=1,2,\ldots,N;k\neq i} Y_{ik}, & \text{if } i = j \\ -Y_{ij}, & \text{if } i \neq j \end{cases} \tag{C.12}$$

Matpower

Matpower [19] is a package of Matlab m-files for solving power flow and power flow related problems. The manual of the package can be found in [20]. In this work, only part of the Matpower functions are used, which is to solve a power flow using the NewtonRaphson method to solve for the steady-state AC power flow of the 5 bus system. The inputs to the Matpower are the parameters of the system and the known quantities of each bus as described in the previous section.

To be more specific, in the 5-bus system shown in Figure 1.1, for the infinite bus, which is chosen to be the slack bus, the voltage magnitude and the angle are the

inputs; for the generator bus at bus 5, the active power and the voltage magnitude are the inputs. For the load bus at bus 2, the total active and reactive power of the loads consumed by the two induction machines and the constant admittance are the inputs. For bus 3 and bus 4, which are not generating power for the system, it is treated the same way as the load bus with active and reactive power consumption set to 0. In addition, the transmission lines and the LTC transformer admittance used to generate the admittance matrix is also provided as branch information between buses. The sample input script for the sample operating point described in the appendix A are shown next page.

```
%%-----  Power Flow Data  -----%%
%% system MVA base
mpc.baseMVA = 500;

%% bus data
%bus_i   type    Pd      Qd      Gs      Bs      area    Vm      Va      baseKV  zone    Vmax    Vmin
mpc.bus = [
1       3       0       0       0       0       1       1.05    0   225 1       1.07    0.95;
2       2       0       0       0       0       1       1       0   225 1       1.07    0.95;
3       1       400     80      0       0       1       1       0   225 1       1.07    0.95;
4       1       0       0       0       0       1       1       0   225 1       1.07    0.95;
5       1       0       0       0       0       1       1       0   225 1       1.07    0.95;
];

%% generator data
%       bus     Pg      Qg      Qmax    Qmin    Vg      mBase   status  Pmax    Pmin    Pc1     Pc2     Qc1min  Qc1max  Qc2min  Qc2max
    ramp_agc        ramp_10 ramp_30 ramp_q  apf
mpc.gen = [
        1  0       0    300      -300  1.05  100  1      750     0 0     0 0     0 0     0 0     0 0     0 0;
        2  300     0    300      -300  1.0   100  1      750     0 0     0 0     0 0     0 0     0 0     0 0;
];

%% branch data
%       fbus    tbus    r       x       b       rateA   rateB   rateC   ratio   angle   status  angmin  angmax
mpc.branch = [
        1       5       r51     x51     b51     60      0       0       0   0   1       -360    360;
        5       4       r54     x54     b54     60      0       0       0   0   1       -360    360;
        5       3       r35     x35     0       60      0       0       n1  0   1       -360    360;
        4       2       r42     x42     0       60      0       0       n2  0   1       -360    360;
];

%% run power flow
PFsol = runpf(mpc);
BUS.Vbus = PFsol.bus(:,8);
BUS.Vang = PFsol.bus(:,9);
BUS.Pgen = PFsol.gen(:,2);
BUS.Qgen = PFsol.gen(:,3);

BUS.Pbranch = [PFsol.branch(:,14);PFsol.branch(:,16)];
BUS.Qbranch = [PFsol.branch(:,15);PFsol.branch(:,17)];
```

The useful output of the Matpower in this work are all the bus information including voltage magnitude and angle of each, the complex power the bus generates/consumes and the power flow on each branches (transmission lines and the transformer) after the command **runpf**. For example, The output of the sample operating point is:

```
MATPOWER Version 7.0, 20-Jun-2019 -- AC Power Flow (Newton)

Newton's method power flow (power balance, polar) converged in 4 iterations.

Converged in 0.00 seconds
Converged in 0.00 seconds
================================================================================
|     System Summary                                                           |
================================================================================

How many?                How much?              P (MW)            Q (MVAr)
---------------------    -------------------  -------------  -----------------
Buses              5     Total Gen Capacity    1500.0        -600.0 to 600.0
Generators         2     On-line Capacity      1500.0        -600.0 to 600.0
Committed Gens     2     Generation (actual)    401.2             112.9
Loads              1     Load                   400.0              80.0
  Fixed            1       Fixed                400.0              80.0
  Dispatchable     0       Dispatchable          -0.0 of -0.0       -0.0
Shunts             0     Shunt (inj)            -0.0               0.0
Branches           4     Losses (I^2 * Z)        1.19             81.30
Transformers       2     Branch Charging (inj)     -              48.4
Inter-ties         0     Total Inter-tie Flow    0.0               0.0
Areas              1

                         Minimum                      Maximum
                ------------------------  --------------------------------
Voltage Magnitude   1.000 p.u. @ bus 3          1.050 p.u. @ bus 1
Voltage Angle      -7.66 deg   @ bus 3          4.21 deg   @ bus 2
P Losses (I^2*R)             -                 0.63 MW    @ line 1-5
Q Losses (I^2*X)             -                41.61 MVAr  @ line 5-3

================================================================================
|     Bus Data                                                                 |
================================================================================
 Bus      Voltage          Generation             Load
  #   Mag(pu) Ang(deg)   P (MW)   Q (MVAr)   P (MW)   Q (MVAr)
----- ------- --------  --------  --------  --------  --------
```

1	1.050	0.000*	101.19	60.36	-	-
2	1.000	4.212	300.00	52.58	-	-
3	1.000	-7.655	-	-	400.00	80.00
4	1.018	-1.013	-	-	-	-
5	1.015	-2.055	-	-	-	-
			---	---	---	---
		Total:	401.19	112.94	400.00	80.00

Branch Data								
Brnch #	From Bus	To Bus	From Bus Injection P (MW)	From Bus Injection Q (MVAr)	To Bus Injection P (MW)	To Bus Injection Q (MVAr)	Loss (I^2 * Z) P (MW)	Loss (I^2 * Z) Q (MVAr)
1	1	5	101.19	60.36	-100.55	-96.12	0.633	6.33
2	5	4	-299.45	-25.49	300.00	24.75	0.554	5.54
3	5	3	400.00	121.61	-400.00	-80.00	-0.000	41.61
4	4	2	-300.00	-24.75	300.00	52.58	0.000	27.83
							---	---
						Total:	1.187	81.30

By using the bus and branch information above, the initial condition of the states can be calculated based on the description each of the models. The other command used in this work is the **makeYbus**, which will give the admittance matrix of the system and it is used in the reduced-order model. In addition, in the behavioral model, the power flow is being solved repeatedly at at each sample with updated initial guesses.